HAL
open science

Asymptotics of plasmonic resonnances of rectangular cavities

Abdelfatah Gtet

To cite this version:

Abdelfatah Gtet. Asymptotics of plasmonic resonnances of rectangular cavities. General Mathematics [math.GM]. Université Grenoble Alpes, 2017. English. NNT : 2017GREAM096 . tel-01885548

HAL Id: tel-01885548

https://theses.hal.science/tel-01885548v1

Submitted on 2 Oct 2018

HAL is a multi-disciplinary open access archive for the deposit and dissemination of scientific research documents, whether they are published or not. The documents may come from teaching and research institutions in France or abroad, or from public or private research centers.

L'archive ouverte pluridisciplinaire **HAL**, est destinée au dépôt et à la diffusion de documents scientifiques de niveau recherche, publiés ou non, émanant des établissements d'enseignement et de recherche français ou étrangers, des laboratoires publics ou privés.

Communauté UNIVERSITÉ Grenoble Alpes

THÈSE

Pour obtenir le grade de

DOCTEUR DE LA COMMUNAUTÉ UNIVERSITÉ GRENOBLE ALPES

Spécialité : Mathématiques Appliquées

Arrêté ministériel : 25 mai 2016

Présentée par

ABDELFATAH GTET

Thèse dirigée par **Faouzi TRIKI**,
codirigée par **Eric BONNETIER** Université Grenoble Alpes
préparée au sein du **Laboratoire Laboratoire Jean Kuntzmann**
dans **l'École Doctorale Mathématiques, Sciences et technologies de l'information, Informatique**

Calcul asymptotique de résonances de plasmon de cavités rectangulaires

Asymptotics of plasmonic resonnances of rectangular cavities

Thèse soutenue publiquement le **19 décembre 2017**,
devant le jury composé de :

Monsieur ERIC BONNETIER
PROFESSEUR, UNIVERSITE GRENOBLE ALPES, Co-directeur de thèse
Monsieur FAOUZI TRIKI
MAITRE DE CONFERENCES, UNIVERSITE GRENOBLE ALPES, Directeur de thèse
Monsieur MOURAD SINI
DIRECTEUR DE RECHERCHE, ACADEMIE AUTRICHIENNE DES SCIENCES, Rapporteur
Madame MIKYOUNG LIM
PROFESSEUR, KAIST - COREE DU SUD, Rapporteur

Monsieur GREGORY VIAL
PROFESSEUR, ECOLE CENTRALE DE LYON, Président
Monsieur FERNANDO GUEVERA VASQUEZ
PROFESSEUR ASSISTANT, UNIVERSITE D'UTAH - ETATS-UNIS, Examinateur
Monsieur SEBASTIEN TORDEUX
MAITRE DE CONFERENCES, UNIVERSITE DE PAU ET DES PAYS DE L'ADOUR, Examinateur

Asymptotic Analysis of Plasmonic Resonances of some Metallic Structures

GTET Abdelfatah

October 20, 2017

Contents

Introduction **5**

1 Introduction to surface plasmon polaritons **9**
1.1 Introduction 9
1.2 The dielectric permittivity of a metal 10
1.2.1 Drude Model 10
1.2.2 Contribution of inter-band Transitions 11
1.3 Surface Plasmons Polaritons 13
1.3.1 Plasmon, surface plasmon, polariton, surface plasmon polariton, resonances 13
1.3.2 Surface plasmon polaritons at metal /insulator interfaces 14
1.3.3 Subwavelength grating 23

2 Asymptotic of resonances of a real metallic plane perturbed by a subwavelength rectangular cavity **25**
2.1 Introduction 25
2.2 Formulation of the problem 28
2.2.1 Notations 28
2.2.2 Problem Formulation 28
2.3 Integral representation 30
2.3.1 The Green function in the half-space $\mathbb{R}^2_+$ 30
2.3.2 The Green function in the rectangular cavity 32
2.3.3 Integral equations 36
2.4 Asymptotics 37
2.4.1 Asymptotic of G_i 37
2.4.2 Asymptotic of G_e 53
2.4.3 Asymptotic of $S(w, k)$ 57
2.4.4 Asymptotic of resonant frequencies 58

3 Asymptotic of resonances of a periodic array of metallic subwavelength cavities **63**
3.1 Introduction 64
3.2 Position of the problem 65

3.2.1 Description of the geometry and notations 65
3.2.2 Formulation of the problem 66
3.2.3 Quasi-periodicity 67
3.2.4 The radiation condition 68
3.2.5 The periodic problem 73
3.3 Wellposedness of the problem 73
3.3.1 θ-periodic functional spaces 74
3.3.2 Truncation of the domain 76
3.3.3 The variational formulation 77
3.3.4 Characterization of singular frequencies 79
3.4 Reduction of the problem to an integral equation 80
3.4.1 The Green function in Ω_i 80
3.4.2 The Green function in Ω_e 81
3.4.3 Integral representation 82
3.5 Asymptotics 85
3.5.1 The case d is independent of w 85
3.5.2 The case $d = mw$ 101

4 Green's function for a real metallic slab cladded in a dielectric media 111
4.1 Introduction 111
4.2 Position of the problem 112
4.2.1 Description of the geometry and notations 112
4.2.2 Problem formulation 113
4.2.3 Drude's model for real conductor permittivity 114
4.3 Thin layer limit model 115
4.3.1 Motivation 115
4.3.2 The Green function of the limiting problem 116
4.3.3 Behavior of G_0 as a function of the contrast η 126
4.4 Numerical results 132

Conclusion 135

Bibliography 137

Introduction

Rough metallic surfaces with subwavelength structurations possess extraordinary diffractive properties: at certain frequencies, one may observe fine localization and very large enhancement of the electromagnetic fields. The discovery of these phenomena has raised considerable interest as potential applications are numerous (optical switches, sensors, devices for microscopy). This behavior results from the combination of very complex interaction between the incident excitation, the geometry and the material properties of the scatterer. The main goal of this thesis is to better understand these phenomena from the mathematical point of view.

In mathematical terms, the localization and concentration of the fields is the mark of a resonance phenomenon. In our context, the corresponding resonant field may be surface plasmons, i.e., waves that propagate along the interface of the grating, and that decay exponentially away from it. Another type of resonance is due to possible cavity modes. Thus, the study of these phenomena pertains to eigenvalue problems for the solutions of the Maxwell system, in geometric configurations where in the whole of a dielectric (generally air) and a metal are separated by an infinite rough interface.

Our main objective is to derive asymptotic limits for such gratings, as the parameters that measure the roughness tend to 0. The asymptotic models are indeed very interesting for optimization and design purposes. They correspond to configurations where the metal and the dielectric are separated by a planar interface, and one may derive dispersion relations that are better suited for precise numerical approximation of the resonance frequencies.

We are interested in particular micro-structured devices, namely metallic surfaces that contain rectangular grooves with sub-wavelength apertures, and thin plane layers. Configurations of this type can be manufactured quite precisely and have been subject to experimental work and theoretical studies [1, 2, 3, 4, 5, 6]. The simple geometry of the structures allows to transform the eigenvalue problem for the Maxwell system into a nonlinear eigenvalue problem for an integral operator that depends on a small parameter, which, using tools from analytic perturbation theory, lends itself to a precise asymptotic analysis.

In chapter two and three, we considered the spectral problem for Maxwell equations. where the frequency is the eigenvalue, in unbounded domains de-

limited by an infinite plane interface containing rectangle cavities of width w. Our goal is to derive the asymptotic expansion of the resonances as w goes to zero. Our strategy is (1) to reformulate the eigenvalue problem in the whole unbounded domain occupied by the structure, as a nonlinear eigenvalue problem on a small bounded set of lower dimensionality w (such as the aperture of the cavities); (2) to study the associated integral operators $S(w,k)$ and determine their asymptotic as w tends to 0; (3) to derive the asymptotic expansion of the resonant frequencies, using the generalized Rouché Theorem and Fredholm theory for operator valued functions.

The enhancement and confinement of electromagnetic fields in the considered metallic structures, can indeed be quantified in term of the imaginary part of the resonance frequencies. The reduced nonlinear spectral problem takes the form

$$S(w,k)\varphi = 0$$

where $S(w,k)$ is a weakly singular integral operator that contains the different interactions between surface plasmon waves or cavity modes and the incident fields on both sides of the interface metal-dielectric. For example, in the case of a real metal planar interface which contains a single sub-wavelength rectangular cavity, the operator-valued function takes the following form:

$$S(w,k)\varphi(x_1) = \int_{-1}^{1} \left(G_e(wx_1,0;wy_1,0) + G_i(wx_1,0;wy_1,0)\right)\varphi(y_1)dy_1$$

where $(-1,1)$ is the rescaled opening of the cavity of width w, and G_i, G_e are respectively the Green functions of the Helmholtz operator inside and outside the cavity, which are known explicitly. In the second chapter we showed that the resonance frequencies of the micro-cavity are exactly the zeros of the function $k \to S(w,k)$. More specifically, based on the Fredholm theory and a rigorous analysis of the properties of the meromorphic function we have obtained the following behavior near a resonance frequency say $k_n(w)$:

$$S^{-1}(w,k) \quad = \quad \frac{S_{-1,n}}{k-k_n} + R_n(k).$$

The rest $R_n(k)$ is holomorphic in a small neighborhood of k_n, and $S_{-1,n}$ is a finite rank operator. The confinement and exaltation of the electromagnetic fields around the cavity occur at a frequency of the incident plane wave (which is always real), close to $\mathrm{Re}(k_n)$ if the imaginary part $\mathrm{Im}(k_n)$ is small enough. Consequently, the behavior of operator $S_{-1,n}$ as tends to zero can gauge the localization and the enhancement of the electromagnetic fields near the cavity. Using the Generalized Rouché Theorem, we derived

in chapters two and three the asymptotic expansions of k_n as w tends to 0.

In the fourth chapter we focus on a simple plasmonic waveguide that consists in a metallic slab cladded in a dielectric media. Our objective is to study the quasi-static resonances of the system that correspond to the case where the thickness of the metal layer is too small compare to the wavelength. These resonant frequencies correspond to plasmonic surface waves.

The work we propose here intends to apply techniques developed in [4, 5, 6] to more complex and more realistic situations (real metal, periodic gratings, thin metallic layers). In the first chapter, we present the physical setting of the considered mathematical models. We first describe the optical properties of metals through their dielectric permittivities which are responsible for the response of the material to an applied electromagnetic field. We focus on the Drude model which gives a good approximate expression of the dielectric permittivity for the range of frequencies considered. Then, we introduce the physical modeling of surface plasmon waves via the Maxwell equations.

In the second chapter, we consider an open sub-wavelength metallic cavity. At the interface dielectric /metal, we consider an impedance boundary condition called the impedance condition. We present a theoretical study of the electromagnetic diffraction. We begin by writing an integral representation of the magnetic field on the aperture of the cavity. The integral problem is equivalent to the Helmholtz one. We then derive a rigorous asymptotic of the Green functions outside and inside the cavity which represent the kernel of the integral equation. Using an operator version of the Rouché theorem, we show that the resonances are the poles of the kernel and we derive the asymptotic expansion of the resonant frequencies when the width of the cavity shrinks to zero.

The third chapter deals with a periodic array of rectangular metallic sub-wavelength cavities. Here we consider a perfect metal and a Neumann boundary condition is imposed on the interface dielectric/metal. We begin by formulating the problem and unrolling some well-posedness results. Then, thanks to the periodicity of the geometry, we reduce the problem to the principal periodicity cell. We find an equivalent integral problem at the aperture of the single cavity in the principal periodic unit cell. Using the same strategy as in the second chapter, we compute an asymptotic of the resonances of the problem when the width of the cavities goes to zero. We studied two asymptotic regimes: the first deals with the case where only the width of the aperture goes to zero while the period of the array remains constant, and the second is related to the case where the period and the width shrinks together to zero.

In the fourth chapter, we study the enhancement and confinement of electromagnetic fiels in a plasmonic waveguide that consists of a thin layer of metal positioned between two infinite dielectrics. The aim of this chapter is to analyse the resonances frequencies associated to guided modes confined along the interface between the metal and the dielectric. We start by formulating the problem as a Helmholtz equation with the adequate transmission conditions. We first compute the Green function of the quasi-static limiting system using Fourier techniques. We then investigate the set of frequencies and the spatial region where it blows up.

Chapter 1

Introduction to surface plasmon polaritons

Sommaire

1.1 Introduction 9

1.2 The dielectric permittivity of a metal 10

1.2.1 Drude Model 10

1.2.2 Contribution of inter-band Transitions 11

1.3 Surface Plasmons Polaritons 13

1.3.1 Plasmon, surface plasmon, polariton, surface plasmon polariton, resonances 13

1.3.2 Surface plasmon polaritons at metal /insulator interfaces 14

1.3.3 Subwavelength grating 23

1.1 Introduction

Surface plasmon polaritons are electromagnetic excitations that propagates at the interface between a dielectric and a metal. They are evanescent and confined in the perpendicular direction to the interface. These surface waves occur via the coupling of the electromagnetic fields to the oscillations of the metam's electron plasma. The first part of this chapter describes the Drude model of the dielectric permittivity of a metal in the visible range. The second part deals with the physical modeling of surface plasmon polaritons along flat interfaces between metal and dielectric using Maxwell systems.

1.2 The dielectric permittivity of a metal

In plasmonic field the dielectric permittivity is one of the fundamental material parameters that affects the behavior of electromagnetic fields within the metallic structures. The response of a non-magnetic material to an electromagnetic wave is directly related to the interactions between the wave and the electrons of the material under consideration. The dielectric permittivity of a material is the physical quantity that manages its linear response to the propagation of electromagnetic waves inside of it.

1.2.1 Drude Model

An isolated atom has a positively charged nucleus surrounded by *core* electrons and then one or more valence electrons. In the case of metals, this atomic structure is preserved with the exception that the valence electrons find themselves delocalized and free to move in the crystal lattice. Thus, a metal consists of a lattice of atoms, each with an outer shell of electrons that freely dissociate from their parent atoms and travel through the lattice. The free electrons are called conduction electrons and form a gas (or sea) of negatively charged free electrons. Atomic nuclei surrounded by core electrons form a fixed crystal structure positively charged also known as a positive ionic lattice.

Drude in 1900 [7], [8] considered the metal as a Free Electron Gas or plasma and introduced his famous model. The Drude model is based on certain assumptions about the movement of free electrons. Electron-electron interactions are neglected and the movement of electrons is only perturbed by collisions with the crystal lattice. When an electromagnetic field is applied, the free electrons oscillate and their motion is damped via collisions occurring with a characteristic collision frequency $\gamma = \frac{1}{\tau}$. The constant τ is the relaxation time of the free electron gas defined as the mean time between two successive collisions. Sommerfeld extended this classic model to quantum-mechanics by incorporating Fermi-Dirac statistics for electrons [9].

The trajectory of an electron of mass m in the presence of an electric field E is described by the fundamental relation of the dynamics. The different possible forces applied to the electrons are: the force produced by the electric field E itself, and the damping force due to collisions with the ions network. The temporal evolution of the position x of the electrons is then described by:

$$m\frac{\partial^2 x}{\partial t^2} + m\gamma\frac{\partial x}{\partial t} = -eE \tag{1.2.1}$$

where e is the elementary charge of an electron. Assuming a harmonic time dependence $E(t) = E_0 e^{-i\omega t}$ of the driving field and a harmonic motion of

the electron, a solution to the latter equation is given by:

$$x(t) = \frac{e}{m(\omega^2 + i\omega\gamma)} E_0 e^{-i\omega t} \tag{1.2.2}$$

The microscopic displacement of the free electron gas results in a macroscopic polarization $P = -nex(t)$, that is

$$P = -\frac{ne^2}{m(\omega^2 + i\omega\gamma)} E_0 e^{-i\omega t}$$

where n is the free electrons density. Recalling that the permittivity in a linear, homogeneous and isotropic material obeys to

$$D = \epsilon_0 E + P = \epsilon_0 \epsilon_d E$$

where D is the dielectric displacement, one can find that the dielectric permittivity is given by:

$$\epsilon_d(\omega) = 1 - \frac{\omega_p^2}{\omega^2 + i\omega\gamma} \tag{1.2.3}$$

where $\omega_p = \sqrt{\frac{ne^2}{\epsilon_0 m}}$ is the plasma frequency of the free electron gas. For noble metals (e.g Au, Ag, Cu) an extension of this model is needed for $\omega > \omega_p$ due to residual polarization of ions. More precisely we need to introduce a dielectric constant ε_∞ ($1 \leq \varepsilon_\infty \leq 10$) to describe this effect. Then, the permittivity can be rewritten as:

$$\varepsilon(\omega) = \varepsilon_\infty - \frac{\omega_p^2}{\omega^2 + i\gamma\omega}. \tag{1.2.4}$$

The validity limits of the free-electron description for the case of gold (1.2.4) are illustrated in the Figure 1.1. It shows the real and imaginary parts of the Drude dielectric function fitted to the experimental dielectric function of the gold [10]. Clearly, the applicability of the free-electron model fails to match the experimental graph at visible frequencies due to the occurrence of inter-band transitions. This will be discussed in the next section.

1.2.2 Contribution of inter-band Transitions

A more rigorous consideration of the electronic structure of materials is provided by the quantum theory of bands which consists in representing the possible energy levels of the set of electrons in a solid [11]. The electrons of an isolated atom can occupy only discrete states of energy, and the association of several atoms extends the number of energetic states by hybridization of the atomic orbitals in various electronic layers. In a solid, the permissible energies form a continuum in given intervals, called energy bands, and may

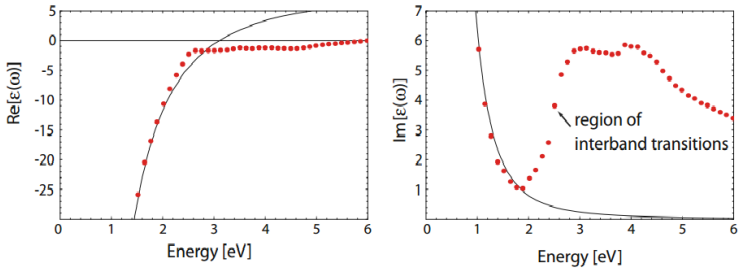

Figure 1.1: Drude dielectric function (solid line) fitted to the literature values of the dielectric function (dots) for gold [7].

have very complex structures, with possible overlaps. The difference between metallic, semiconductor or insulating materials can be carried out from their electronic band structure calculated at zero temperature. The valence band is the last band completely filled, by localized electrons that participate in the cohesion of the material. The conduction band is the band immediately higher in energy than that of valence, with a possible overlap between this and the valence band. The electrons of this conduction band are then delocalized and participate in the electrical and thermal conduction of the material. The presence of a band of forbidden energy (band gap) between the valence band and the conduction band is responsible of the nature of the material. In the case of insulators, the conduction band is entirely above the valence band and is empty, and the band gap is wide enough to prevent the passage of electrons from the valence band to the conduction band. For semiconductors, the conduction band is also entirely above that of valence, with a relatively narrow band gap allowing a transition of the electrons from the valence band to the conduction band by thermal effect or light excitation . Finally, the case of metals is a little more complex, for the alkali metals for example, the band which is not completely filled plays the role of both valence and conduction bands. For transition metals, the conduction band is partially superimposed on that of valence, each of which may be partially fulfilled. The metals have a non-empty conduction band, which explains the excellent conductivity of these materials.

The Drude model presented in the previous paragraph considers only the conduction electrons in the metal response (this model is said to describe inter-band transitions). However, electron transitions from one band to another may in some cases play a non-negligible role in the response of metals. In other words, the Drude model adequately describes the optical response of metals only for photon energies below the threshold of transitions between electronic bands. For some noble metals, inter-band effects already

start to occur for energies that exceed $1eV$ (corresponding to a wavelength $\lambda \approx 1\mu m$). In the case of gold, its validity breaks down already at the boundary between the near-infrared and the visible [12]. To overcome this inadequacy of the model for some frequencies, the relative dielectric permittivity can be rewritten taking into account the inter-band transitions [13]

$$\epsilon(\omega) = \epsilon_d(\omega) + \epsilon_{interband}(\omega) \tag{1.2.5}$$

where $\epsilon_{interband}(\omega)$ is the added term due to inter-band transitions. To compute the latter term, we consider the equation governing the motion of a bound electron:

$$m_b \frac{\partial^2 x}{\partial t^2} + m_b \gamma_b \frac{\partial x}{\partial t} + \alpha x = -eE \tag{1.2.6}$$

where m_b is the effective mass of the bound electrons, γ_b is another damping term, and α is the constant of the potential retaining the electrons in place. By analogy to the calculations made in the Drude model section, we find that:

$$\epsilon_{interband}(\omega) = 1 + \frac{\omega_{pb}^2(\omega_0 - \omega^2)}{(\omega_0^2 - \omega^2)^2 + \omega^2\gamma_b^2} + i\frac{\gamma_b \omega_{pb}^2 \omega}{(\omega_0^2 - \omega^2)^2 + \omega^2\gamma_b^2} \tag{1.2.7}$$

where the frequency $\omega_{pb} = \sqrt{\frac{n_b e^2}{\epsilon_0 m_b}}$ is analogous to the plasma frequency of the metal in the model of Drude-Sommerfeld, $\omega_0 = \sqrt{\frac{\alpha}{m_b}}$, and n_b is the bound electrons density.

1.3 Surface Plasmons Polaritons

1.3.1 Plasmon, surface plasmon, polariton, surface plasmon polariton, resonances

Plasmons

The Drude model considers the metal as a mass of positively charged ions from which a number of *free electrons* were detached. These free electrons are oscillating naturally (due to thermal energy) and their motion may increase in the presence of an electric field. In fact when the free electrons within the metal are displaced, the atomic nuclei surrounded by core electrons positively charged perform a little motion due to their large mass, and hence exert on these electrons an attractive Coulomb force. The electrons will therefore return to their initial position, and so on. These oscillations can be similarly found in plasma state. They are called Plasma oscillations, also known as "Langmuir waves" (after Irving Langmuir) [14]. Plasmon is a quantum of

plasma oscillation. Just like an optical oscillation(light) consists of photons, the plasma oscillation consists of plasmons. The plasmon can be considered as a quasiparticle since it arises from the quantization of plasma oscillations. Thus, plasmons are collective (a discrete number) oscillations of the free electron gas density.

Surface plasmon

Surface plasmons are plasmons that exist at the interface between any two materials where the real part of the dielectric function changes sign across the interface (e.g. a metal-dielectric interface, such as a metal layer in air). The existence of surface plasmons was first predicted in 1957 by Rufus Ritchie [15].

Polariton

Polaritons are quasi particles resulting from strong coupling of electromagnetic waves with an electric or magnetic dipole carrying excitation (polarization wave) [16].

Surface plasmon polariton

Surface plasmon polariton is a special case of surface plasmon when there is coupling between electromagnetic wave coming from a dielectric medium and a plasmon in a metal (the electric dipole carrying excitation). At wavelengths capable of supporting plasmons, the light wave can not penetrate into the metal, however coupling can take place at the metal / dielectric interface. Such a surface wave is thus called a surface polariton plasmon [17]. Surface plasmon polariton can be excited by both electrons and photons. Excitation by electrons is created by firing electrons into the bulk of a metal however excitation by photons occurs when both photon and Surface plasmon plariton have the same frequency and momentum.

1.3.2 Surface plasmon polaritons at metal /insulator interfaces

In order to investigate the physical properties of surface plasmon polaritons, we start by considering the diffraction of an electromagnetic wave by a plane interface between two media, one is a metal and the other is a dielectric.

Diffraction by a flat interface

We begin by applying the Maxwell's equations to the flat interface between a metal and a dielectric. We present Maxwell's equations at the macroscopic level in the following form:

$$\nabla.\mathbf{D} = \rho_{ext} \tag{1.3.1}$$

$$\nabla.\mathbf{B} = 0 \tag{1.3.2}$$

$$\nabla \otimes \mathbf{E} = -\frac{\partial \mathbf{B}}{\partial t} \tag{1.3.3}$$

$$\nabla \otimes \mathbf{H} = \mathbf{J}_{ext} + \frac{\partial \mathbf{D}}{\partial t} \tag{1.3.4}$$

These equations link the four macroscopic fields : the dielectric displacement D, the electric field E, the magnetic field H, and the magnetic induction or magnetic flux density B with the external charge ρ_{ext} and current densities J_{ext}. The media is supposed to be linear, isotropic and nonmagnetic. One can define the constitutive relations

$$\mathbf{D} = \epsilon_0 \epsilon \mathbf{E}$$

$$\mathbf{B} = \mu_0 \mu \mathbf{H}$$

where ϵ_0 and μ_0 are the electric permittivity and magnetic permeability of vacuum, respectively. ϵ is called the dielectric constant or relative permittivity and $\mu = 1$ the relative permeability of the nonmagnetic medium. In the absence of external charge and current densities, the curl of equations (1.3.3, 1.3.4) can be combined to yield

$$\nabla \otimes \nabla \otimes \mathbf{E} = -\mu_0 \frac{\partial^2 \mathbf{D}}{\partial t^2} \tag{1.3.5}$$

Using the identity $\nabla \otimes \nabla \otimes \mathbf{E} = \nabla(\nabla.\mathbf{E}) - \nabla^2 \mathbf{E}$, it becomes

$$\nabla^2 \mathbf{E} - \frac{\epsilon}{c^2} \frac{\partial^2 \mathbf{E}}{\partial t^2} = 0 \tag{1.3.6}$$

To look for the solutions to the problem, this equation has to be solved separately in regions of constant ϵ, and the obtained solutions have to be matched using appropriate boundary conditions. We assume a harmonic time dependence of the electric field $\mathbf{E}(r,t) = \mathbf{E}(r)e^{-i\omega t}$, which gives the following Helmholtz equation

$$\nabla^2 \mathbf{E} - k_0^2 \epsilon \mathbf{E} = 0 \tag{1.3.7}$$

where $k_0 = \frac{\omega}{c}$ is the wave vector of the propagating wave in vacuum.

Following the cartesian coordinates shown in Figure 1.2, the plane $z = 0$ coincides with the interface separating the two media, and the waves are

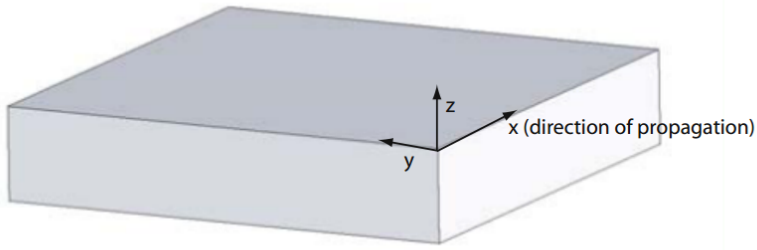

Figure 1.2: The flat interface sustaining the surface plasmon polariton

chosen to be propagate along the x-direction, presenting no spatial variations in the y-direction.

Due to spatial invariance arguments, the electromagnetic field can be described as $\mathbf{E}(x, y, z) = \mathbf{E}(z)e^{i\beta x}$ and $\mathbf{H}(x, y, z) = \mathbf{H}(z)e^{i\beta x}$. The complex parameter β is called the propagation constant of the propagating wave and corresponds to the component of the wave vector in the direction of propagation. Inserting this expression into (1.3.7) gives

$$\frac{\partial^2 \mathbf{E}}{\partial z^2} + (k_0^2\epsilon - \beta^2)\mathbf{E} = 0 \tag{1.3.8}$$

Naturally, the magnetic field $\mathbf{H}$ verifies a similar equation. We further solve these equations in order to recover the spatial field profile and dispersion of the propagating waves. Back to the equations (1.3.3,1.3.4), we can combine them in the following system

$$\frac{\partial E_z}{\partial y} - \frac{\partial E_y}{\partial z} = i\omega\mu_0 H_x \tag{1.3.9}$$

$$\frac{\partial E_x}{\partial z} - \frac{\partial E_z}{\partial x} = i\omega\mu_0 H_y \tag{1.3.10}$$

$$\frac{\partial E_y}{\partial x} - \frac{\partial E_x}{\partial y} = i\omega\mu_0 H_z \tag{1.3.11}$$

$$\frac{\partial H_z}{\partial y} - \frac{\partial H_y}{\partial z} = -i\omega\epsilon_0\epsilon E_x \tag{1.3.12}$$

$$\frac{\partial H_x}{\partial z} - \frac{\partial H_z}{\partial x} = -i\omega\epsilon_0\epsilon E_y \tag{1.3.13}$$

$$\frac{\partial H_y}{\partial x} - \frac{\partial H_x}{\partial y} = -i\omega\epsilon_0\epsilon E_z \tag{1.3.14}$$

Along the x-direction $\frac{\partial}{\partial x} = i\beta$ and the y-direction $\frac{\partial}{\partial y} = 0$, the above system

simplifies to

$$
\begin{aligned}
&\frac{\partial E_y}{\partial z} = -i\omega\mu_0 H_x \\
&\frac{\partial E_x}{\partial z} - i\beta E_z = i\omega\mu_0 H_y \\
&i\beta E_y = i\omega\mu_0 H_z \\
&\frac{\partial H_y}{\partial z} = i\omega\epsilon_0\epsilon E_x \\
&\frac{\partial H_x}{\partial z} - i\beta H_z = -i\omega\epsilon_0\epsilon E_y \\
&i\beta H_y = -i\omega\epsilon_0\epsilon E_z
\end{aligned}
\tag{1.3.15}
$$

Regarding these equations, one can notice that they can be decomposed into two sets of self-consistent systems of equations. The first governs the components E_x, E_z and H_y, corresponds to the transverse magnetic (TM or p) polarization, while the second governs H_x , H_z and E_y and is related to the transverse electric (TE or s) polarization.

For TM modes, the system of governing equations 1.3.15 reduces to

$$E_x = -i\frac{1}{\omega\epsilon_0\epsilon}\frac{\partial H_y}{\partial z} \tag{1.3.16}$$

$$E_z = -\frac{\beta}{\omega\epsilon_0\epsilon}H_y \tag{1.3.17}$$

and, the wave equation is

$$\frac{\partial^2 H_y}{\partial z^2} + (k_0^2\epsilon - \beta^2)H_y = 0 \tag{1.3.18}$$

For TE modes, the system of governing equations 1.3.15 reduces to

$$H_x = i\frac{1}{\omega\mu_0}\frac{\partial E_y}{\partial z} \tag{1.3.19}$$

$$H_z = \frac{\beta}{\omega\mu_0}E_y \tag{1.3.20}$$

and the wave equation is

$$\frac{\partial^2 E_y}{\partial z^2} + (k_0^2\epsilon - \beta^2)E_y = 0. \tag{1.3.21}$$

Thus, the recovery of only the magnetic field H_y will give a full charateri-sation of the TM polarization. Similarly the knowledge of electric field E_y is is enough to describe the propagation of electromagnetic waves in TE polarization.

Surface plasmons polariton

We consider here a dielectric material occupying the half space ($z > 0$) with a real dielectric constant $\epsilon_2 > 0$ and a metal occupying the half space ($z < 0$) with a complex dielectric permittivity $\epsilon_1(\omega)$. Our aim here is to show the existence of surface waves that are confined along the interface between the two materials, i.e. they are evanescent in the perpendicular z-direction, and propagate in the x-direction. The transmission relations between the two media yield

$$\mathbf{n} \otimes (\mathbf{E}^1 - \mathbf{E}^2) = 0 \tag{1.3.22}$$

$$\mathbf{n}.(\mathbf{D}^1 - \mathbf{D}^2) = \rho_s \tag{1.3.23}$$

$$\mathbf{n}.(\mathbf{B}^1 - \mathbf{B}^2) = 0 \tag{1.3.24}$$

$$\mathbf{n} \otimes (\mathbf{H}^1 - \mathbf{H}^2) = \mathbf{J}_s \tag{1.3.25}$$

where $\mathbf{D}^1 = \epsilon_1(\omega)\mathbf{E}^1$ and $\mathbf{D}^2 = \epsilon_2\mathbf{E}^2$ are the electric displacement fields in the metallic medium and the dielectric respectively. $\mathbf{B}^1 = \mu\mathbf{H}^1$ and $\mathbf{B}^2 = \mu\mathbf{H}^2$ are the magnetic field ($\mu = 1$) in the dielectric and metallic medium respectively. ρ_s is the surface charge density and $\mathbf{J}_s$ is the surface current.

Considering first the TM modes, using the equations (1.3.16,1.3.17,1.3.18) on both sides of the interface, we find:

For $z > 0$

$$H_y(x, z) = A_2 e^{i\beta x} e^{-k_2 z} \tag{1.3.26}$$

$$E_x(x, z) = iA_2 \frac{1}{\omega\epsilon_0\epsilon_2} k_2 e^{i\beta x} e^{-k_2 z} \tag{1.3.27}$$

$$E_z(x, z) = -A_2 \frac{\beta}{\omega\epsilon_0\epsilon_2} e^{i\beta x} e^{-k_2 z} \tag{1.3.28}$$

For $z < 0$

$$H_y(x, z) = A_1 e^{i\beta x} e^{k_1 z} \tag{1.3.29}$$

$$E_x(x, z) = -iA_1 \frac{1}{\omega\epsilon_0\epsilon_2} k_1 e^{i\beta x} e^{k_1 z} \tag{1.3.30}$$

$$E_z(x, z) = -A_1 \frac{\beta}{\omega\epsilon_0\epsilon_2} e^{i\beta x} e^{k_1 z} \tag{1.3.31}$$

$k_i, i = 1, 2$ is the component of the wave vector in the z direction.
The equations (1.3.22..1.3.25) in the case of TM polarization insure the continuity of H_y and ϵE_z, and E_x at the interface, which in turn yields

$$A_1 = A_2 \tag{1.3.32}$$

$$\frac{k_2}{\epsilon_2} = -\frac{k_1}{\epsilon_1}. \tag{1.3.33}$$

The surface plamson polaritons are waves that are confined at the interface separating the two materials. The confinement can be seen in (1.3.26,1.3.29) from the facts that $\mathrm{Im}(k_i)$ is too mall compare to $\mathrm{Re}(k_i)$ (waves are not propagative) and $\mathrm{Re}(k_i) > 0$ (exponential decay). We deduce from 1.3.33, that $Re(\epsilon_1) > 0$ if $\epsilon_2 > 0$. This fact confirms the observations of physicists that the surface waves exist only at interfaces when the dielectric permittivities of two materials have real parts opposite signs. The expression for H_y has to fulfill the wave equation (1.3.18), yielding

$$k_i^2 = \beta^2 - k_0^2 \epsilon_i \tag{1.3.34}$$

The equation (1.3.34) combined with the equation (1.3.33) gives us the dispersion relation of surface plasmon polaritons propagating at the interface between the dielectric and the metal.

$$\beta = k_0 \sqrt{\frac{\epsilon_1 \epsilon_2}{\epsilon_1 + \epsilon_2}} \tag{1.3.35}$$

Considering now the TE polarization, using the equations (1.3.19,1.3.20,1.3.21), we obtain

For $z > 0$

$$E_y(x,z) = A_2 e^{i\beta x} e^{-k_2 z} \tag{1.3.36}$$

$$H_x(x,z) = -iA_2 \frac{1}{\omega\mu_0} k_2 e^{i\beta x} e^{-k_2 z} \tag{1.3.37}$$

$$H_z(x,z) = A_2 \frac{\beta}{\omega\mu_0} e^{i\beta x} e^{-k_2 z} \tag{1.3.38}$$

For $z < 0$

$$E_y(x,z) = A_1 e^{i\beta x} e^{k_1 z} \tag{1.3.39}$$

$$H_x(x,z) = iA_1 \frac{1}{\omega\mu_0} k_1 e^{i\beta x} e^{k_1 z} \tag{1.3.40}$$

$$H_z(x,z) = A_1 \frac{\beta}{\omega\mu_0} e^{i\beta x} e^{k_1 z} \tag{1.3.41}$$

The continuity of E_y, H_z and H_x at the interface implies

$$A_1 = A_2 \tag{1.3.42}$$

$$A_1(k_1 + k_2) = 0 \tag{1.3.43}$$

The confinement of the fields at the interface $z = 0$ requires that $\mathrm{Re}(k_i) > 0$ which is fulfilled only if $A_2 = A_1 = 0$. Consequently, surface plasmon polaritons do not exist under TE polarization, they only occur under TM polarization.

Dispersion relations

We consider the dispersion relation (1.3.35). We assume that $\epsilon_1(\omega)$ obey to the Drude model. For the sake of simplicity we further suppose that the metal has a zero damping, that is

$$\epsilon_1(\omega) = 1 - \frac{\omega_p^2}{\omega^2}.$$

The plots of the constant (1.3.35) for an air/metal interface with $\epsilon_2 = 1$ are given in Figure 1.3. We deduce from the dispersion relation (1.3.35) that

For $\omega > \omega_p$, and $\omega < \frac{\omega_p}{\sqrt{1+\epsilon_2}}$, the propagation constant β is real. Otherwise, β is purely imaginary.

For $\frac{\omega_p}{\sqrt{1+\epsilon_2}} < \omega < \omega_p$, β is purely imaginary and thus in this zone, there is no propagation at the interface.

Therefore the radiation into the metal occurs in the transparency regime $\omega > \omega_p$ whereas the surface plasmon polaritons excitations correspond to the part of the dispersion curves lying under the light line. Thus, special phase-matching techniques such as grating or prism coupling are required for their excitation.

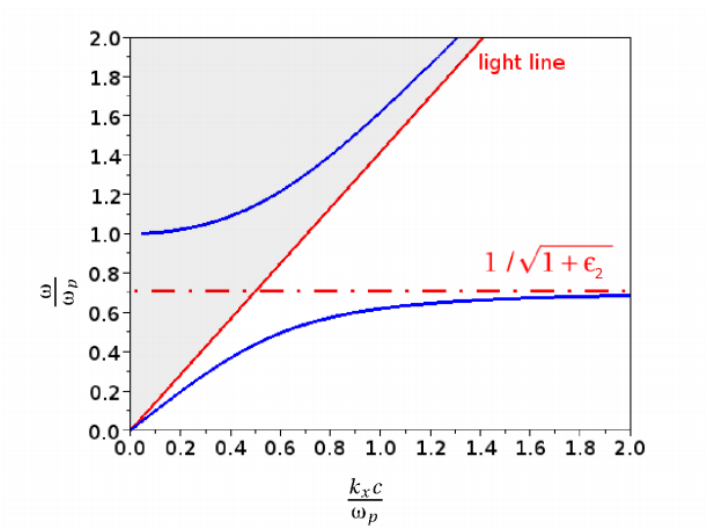

Figure 1.3: Dispersion of surface plasmons polatitons (blue lline) and light line (red line). Here ω is normalized to the plasma frequency ω_p , the real part of β is the continuous curve and its imaginary part is the broken one.

Penetration depth in real metals

When the metal is real, the dielectric and the propagation constants ϵ_1 and β respectively are complex numbers. The real part of β determines the physical wavelength λ_{spp} of the surface plasmon polariton

$$\mathrm{Re}(\beta) = \frac{2\pi}{\lambda_{spp}} \tag{1.3.44}$$

while the imaginary part of β controls the plasmonic losses during propagation. The distance at which the SPP intensity falls by a factor of $\frac{1}{e}$ is called the propagation length L_{spp}, and is given by

$$L_{spp} = \frac{1}{2\mathrm{Im}(\beta)}. \tag{1.3.45}$$

Due to strong confinement at the boundary between the two materials, surface plasmon ploaritons are called evanescent waves, i.e the amplitude of their electromagnetic field decays exponentially along normal direction to the surface both in the metal and in the dielectric layers. It is described by the penetration depth in both metal and dielectric $L_{z,i}$

$$L_{z,i} = \frac{1}{2\mathrm{Re}(k_i)}. \tag{1.3.46}$$

In order to quantify the huge confinement of surface plasmon polaritons , we give some examples at a silver/air interface: for $\lambda_0 = 450nm$, $L_{z,2} = 180nm$; and for $\lambda_0 = 1.5\mu m$, $L_{z,2} = 2.6\mu m$ [**?**].

Excitation of surface plasmon polaritons at planar interfaces

We can observe in Figure 1.3 that the surface plasmon polaritons dispersion curve is located under the light cone. It will therefore never be possible to excite the surface plasmon directly with a light wave from the air. There are, however, several methods for coupling the surface plasmon with light excitation. A plane wave which impinges on the interface with an angle of incidence θ can only excite a mode whose wavevector along the x direction matches $k_0 \sin\theta$. As the wavevector of the SPP is greater than the one of the incident light, one needs to find ways to increase the wavevector of the incident wave to match that of the surface plasmon polariton.

Prism coupling In 1968 Otto proposed a first approach for coupling photons to surface plasmons using a prism of refractive index $n > 1$ [18]. The total reflection of the incoming light with an incident angle θ as shown in Figure 1.4 gives rise to an evanescent wave at the back of the prism with a wavevector $k = nk_0 \sin\theta$. Thus, the wavevector of the evanescent wave is

increased compared to the initial plane wave one. Which can excite a surface plasmon polariton on a metallic surface facing the prism. The prism is placed at a distance less than the wavelength to the metallic surface, i.e. at a distance smaller than the decay of the evanescent wave. The control of the relative positions of the prism and the metallic surface seems to be difficult. Kretschmann [19] then proposed a very similar but simpler configuration to put in place because it no longer requires the control of the distance between the prism and the surface. The excitation of the surface plasmon is made by illuminating a prism on which the metal is directly deposited in the form of a thin film. The surface plasmon polariton is then excited on the side which is not in contact with the prism as shown in Figure 1.4.

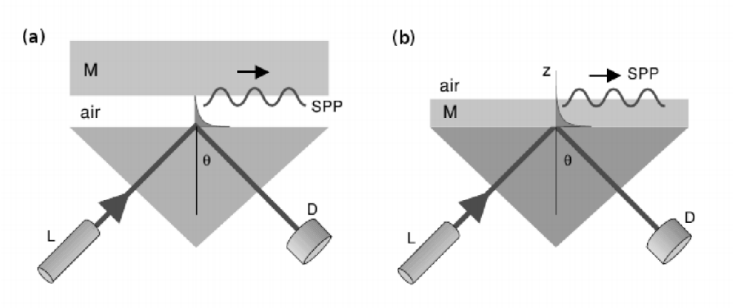

Figure 1.4: Experimental set -up to excite Surface plasmon polaritons: in (a) the Otto configuration and in (b) the Kretschmann configuration [20]

Grating coupling. An other way of coupling the surface plasmon polaritons with light is to use gratings. The wavevector of the incident light is increased via periodic metallic grating whose periodicity d induces a pseudo momentum $m\frac{2\pi}{d}$ parallel to the interface, with m is the order of diffraction. This pseudo momentum is added to the momentum of light $k_0 \sin\theta$ to equal the momentum β of surface plasmon polariton. More generally, each time the following condition

$$\beta = \pm k_0 \sin\theta + m\frac{2\pi}{d} \tag{1.3.47}$$

is fulfilled, a surface plasmon polariton mode is excited. The surface plasmon polariton excitations by a plane wave impinging with an incidence angle θ correspond to the intersections of the dispersion branches of the different modes with the light cone as shown in the Figure 1.5.

Generally, any rough surface may contribute to the coupling of the surface plasmon polaritons with light.

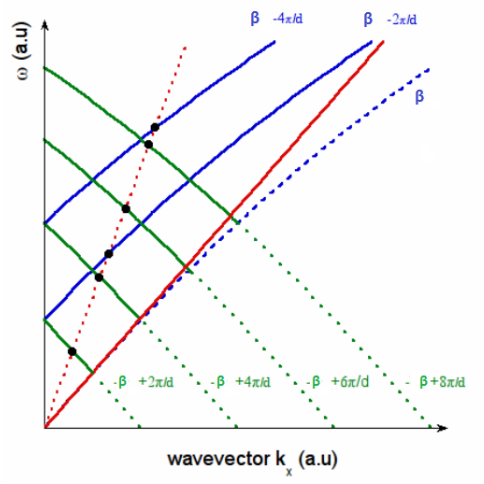

Figure 1.5: Dispersion curve of the SPP surface modes of a grating (blue and green lines). Modes which can be excited by TM polarized light are in solid lines whereas the modes which cannot are in dashed lines. The red curves represent the light line (solid line) and the dispersion curve of a plane wave impinging with an angle θ of pulsation ω (dashed line). The modes excited by a plane wave impinging with an angle θ of pulsation ω are indicated by black dots.

1.3.3 Subwavelength grating

Metallic gratings are one of the most used techniques in applications to couple directly an incident plane wave and plasmonic surface modes. But the particularity of the used gratings is that the amplitude of the groove is of the order of magnitude of the wavelength of the incident electromagnetic field. This specificity creates an additional cavity resonance contributing to more localization and confinement of the electromagnetic wave inside the groove itself. Hessel and Oliner were the first to theoretically investigate electromagnetic resonances in such subwavelength structures [21], they estimate that deep grooves of metallic subwavelength gratings may support additional modes to the surface modes. The additional modes consist in a Fabry-Perot-like resonance of a propagative electromagnetic wave guided in the groove. Many studies after were conducted in the same context by T. Lopez-Rios and A. Wirgin [22, 23, 5, 6]. An experimental confirmation of the thesis of Hessel and Oliner was observed later in [24]. Finally, two kinds of resonances are ooccuring in the subwavelength metallic gratings : waveguide or cavity modes and surface plasmon polaritons (SPP). One of the objective of this thesis is to study how the cavity modes can be coupled with surface waves.

Chapter 2

Asymptotic of resonances of a real metallic plane perturbed by a subwavelength rectangular cavity

Sommaire

2.1 Introduction **25**
2.2 Formulation of the problem **28**
2.2.1 Notations 28
2.2.2 Problem Formulation 28
2.3 Integral representation **30**
2.3.1 The Green function in the half-space $\mathbb{R}^2_+$ 30
2.3.2 The Green function in the rectangular cavity . . . 32
2.3.3 Integral equations 36
2.4 Asymptotics **37**
2.4.1 Asymptotic of G_i 37
2.4.2 Asymptotic of G_e 53
2.4.3 Asymptotic of $S(w, k)$ 57
2.4.4 Asymptotic of resonant frequencies 58

2.1 Introduction

Optical micro-cavities are structures that can confine light in a small spot, where the size of the spot is on the order of the optical wavelength. The local amplification of the fields near the aperture can be strikingly high, sometimes

up to a factor 10^6. They are especially useful to enhance light-matter interactions, since light can be strongly localized in the micro-cavities. Optical micro-cavities have found many applications, including integrated optical circuits, low-threshold lasers, low-power switches, adiabatic wavelength conversion, etc. Other applications include spectroscopy and imaging: For instance, commercial devices for detection of single homoglobin proteins based on local enhancement of optical fields are already on the market [25]. Modeling and numerical simulations are essential in the design and optimization of micro-cavities for various applications.

In mathematical terms, the localization and concentration of the fields is the mark of a resonance phenomenon. In our context, the corresponding resonant field may be surface plasmons, i.e., waves that propagate along the interface of the grating, and that decay exponentially away from it. Another type of resonance is due to possible cavity modes. Thus, the study of these phenomena pertains to eigenvalue problems for the solutions of the Maxwell system, in geometric configurations where a dielectric (generally air) and a metal are separated by an infinite rough interface.

We are interested in metallic surfaces that contain rectangular grooves, which have been studied experimentally in [3, 1]. Our objective is to understand the role played by the rugosity of the surfaces in the creation of resonant modes. The case of planar devices with rectangular cavities is particularly interesting. On the one hand, they can be manufactured with controlled precision by current lithographic processes at the appropriate scales, and are widely used in opto-electronics. On the other hand, their simple geometry allows one to develop the mathematical analysis very far. Experimental results suggest that the amplification factors of the fields depend on the width of the cavities. In [5], the case of a half plane containing a single cavity of width w was considered. The authors studied the asymptotic of the Green function as $w \to 0$ using techniques based on integral representation [4, 5, 26], which are well adapted to such geometry. The limiting Green function turns out to be that of an infinite half plane on which a dipole is placed.

The paper [6] extended the analysis of [5] to two sub-wavelength cavities separated by a sub-wavelength distance, and studied the interaction between the cavities. The authors obtained the localization of two types of cavity resonances, the symmetric and anti-symmetric in a small neighborhood of each zero of some explicit function, associated to the limiting geometry. For the symmetric modes, the fields in the cavities interact in phase, and the system of two cavities essentially acts as a dipole. In the anti-symmetric case, the fields oscillate in anti-phase, and the system behaves like a quadripole.

In this chapter, we would like to study the resonances of a single sub-wavelength rectangular cavity in the case where the metal is real. A first step will be to consider the case of a single cavity in a half plane, when an impedance boundary condition is imposed instead of a homogeneous Neumann condition for a perfect metal. An impedance boundary condition on the interface is an intermediate regime between the perfect and real metal. The open problem of deriving the adequate radiation conditions in unbounded domain with impedance boundary condition is solved recently by J-C Nédélec and al. [27].

Due to geometrical considerations and to the choice of a time harmonic incident field [3, 5], the scattering problem can be reduced to a Helmholtz equation. Using the Green formula we reformulate the Helmholtz equation as a system of integral equations defined on the aperture of the of the cavity. The formalism of integral equations naturally leads itself to asymptotic analysis, as the width w of the cavity tends to 0 while the wavelength is fixed. Using an operator version of the Rouché theorem, we are able derive the asymptotic of the resonant frequencies $k_n(w)$ of our system.

The outline of the chapter is as follows. Section 2 describes the scattering problem. In section 3, an integral representation of the solution to the diffraction problem. We reduce the Helmholtz equation in the unbounded diffraction domain to a linear system of integral equations on the aperture of the cavity (2.3.10). By rescaling the obtained integral equation we show that the resonances are exactly the zeros of a given operator valued function $S(w, k)$.

Section 4 is devoted to the asymptotic expansion of kernel of $S(w, k)$. Using the fact that this latter kernel is the sum of Green functions in simple geometries we obtain the asymptotic behavior of $S(w, k)$ as w tends to zero through the nontrivial asymptotic expansions of these Green functions (Theorem 8 and Corollary 9).

Finally, we derive the asymptotic expansion of the resonances $k_n(\omega)$ by using the Generalized Rouché Theorem and the properties of the integral operators appearing in the asymptotic of $S(w, k)$ (Theorem 10).

2.2 Formulation of the problem

2.2.1 Notations

We consider the geometry shown in Figure 1 to study the scattering of electromagnetic waves by an optical device, that contains a small subwavelength cavity. The scattering domain (the air above the device) is invari-

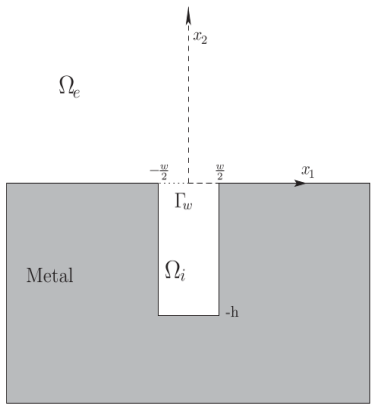

Figure 2.1: The diffracting domain Ω

ant in the x_3-direction and has the form $\Omega \times \mathbb{R}$. Its cross-section Ω consists of the union of the upper-half plane $\Omega_e = \mathbb{R}^2_+$ and of the open cavity $\Omega_i = (-h, 0] \times (-w, w)$, of width $2w$ and depth h. We denote by $\Gamma_w \times \{x_2 = 0\} = (-w, w) \times \{x_2 = 0\}$ the aperture of the cavity, and by $X = (x_1, x_2)$ a point in $\mathbb{R}^2$.

2.2.2 Problem Formulation

We assume that Ω is filled with a homogeneous dielectric material of magnetic permeability μ, and electric permittivity ε. The time-dependent, linear Maxwell equations take the form

$$\begin{aligned} \nabla \times \mathbf{E} + \mu \frac{\partial \mathbf{H}}{\partial t} &= 0 \quad \text{in } \Omega \times \mathbb{R} \times \mathbb{R}_+, \\ \nabla \times \mathbf{H} - \varepsilon \frac{\partial \mathbf{E}}{\partial t} &= 0 \quad \text{in } \Omega \times \mathbb{R} \times \mathbb{R}_+, \end{aligned}$$

where $\mathbf{E} \in \mathbb{R}^3$ and $\mathbf{H} \in \mathbb{R}^3$ respectively denote the electric and magnetic fields. In this paper we only consider time-harmonic solutions, i.e., special solutions of the form

$$\mathbf{E}(x,t) = Re(E(x)e^{-i\omega t}) \quad \text{and} \quad \mathbf{H}(x,t) = Re(H(x)e^{-i\omega t}),$$

where ω denotes the time pulsation and the complex fields $E(x)$ and $H(x)$ satisfy

$$\nabla \times E - i\omega\mu H = 0, \tag{2.2.1}$$

$$\nabla \times H + i\omega\varepsilon E = 0. \tag{2.2.2}$$

Since the open cavity is deposited on a real thick conducting medium the electric field satisfies on $\partial\Omega \times \mathbb{R}$ the following impedance boundary condition:

$$\mathbf{n} \times (\nabla \times H) - i\omega\sqrt{\varepsilon\mu}\,\beta H = 0, \tag{2.2.3}$$

where $\mathbf{n} = (n, 0)$, the quantity n is the outward normal vector on $\partial\Omega$ and and $\beta > 0$ is the relative surface impedance that only depends on the electric permittivity of the metal.

The diffraction of (time harmonic) incident fields E^{inc}, H^{inc} by the surface $\partial\Omega$ gives rise to reflected and scattered fields. We write

$$\begin{aligned} E &= E^{inc} - E^{ref} + E^s, \\ H &= H^{inc} + H^{ref} + H^s, \end{aligned}$$

where E^{ref} and H^{ref} are the electromagnetic fields generated by the reflection of the incident fields by the whole plane interface without the cavity.

Since the scattering domain is unbounded, we require that the scattered fields (E^s, H^s) satisfy radiation conditions that fix the behavior of the solution at infinity. The impedance boundary conditions produce surface waves propagating along the interface that can not be separated from the total field. Hence, the scattered field does not verify the classical Sylver-Müller radiation condition. Nédélec and al. have obtained recently a new type of radiation conditions that describe well the behavior of the scattered fields close and far away from the boundary.

As in [3], we focus on the transverse magnetic polarization (TM), where the magnetic field is transverse to the invariant dimension. In this case, $H^s = (0, 0, H_3(x_1, x_2))$ and the x_3-component of the magnetic field verifies the Helmholtz equation

$$\Delta H_3(X) + k^2 H_3(X) = 0, \qquad X \in \Omega,$$

with $k = \omega\sqrt{\varepsilon\mu}$. As in [3], the impedance boundary approximation (2.2.3) can be formulated as follows:

$$\frac{\partial H_3}{\partial n} + ik\beta H_3 = f \qquad X \in \partial\Omega,$$

where $f = -(\frac{\partial}{\partial n} + ik\beta)(H_3^{inc} + H_3^{ref})$. Since E^{ref} and H^{ref} are the reflected fields by the plane interface, we have $f = 0$ on $\partial\Omega_e \setminus \Gamma_w$, and hence

$f \in \widetilde{H}^{-\frac{1}{2}}(-w,w) = \left(H^{-\frac{1}{2}}(-w,w)\right)'$ (see for instance [5]).

The scattered fields (E^s, H^s) satisfy radiation conditions developed in [27]: For large r and a fixed $\alpha \in (0, \frac{1}{2})$,

$$\begin{cases} |\dfrac{\partial H_3^s}{\partial r} - ikH_3^s| & < & cr^{\alpha-1}, & \text{for} & y > cr^{\alpha} \\ |\dfrac{\partial H_3^s}{\partial r} - ik\sqrt{1+\beta^2}H_3^s| & < & cr^{-\frac{1}{2}}, & \text{for} & cr^{\alpha-1} < y < cr^{\alpha} \\ |\dfrac{\partial H_3^s}{\partial r} - ik\sqrt{1+\beta^2}H_3^s| & < & cr^{\alpha-1}, & \text{for} & y < cr^{\alpha-1} \end{cases}$$

where (r, θ) are the polar coordinates, that is $x = r\cos\theta$ and $y = r\sin\theta$.

The whole system is reduced to a Helmholtz equation, as the components of E can be recovered from H_3 by (2.2.2).

The scattering resonances are the values of $k \in \mathbb{C}$ such that the previous system satisfied by H_3, has a non trivial solution with f is identically zero. The asymptotic expansion of the scattering resonances is derived in Theorem 10.

2.3 Integral representation

In this section, we aim to obtain an integral representation of the field H^s. To do so we need to first determine the Green functions of the Helmholtz equation inside and outside the rectangular cavity.

2.3.1 The Green function in the half-space $\mathbb{R}^2_+$

Let $G_e(k, X, Y)$ be the Green function of the Helmholtz equation with impedance boundary condition in the half space $\mathbb{R}^2_+$.

Here the source point $Y = (y_1, y_2)$ is fixed in Ω_e with y_1 is the horizontal coordinate and y_2 is the vertical one. Also when k is fixed and if there's no confusion, we simply denote $G_e(X, Y)$ instead of $G_e(k; X, Y)$.

Since there is no horizontal variation in the geometry of the problem, we can suppose without loss of generality that $y_1 = 0$. $G_e(k; X, Y)$ is the solution of the boundary value problem:

$$\begin{cases} \Delta G_e(x_1, x_2; 0, y_2) + k^2 G_e(x_1, x_2; 0, y_2) & = & \delta(x_1)\delta(x_2 - y_2), & X \in \Omega_e \\ -\dfrac{\partial G_e}{\partial x_2} + ik\beta G_e & = & 0, & x_2 = 0 \end{cases}$$

Considering the fact that Ω_e is invariant in the horizontal direction, and taking the Fourier transform with respect to x_1, we get the following differential equation (with initial condition) in the vertical variable x_2:

$$\begin{cases} \dfrac{\partial^2 \widehat{G_e}}{\partial x_2^2}(\xi, x_2; 0, y_2) + (k^2 - \xi^2)\widehat{G_e}(\xi, x_2; 0, y_2) & = \frac{\delta(x_2 - y_2)}{\sqrt{2\pi}}, & x_2 > 0 \\ -\dfrac{\partial \widehat{G_e}}{\partial x_2} + ik\beta\widehat{G_e} & = 0, & x_2 = 0 \end{cases}$$

A particular solution of the diffrential equation above is given by:

$$g_p = -\frac{e^{-\sqrt{\xi^2-k^2}|x_2-y_2|}}{2\sqrt{\xi^2-k^2}\sqrt{2\pi}}$$

The solution of the homogeneous equation has the form:

$$g_h = \alpha e^{\sqrt{\xi^2-k^2}\,x_2} + \eta e^{-\sqrt{\xi^2-k^2}x_2}$$

The physical solutions of this equation are those which are bounded at infinity. So we keep only the following homogenous solutions:

$$g_h = \eta e^{-\sqrt{\xi^2-k^2}\,x_2}$$

Hence, the general solution is:

$$\widehat{G_e} = \eta e^{-\sqrt{\xi^2-k^2}\,x_2} - \frac{e^{-\sqrt{\xi^2-k^2}|x_2-y_2|}}{2\sqrt{\xi^2-k^2}\sqrt{2\pi}}$$

and $-\frac{\partial \widehat{G_e}}{\partial x_2} = \sqrt{\xi^2-k^2}\eta e^{-\sqrt{\xi^2-k^2}\,x_2} + \frac{e^{-\sqrt{\xi^2-k^2}|x_2-y_2|}}{2\sqrt{2\pi}}$.

The condition $-\frac{\partial \widehat{G_e}}{\partial x_2}(x_2 = 0) + ik\beta\widehat{G_e}(x_2 = 0) = 0$ implies that:

$$\eta = -\frac{(\sqrt{\xi^2-k^2} - ik\beta)e^{-\sqrt{\xi^2-k^2}y_2}}{\sqrt{8\pi}\sqrt{\xi^2-k^2}(\sqrt{\xi^2-k^2} + ik\beta)}$$

Thus:

$$\widehat{G_e} = \frac{1}{\sqrt{8\pi}}\left(-\frac{\sqrt{\xi^2-k^2} - ik\beta}{\sqrt{\xi^2-k^2} + ik\beta}\,\frac{e^{-\sqrt{\xi^2-k^2}(x_2+y_2)}}{\sqrt{\xi^2-k^2}} - \frac{e^{-\sqrt{\xi^2-k^2}|x_2-y_2|}}{\sqrt{\xi^2-k^2}}\right).$$

$\widehat{G_e}$ is called the spectral Green's function.

Using the inverse Fourier Transform, the spatial Green function has the expression:

$$G_e(x_1, x_2; y_1, y_2) =$$
$$\frac{1}{4\pi}\int_{-\infty}^{+\infty}\left(-\frac{\sqrt{\xi^2-k^2}-ik\beta}{\sqrt{\xi^2-k^2}+ik\beta}\,\frac{e^{-\sqrt{\xi^2-k^2}(x_2+y_2)}}{\sqrt{\xi^2-k^2}}-\frac{e^{-\sqrt{\xi^2-k^2}|x_2-y_2|}}{\sqrt{\xi^2-k^2}}\right)e^{-i(x_1-y_1)\xi}d\xi. \tag{2.3.1}$$

In the previous expression, we have taken the general case $y_1 \neq 0$.

2.3.2 The Green function in the rectangular cavity

Let $Y = (y_1, y_2)$ be the source point fixed in Ω_i. Let $G_i(w, k; X, Y)$ be the Green function of the Helmholtz equation with impedance boundary condition in the rectangular cavity. If there is no confusion, we simply denote $G_i(X, Y)$ instead of $G_i(w, k; X, Y)$.

Assume that k^2 is not an eigenvalue of the Helmholtz equation with impedance boundary condition. The Green function $G_i(X, Y)$ satisfies:

$$\begin{cases} \Delta G_i(X,Y) + k^2 G_i(X,Y)) &= \delta(X-Y) \qquad X \in \Omega_i \\ \partial_{n_i} G_i + ik\beta G_i &= 0, \qquad X \in \partial\Omega_i/\Gamma_w \\ \partial_{n_i} G_i - ik\beta G_i &= 0, \qquad X \in \Gamma_w \end{cases}$$

Where n_i denotes the outward normal vector to $\partial\Omega_i$, $X = (x_1, x_2)$ and $Y = (y_1, y_2)$.

Next, we proceed by separation of variables to derive a spectral decomposition of the Green function. We first determine a complete set of eigenvectors in $L^2(-w, w)$ associated to a 1d Helmholtz equation with impedance boundary condition.

Let $v_n(x_1) \in H^1(-w, w)$ et $k_{1,n} \in \mathbb{C}_+$ be such that

$$\begin{cases} v_n''(x_1) + k_{1,n}^2 v_n(x_1) &= 0, \qquad x_1 \in]-w, w[\\ v_n'(w) + ik\beta v_n(w) &= 0 \\ -v_n'(-w) + ik\beta v_n(-w) &= 0 \end{cases} \tag{2.3.2}$$

Then $v_n(x_1)$ can be written in the following form

$$v_n(x_1) = \alpha e^{ik_{1,n}x_1} + \eta e^{-ik_{1,n}x_1}$$

The boundary condition gives the following relation:

$$\alpha = -\eta \frac{-k_{1,n} + k\beta}{k_{1,n} + k\beta} e^{-2ik_{1,n}w}$$

Therefore, the eigenvector $v_n(x_1)$ is given by:

$$v_n(x_1) = \kappa_n \left(\frac{k_{1,n} - k\beta}{k_{1,n} + k\beta} e^{-2ik_{1,n}w} e^{ik_{1,n}x_1} + e^{-ik_{1,n}x_1} \right)$$

where $\kappa_n \in \mathbb{C}$ is a normalization constant that will be choosen later, and $k_{1,n}$ verifies this dispersion relation:

$$e^{-2ik_{1,n}w} = \tau_n \frac{k\beta + k_{1,n}}{k\beta - k_{1,n}} \tag{2.3.3}$$

where $\tau_n = \pm 1$. Hence

$$v_n(x_1) = \kappa_n \left(-\tau_n e^{ik_{1,n}x_1} + e^{-ik_{1,n}x_1} \right) \tag{2.3.4}$$

We can easily check that $-k\beta$ and $k\beta$ are not eigenvalues of the problem in order to ensure that $(k_{1,n} + k\beta)$ and $(-k_{1,n} + k\beta)$ are different from zero. In fact, if $-k\beta$ is an eigenvalue, then

$$v_n(x_1) = \alpha e^{-ik\beta x_1} + \eta e^{ik\beta x_1}$$

On the other hand the equalities

$$v_n'(w) + ik\beta v_n(w) = 0 \qquad \text{and} \qquad -v_n'(-w) + ik\beta v_n(-w) = 0$$

imply respectively that $\eta = 0$ and $\alpha = 0$. So $v_n(x_1) = 0$, which contradicts the fact that v_n is an eigenvector. The same analysis also applies to the value $k\beta$.

We further choose the complex number κ_n such that v_n becomes real. Let $\kappa(s)$ be a fixed complex function that satisfies $\kappa(-1) = \frac{1}{2}$ and $\kappa(1) = -\frac{1}{2i}$. We set

$$\kappa_n = \kappa(\tau_n)$$

According to this choice of normalization, we get

$$v_n(x_1) = \begin{cases} \cos(k_{1,n}x_1) & \text{if} \quad \tau_n = -1 \\ \sin(k_{1,n}x_1) & \text{if} \quad \tau_n = 1 \end{cases}$$

We choose the indexing of $k_{1,n}$ by:

$$\tau_n = \begin{cases} -1 & \text{if} \quad n \text{ is even} \\ +1 & \text{if} \quad n \text{ is odd} \end{cases}$$

this choice is justified in the part of "asymptotic of $k_{1,n}$". Then, we obtain that:

$$v_n(x_1) = \cos(k_{1,n}x_1 + \frac{n\pi}{2}). \tag{2.3.5}$$

Proposition 1. *Let $k_{1,n}$ be the eigenvalues of (2.3.2) associated to the eigenfunction $v_n(x_1)$ defined by (2.3.5). Then*

$$\begin{aligned} Re(k_{1,n}^2) &= \frac{\int_{-w}^{w} |v_n'|^2}{\int_{-w}^{w} |v_n|^2} \\ Im(k_{1,n}^2) &= k\beta \frac{|v_n|^2(w) + |v_n|^2(-w)}{\int_{-w}^{w} |v_n|^2} > 0 \end{aligned}$$

Proof. We proceed by multiplying the equation (2.3.2) by $\overline{v_n}$ and integrating by parts to obtain the result. □

Remark 2. *The eigenvalues $k_{1,n}$ are not real because the spectral problem (2.3.2) is not self-adjoint. We observe that $k_{1,n}$ become real and coincide with the Neumann eigenvalues if $\beta = 0$.*

Proposition 3. *Let $k_{1,n}$ be the eigenvalues of (2.3.2) associated to the eigenfunction $v_n(x_1)$ defined by (2.3.5). Then*

$$\int_{-w}^{w} v_n v_m = \begin{cases} 0 & \text{if} \quad n \neq m \\ \int_{-w}^{w} v_n^2 \neq 0 & \text{if} \quad n = m \end{cases}$$

Proof. We proceed by multiplying the equation (2.3.2) by v_m and integrating by parts to find the result. □

Lemma 2.3.1. *There exists w_0, such that for $w < w_0$ the set $(v_n)_n$ is a complete set of $L^2(]-w, w[)$.*

Proof. The proof is based on the asymptotic expansion of the eigenfunctions v_n as w tends to zero. In fact we will prove later in section 2.4 that v_n converge uniformly to the Fourier basis (subsection Asymptotic of $v_n(wx)$). □

Now, we reconstruct $g(\lambda; x_2, y_2)$, the Green function of the 1d Helmholtz equation with impedance boundary condition on $(-h, 0)$. For $x_2 \neq y_2$, we have

$$\begin{cases} g''(x_2) + \lambda^2 g(x_2) = \delta(x_2 - y_2), \qquad x_2 \in]-h, 0[\\ g'(0) - ik\beta g(0) = 0 \\ -g'(-h) + ik\beta g(-h) = 0 \end{cases} \tag{2.3.6}$$

We first look for a function $\varphi^-(x_2)$ solution to the Helmholtz equation in $(-h, 0)$ satisfying the impedance boundary condition at $-h$, that is:

$$\begin{cases} \varphi^{-\prime\prime}(x_2) + \lambda^2\varphi^-(x_2) &= 0, \qquad x_2 \in]-h, 0[\\ -\varphi^{-\prime}(-h) + ik\beta\varphi^-(-h) &= 0 \end{cases}$$

Then

$$\varphi^-(x_2) = e^{i\lambda x_2} + \frac{\lambda - k\beta}{\lambda + k\beta} e^{-2i\lambda h} e^{-i\lambda x_2}$$

Afterwards, we seek a function $\varphi^+(x_2)$ solution to the Helmholtz equation in $(-h, 0)$ satisfying the impedance boundary condition at 0, that is:

$$\begin{cases} \varphi^{+\prime\prime}(x_2) + \lambda^2\varphi^+(x_2) &= 0, \qquad x_2 \in]-h, 0[\\ \varphi^{+\prime}(0) - ik\beta\varphi^+(0) &= 0 \end{cases}$$

We similarly find

$$\varphi^+(x_2) = e^{i\lambda x_2} + \frac{\lambda - k\beta}{\lambda + k\beta} e^{-i\lambda x_2}$$

The Green function g is then given by

$$g(\lambda^2; x_2, y_2) = \frac{1}{W(y_2)} \begin{cases} \varphi^+(x_2)\varphi^-(y_2), & \text{if} \quad y_2 \leq x_2 \\ \varphi^+(y_2)\varphi^-(x_2), & \text{if} \quad y_2 \geq x_2 \end{cases}$$

where $W(y_2)$ is the Wronskian of φ^+ and φ^- at $x_2 = y_2$, that means

$$\begin{aligned} W(y_2) &= (\varphi^+)'(y_2)\varphi^-(y_2) - (\varphi^-)'(y_2)\varphi^+(y_2) \\ &= 2i\lambda \frac{\lambda - k\beta}{\lambda + k\beta} \left(e^{-2i\lambda h} - 1\right) \end{aligned}$$

So,

$$\begin{aligned} g(\lambda^2; x_2, y_2) = \frac{1}{2i\lambda(e^{-2i\lambda h} - 1)} \{ & \frac{\lambda + k\beta}{\lambda - k\beta} e^{i\lambda(x_2+y_2)} + e^{-2i\lambda h} e^{i\lambda|x_2-y_2|} + e^{-i\lambda|x_2-y_2|} \\ & + \frac{(\lambda - k\beta)}{(\lambda + k\beta)} e^{-2i\lambda h} e^{-i\lambda(x_2+y_2)} \} \end{aligned} \tag{2.3.7}$$

Using Lemma (2.3.1) and Proposition (3), we obtain

$$G_i(X, Y) = \sum_{n=0}^{\infty} \frac{v_n(x_1)v_n(y_1)}{\int_{-w}^{w} v_n^2} g(k^2 - k_{1,n}^2; x_2, y_2) \tag{2.3.8}$$

2.3.3 Integral equations

We recall that the scattered field satisfies

$$\begin{cases} \Delta H^s(X) + k^2 H^s(X) &= 0, \qquad X \in \Omega \\ \dfrac{\partial H^s}{\partial n} + ik\beta H^s &= f, \qquad X \in \partial\Omega \end{cases} \tag{2.3.9}$$

Let $Y = (y_1, y_2) \in \Omega_e \cup \Omega_i$. If we multiply the latter system by G_e and integrate over Ω_e we obtain:

$$H^s(Y)\chi_{\Omega_e}(Y) = \int_{\Gamma_w} \left(\frac{\partial H^s}{\partial x_2}(x_1, 0) - ik\beta H^s(x_1, 0) \right) G_e(x_1, 0; Y) d\sigma(x_1) \\ - \int_{\partial\Omega_e \setminus \Gamma_w} f(X) G_e(X; Y) d\sigma(X)$$

And if we multiply the previous equality by G_i and integrate over Ω_i, we obtain:

$$H^s(Y)\chi_{\Omega_i}(Y) = - \int_{\Gamma_w} \left(\frac{\partial H^s}{\partial x_2}(x_1, 0) - ik\beta H^s(x_1, 0) \right) G_i(x_1, 0; Y) d\sigma(x_1) \\ - \int_{\partial\Omega_i \setminus \Gamma_w} f(X) G_i(X; Y) d\sigma(X)$$

Taking the limit $Y \to \Gamma_w$ and adding the two previous equations, we obtain the following integral equation:

$$\int_{\Gamma_w} \left(\frac{\partial H^s}{\partial x_2}(x_1, 0) - ik\beta H^s(x_1, 0) \right) \left(G_i(x_1, 0; y_1, 0) + G_e(x_1, 0; y_1, 0) \right) d\sigma(x_1) \\ = - \int_{\partial\Omega_i \setminus \Gamma_w} f(X) G_i(X; y_1, 0) d\sigma(X) + \int_{\partial\Omega_e \setminus \Gamma_w} f(X) G_e(X; y_1, 0) d\sigma(X). \tag{2.3.10}$$

We further rescale the above equation. Let $\Gamma = (-1, 1)$, and consider the integral operator $S(w, k) : \widetilde{H}^{-\frac{1}{2}}(-1, 1) \to H^{-\frac{1}{2}}(-1, 1)$ defined by

$$S(w, k)\phi(x) := \int_{\Gamma} \left(G_i(wz, 0; wy_1, 0) + G_e(wz, 0; wy_1, 0) \right) \phi(z) d\sigma(z) \tag{2.3.11}$$

We finally have the following integral equation:

$$S(w, k) \left(\frac{\partial H^s}{\partial x_2}(wx_1, 0) - ik\beta H^s(wx_1, 0) \right) \\ = -w^{-1} \left(\int_{\partial\Omega_i \setminus \Gamma_w} f(X) G_i(X; wy_1, 0) d\sigma(X) + \int_{\partial\Omega_e \setminus \Gamma_w} f(X) G_e(X; wy_1, 0) d\sigma(X) \right) \tag{2.3.12}$$

Following the works [5, 6], it can be shown that the plasmonic resonances are exactly the zeros of $S(w,k)$.

The objective of the next section is to derive the asymptotic expansion of $S(w,k)$ when w tends to zero.

2.4 Asymptotics

2.4.1 Asymptotic of G_i

In this section we aim to determine the asymptotic expansion of $G_i(wx_1, 0; wy_1, 0)$ when w tends to zero. The spectral decomposition of G_i is given by:

$$G_i(X,Y) = \sum_{n=0}^{\infty} \frac{v_n(x_1)v_n(y_1)}{\int_{-w}^{w} v_n^2} g(k^2 - k_{1,n}^2; x_2, y_2) \tag{2.4.1}$$

$$G_i(wx_1, 0; wy_1, 0) = \sum_{n=0}^{\infty} \frac{v_n(wx_1)v_n(wy_1)}{\int_{-w}^{w} v_n^2} g(k^2 - k_{1,n}^2; 0, 0)$$

Asymptotic of $k_{1,n}$

Recall that the eigenvalues $k_{1,n}$ verify this dispersion relation (2.3.3):

$$e^{-4ik_{1,n}w} = \frac{(k_{1,n} + k\beta)^2}{(-k_{1,n} + k\beta)^2}$$

We apply the following change of variables $t_n(w) = k_{1,n}(w)w$, and find that $t_n(w)$ is solution of:

$$e^{-4it} = \frac{(t + k\beta w)^2}{(-t + k\beta w)^2}$$

which leads us to define two functions

$$\begin{cases} f_{1,w}(t) &= (t + k\beta w)e^{2it} - (k\beta w - t) \\ f_{2,w}(t) &= (t + k\beta w)e^{2it} + (k\beta w - t) \end{cases}$$

We note $\{t_{1,n}(w),\, n \in I_1\}$ and $\{t_{2,n}(w),\, n \in I_2\}$ the roots of $f_{1,w}(t)$ and $f_{2,w}(t)$ over $\mathbb{C}$ respectively.

Thus

$$\{t_n(w),\, n \in I\} = \{t_{1,n}(w),\, n \in I_1\} \cup \{t_{2,n}(w),\, n \in I_2\},$$

with $I = I_1 \cup I_2$. We now introduce two following functions:

$$\begin{cases} f_{1,0}(t) &= te^{2it} + t \\ f_{2,0}(t) &= te^{2it} - t \end{cases}$$

Similarly, we note $\{t_{1,n}(0)\}$ and $\{t_{2,n}(0)\}$ the roots of $f_{1,0}(t)$ and $f_{2,0}(t)$ over $\mathbb{C}$ respectively.

A simple calculation shows that:

$$\begin{aligned} \{t_{1,n}(0),\, n \in \mathbb{Z}\} &= \{\frac{(2n+1)\pi}{2}, \qquad n \in \mathbb{Z}\} \\ \{t_{2,n}(0),\, n \in \mathbb{Z}\} &= \{n\pi, \qquad n \in \mathbb{Z}\} \end{aligned}$$

We further consider the following indexation

$$\begin{aligned} t_{1,n}(0) &= \frac{(2n+1)\pi}{2} \\ t_{2,n}(0) &= n\pi \end{aligned}$$

If we note $t_n(0) = \frac{n\pi}{2}$, we obtain

$$\{t_n(0),\, n \in \mathbb{Z}\} = \{t_{1,n}(0),\, n \in \mathbb{Z}\} \cup \{t_{2,n}(0),\, n \in \mathbb{Z}\}$$

Then

$$t_{1,n}(0) = t_{2n+1}(0) = \frac{(2n+1)\pi}{2};\ t_{2,n}(0) = t_{2n}(0) = n\pi$$

Remark 4. *$\forall i = 1, 2 : f_{i,w}$ and $f_{i,0}$ are analytic over $\mathbb{C}$, therefore the sets $\{t_{i,n}(w),\, n \in I_i\}$ and $\{t_{i,n}(0),\, n \in \mathbb{Z}\}$ are discrete.*

In order to derive the asymptotic of $k_{1,n}$ when w shrinks to zero, we will first determine the asymptotic of $t_n(w)$. We first localize $\{t_n(w),\, n \in I\}$ in the complex plane.

Let

$C(0, R)$ be the ring in the complex plane centered at the origin with radius R.
$D(0, R)$ be the open disk in the complex plane centered at the origin with radius R.
$D'(0, R)$ the closed disk in the complex plane centered at the origin with radius R.

Proposition 5. *$\forall\, R > 0$ such that $C(0,R) \cap \{t_n(0),\, n \in \mathbb{Z}\} = \emptyset$, $\exists\, w_0$ such that $\forall w < w_0$ and $i = 1, 2$, we have*

$$card\{D'(0,R) \cap \{t_{i,n}(0),\, n \in \mathbb{Z}\}\} = card\{D'(0,R) \cap \{t_{i,n}(w),\, n \in I_i\}\}$$

Hence

$$card\{D'(0,R) \cap \{t_n(0),\, n \in \mathbb{Z}\}\} = card\{D'(0,R) \cap \{t_n(w),\, n \in I\}\}$$

Proof. We first remark that $f_{i,0}$, $i = 1, 2$ is analytic. Therefore

$$\frac{1}{2i\pi}\int_{C(0,R)} \frac{\partial_t f_{i,0}(t)}{f_{i,0}(t)} dt = card\left\{D'(0,R) \cap \{t_{i,n}(0),\, n \in \mathbb{Z}\}\right\}$$

and

$$\frac{1}{2i\pi}\int_{C(0,R)} \frac{\partial_t f_{i,w}(t)}{f_{i,w}(t)} dt = card\left\{D'(0,R) \cap \{t_{i,n}(w),\, n \in I_i\}\right\}$$

On the other hand the function $\dfrac{\partial_t f_{i,w}(t)}{f_{i,w}(t)}$ converges uniformly on each compact subset of the complex plane that does not contain any isolated zero of $f_{i,0}$, to $\dfrac{\partial_t f_{i,0}(t)}{f_{i,0}(t)}$.

Consequently

$$\lim_{w \to 0} \frac{1}{2i\pi}\int_{C(0,R)} \frac{\partial_t f_{i,w}(t)}{f_{i,w}(t)} dt = \frac{1}{2i\pi}\int_{C(0,R)} \frac{\partial_t f_{i,0}(t)}{f_{i,0}(t)} dt$$

Thus $\exists\, w_0$ such as $\quad \forall w < w_0$

$$card\{D'(0,R) \cap \{t_n(0),\, n \in \mathbb{Z}\}\} = card\{D'(0,R) \cap \{t_n(w),\, n \in I\}\}$$

□

In the rest of this section, we will fix a radius R as specified in the previous proposition. Let t varies in $D(0,R)$. We note I_R an indexation of the roots $\{t_n(0),\, n \in \mathbb{Z}\}$ contained in $D(0,R)$, .i.e,

$$\{D'(0,R) \cap \{t_n(0),\, n \in \mathbb{Z}\}\} = \{t_n(0),\, n \in I_R\}$$

Likewise, we note $I_{R,i}$ an indexation of the roots $\{t_{i,n}(0),\, n \in \mathbb{Z}\}$ contained in $D(0,R)$, .i.e,

$$\{D'(0,R) \cap \{t_{i,n}(0),\, n \in \mathbb{Z}\}\} = \{t_{i,n}(0),\, n \in I_{R,i}\}$$

So, we have

$$card(I_R) = card(I_{R,1}) \cup card(I_{R,2})$$

$card\{D'(0,R)\cap\{t_n(0),\, n\in\mathbb{Z}\}\} = card\{D'(0,R)\cap\{t_n(w),\, n\in I\}\} = card(I_R)$

and

$card\{D'(0,R)\cap\{t_{i,n}(0),\, n\in\mathbb{Z}\}\} = card\{D'(0,R)\cap\{t_{i,n}(w),\, n\in I_i\}\} = card(I_{R,i})$

for $i=1,2$.

Proposition 6. *$\exists w_1$ small enough such that $\forall w < w_1 < w_0$, $\forall\, i = 1,2$, $\forall\, n\in I_{R,i}$: $\exists r_{n,i} > 0$ such that $D'(t_{i,n}(0), r_{n,i})\cap\{t_m(0),\, m\in I\} = \{t_{i,n}(0)\}$, and there exists a unique zero of $f_{i,w}(t)$ contained in $D'(t_{i,n}(0), r_{n,i})$. For this zero we will choose the same index as $t_{i,n}(0)$.*

Then

$$D'(t_{i,n}(0), r_{n,i})\cap\{t_{i,m}(w),\, m\in I_i\} = \{t_{i,n}(w)\}$$

Proof. We have

$$\frac{1}{2i\pi}\int_{C(t_{i,n}(0),r_{n,i})}\frac{\partial_t f_{i,0}(t)}{f_{i,0}(t)}dt = 1$$

and $\dfrac{\partial_t f_{i,w}(t)}{f_{i,w}(t)}$ converges uniformly on each compact subset that does not contain any isolated zero of $f_{i,0}$, to $\dfrac{\partial_t f_{i,0}(t)}{f_{i,0}(t)}$. So, there exists $w_{1_{i,n}}$ small enough such that for $w < w_{1_{i,n}} < w_0$

$$\frac{1}{2i\pi}\int_{C(t_{i,n}(0),r_{n,i})}\frac{\partial_t f_{i,w}(t)}{f_{i,w}(t)}dt = 1$$

and we can take w_1 the minimum of $\{w_{1_{i,n}},\, i=1,2,\, n\in I_{R,i}\}$. □

The last result allows us to use the following notation for $t_n(w)$ in analogy with the $t_n(0)$:

$$t_{1,n}(w) = t_{2n+1}(w)$$
$$t_{2,n}(w) = t_{2n}(w)$$

Now, consider the following result which will allow us to compute the asymptotic of $t_n(w)$:

$$t_{i,n}(w) - t_{i,n}(0) = \frac{1}{2i\pi}\int_{C(t_{i,n}(0),r_{n,i})}(t - t_{i,n}(0))\frac{\partial_t f_{i,w}(t)}{f_{i,w}(t)}dt$$

For $i=1$, we have $t_{1,n}(0) = \dfrac{(2n+1)\pi}{2}$, $\dfrac{e^{-it}}{\sin(t)}$ doesn't vanish on $D(0, r_{n,1})$, so $t_{1,n}(w)$ is also the unique zero of $\dfrac{e^{-it}}{2\sin(t)}f_{1,w}(t)$ on $D(0, r_{n,1})$, and we have

$$t_{1,n}(w) - t_{1,n}(0) = \frac{1}{2i\pi}\int_{C(t_{1,n}(0),r_{n,1})}(t - t_{1,n}(0))\frac{\partial_t \frac{e^{-it}}{2\sin(t)}f_{1,w}(t)}{\frac{e^{-it}}{2\sin(t)}f_{1,w}(t)}dt$$

$f_{1,w}(t) = (t + k\beta w)e^{2it} - (k\beta w - t)$ and $\dfrac{e^{-it}}{2\sin(t)} f_{1,w}(t) = t\dfrac{\cos t}{\sin(t)} + iwk\beta.$

We note $\widetilde{f_{1,0}}(t) = t\dfrac{\cos t}{\sin(t)}$. Then

$$t_{1,n}(w) - t_{1,n}(0) = \frac{1}{2i\pi}\int_{C(t_{1,n}(0),r_{n,1})} (t - t_{1,n}(0))\frac{\partial_t \widetilde{f_{1,0}}(t)}{\widetilde{f_{1,0}}(t) + wk\beta i} dt$$

On the other-hand

$$\frac{\partial_t \widetilde{f_{1,0}}(t)}{\widetilde{f_{1,0}}(t) + wk\beta i} = \frac{\partial_t \widetilde{f_{1,0}}(t)}{\widetilde{f_{1,0}}(t)(1 + \frac{wk\beta i}{\widetilde{f_{1,0}}(t)})} = \frac{\partial_t \widetilde{f_{1,0}}(t)}{\widetilde{f_{1,0}}(t)} \sum_{p=0}^{\infty} \left(\frac{-wk\beta i}{\widetilde{f_{1,0}}(t)}\right)^p$$

and also $\widetilde{f_{1,0}(t)} \equiv \partial_t \widetilde{f_{1,0}}(t_{1,n}(0))(t - t_{1,n}(0))$, therefore

$$t_{1,n}(w) - t_{1,n}(0) =$$

$$\frac{1}{2i\pi}\int_{C(t_{1,n}(0),r_{n,1})} \sum_{p=0}^{\infty} \frac{\partial_t \widetilde{f_{1,0}}(t)}{(t - t_{1,n}(0))^p (\partial_t \widetilde{f_{1,0}}(t_{1,n}(0)))^{p+1}} (-wk\beta i)^p dt$$

$$= \frac{1}{2i\pi} \sum_{p=0}^{\infty} \int_{C(t_{1,n}(0),r_{n,1})} \frac{\partial_t \widetilde{f_{1,0}}(t)}{(t - t_{1,n}(0))^p (\partial_t \widetilde{f_{1,0}}(t_{1,n}(0)))^{p+1}} (-wk\beta i)^p dt$$

$$= \frac{1}{2i\pi} \sum_{p=0}^{\infty} \int_{C(t_{1,n}(0),r_{n,1})} \frac{\partial_t \widetilde{f_{1,0}}(t)}{(t - t_{1,n}(0))^p} dt \frac{(-wk\beta i)^p}{(\partial_t \widetilde{f_{1,0}}(t_{1,n}(0)))^{p+1}}$$

On the other hand

$$\partial_t \widetilde{f_{1,0}}(t) = \sum_{m=0}^{\infty} \alpha_m (t - t_{1,n}(0))^m$$

with $\alpha_m = \dfrac{\widetilde{f_{1,0}}^{(m+1)}(t_{1,n}(0))}{m!}$, and by applying the Residue theorem, we find that:

$$t_{1,n}(w) - t_{1,n}(0) = \sum_{p=0}^{\infty} \frac{\alpha_{p-1}}{(\partial_t \widetilde{f_{1,0}}(t_{1,n}(0)))^{p+1}} (-wk\beta i)^p$$

$$t_{1,n}(w) = \frac{(2n+1)\pi}{2} + \sum_{p=0}^{\infty} \frac{\alpha_{p-1}(-ik\beta)^p}{(\partial_t \widetilde{f_{1,0}}(t_{1,n}(0)))^{p+1}} w^p.$$

We will compute α_m, $\alpha_m = \dfrac{\widetilde{f_{1,0}}^{(m+1)}(t_{1,n}(0))}{m!}$

$$\begin{cases} \alpha_{2m-1} &= -2m\frac{2^{2m}(2^{2m}-1)B_{2m}}{(2m)!(2m-1)!} \\ \\ \alpha_{2m} &= -(2n+1)\frac{\pi}{2}\ \frac{2^{2(m+1)}(2^{2(m+1)}-1)B_{2(m+1)}}{(2m)!(2(m+1))!} \end{cases}$$

and,

$$(\partial_t \widetilde{f_{1,0}}(t_{1,n}(0))) = -(2n+1)\frac{\pi}{2}$$

For $i = 2$,

we have $t_{2,n}(0) = n\pi$, $\dfrac{e^{-it}}{\cos(t)} \neq 0$ on $D(0, r_{n,2})$, so $t_{2,n}(w)$ is also the unique zero of $\dfrac{e^{-it}}{2\cos(t)} f_{1,w}(t)$ on $D(0, r_{n,2})$, and

$$t_{2,n}(w) - t_{2,n}(0) = \frac{1}{2i\pi}\int_{C(t_{2,n}(0),r_{n,2})} (t - t_{2,n}(0))\frac{\partial_t \frac{e^{-it}}{2\cos(t)} f_{2,w}(t)}{\frac{e^{-it}}{2\cos(t)} f_{2,w}(t)} dt$$

$f_{2,w}(t) = (t + k\beta w)e^{2it} + (k\beta w - t)$, $\dfrac{e^{-it}}{2\cos(t)} f_{2,w}(t) = it\dfrac{\sin t}{\cos(t)} + wk\beta$

We note $\widetilde{f_{2,0}}(t) = it\dfrac{\sin t}{\cos(t)}$, and so

$$t_{2,n}(w) - t_{2,n}(0) = \frac{1}{2i\pi}\int_{C(t_{2,n}(0),r_{n,2})} (t - t_{2,n}(0))\frac{\partial_t \widetilde{f_{2,0}}(t)}{\widetilde{f_{2,0}}(t) + wk\beta} dt$$

On the other hand

$$\frac{\partial_t \widetilde{f_{2,0}}(t)}{\widetilde{f_{2,0}}(t) + wk\beta} = \frac{\partial_t \widetilde{f_{2,0}}(t)}{\widetilde{f_{2,0}}(t)(1 + \frac{wk\beta}{\widetilde{f_{2,0}(t)}})} = \frac{\partial_t \widetilde{f_{2,0}}(t)}{\widetilde{f_{2,0}(t)}} \sum_{p=0}^{\infty} \left(\frac{-wk\beta}{\widetilde{f_{2,0}(t)}}\right)^p$$

and also $\widetilde{f_{2,0}(t)} \equiv \partial_t \widetilde{f_{2,0}}(t_{2,n}(0))(t - t_{2,n}(0))$, therefore

$$\begin{aligned} t_{2,n}(w) - t_{2,n}(0) \quad = \\ & \frac{1}{2i\pi}\int_{C(t_{2,n}(0),r_{n,2})} \sum_{p=0}^{\infty} \frac{\partial_t \widetilde{f_{2,0}}(t)}{(t - t_{2,n}(0))^p (\partial_t \widetilde{f_{2,0}}(t_{2,n}(0)))^{p+1}} (-wk\beta)^p dt \\ & \frac{1}{2i\pi}\sum_{p=0}^{\infty}\int_{C(0,r_{n,2})} \frac{\partial_t \widetilde{f_{2,0}}(t)}{(t - t_{2,n}(0))^p (\partial_t \widetilde{f_{2,0}}(t_{2,n}(0)))^{p+1}} (-wk\beta)^p dt \\ & \frac{1}{2i\pi}\sum_{p=0}^{\infty}\int_{C(t_{2,n}(0),r_{n,2})} \frac{\partial_t \widetilde{f_{2,0}}(t)}{(t - t_{2,n}(0))^p} dt \frac{(-wk\beta)^p}{(\partial_t \widetilde{f_{2,0}}(t_{2,n}(0)))^{p+1}} \end{aligned}$$

We have

$$\partial_t \widetilde{f_{2,0}}(t) = \sum_{m=0}^{\infty} \eta_m (t - t_{2,n}(0))^m$$

with $\eta_m = \dfrac{\widetilde{f_{2,0}}^{(m+1)}(t_{2,n}(0))}{m!}$ and by applying again the Residue theorem we find that:

$$t_{2,n}(w) - t_{2,n}(0) = \sum_{p=0}^{\infty} \frac{\eta_{p-1}}{(\partial_t \widetilde{f_{2,0}}(t_{2,n}(0)))^{p+1}} (-wk\beta)^p$$

$$t_{2,n}(w) = n\pi + \sum_{p=0}^{\infty} \frac{\eta_{p-1}(-k\beta)^p}{(\partial_t \widetilde{f_{2,0}}(t_{2,n}(0)))^{p+1}} w^p$$

$$\begin{cases} \eta_{2m-1} &= i2m \dfrac{2^{2m}(2^{2m}-1)B_{2m}}{(2m)!(2m-1)!} \\ \eta_{2m} &= in\pi \frac{2^{2(m+1)}(2^{2(m+1)}-1)B_{2(m+1)}}{(2m)!(2(m+1))!} \end{cases}$$

and

$$\partial_t \widetilde{f_{2,0}}(t_{2,n}(0)) = in\pi$$

Finally

$$\begin{cases} t_{1,n}(w) &= t_{2n+1}(w) = \frac{(2n+1)\pi}{2} + \displaystyle\sum_{p=0}^{\infty} \frac{\alpha_{p-1}(-ik\beta)^p}{(\partial_t \widetilde{f_{1,0}}(t_{1,n}(0)))^{p+1}} w^p \\ \\ t_{2,n}(w) &= t_{2n}(w) = n\pi + \displaystyle\sum_{p=0}^{\infty} \frac{\eta_{p-1}(-k\beta)^p}{(\partial_t \widetilde{f_{2,0}}(t_{2,n}(0)))^{p+1}} w^p \end{cases}$$

$$\begin{aligned} t_n(w) = \frac{n\pi}{2} &+ \sum_{m=0}^{\infty} (-1)^m i (k\beta)^{2m+1} \frac{2^{2(m+1)}(2^{2(m+1)}-1)B_{2(m+1)}}{(2m)!(2(m+1))!} \frac{w^{2m+1}}{(\frac{n\pi}{2})^{2m+1}} \\ &+ \sum_{m=1}^{\infty} (-1)^m (k\beta)^{2m} (2m) \frac{2^{2m}(2^{2m}-1)B_{2m}}{(2m)!(2m-1)!} \frac{w^{2m}}{(\frac{n\pi}{2})^{2m+1}} \end{aligned}$$

We remark that the first terms in the asymptotic expansion of the impedance eigenvalues are the Neumann eigenvalues of the same Helmholtz operator.

Consequently for $n \neq 0$:

$$k_{1,n}(w) = \tag{2.4.2}$$
$$\frac{n\pi}{2w} + \sum_{m=0}^{\infty} (-1)^m \; i \; (\beta)^{2m+1} \; \frac{2^{2(m+1)}(2^{2(m+1)}-1)B_{2(m+1)}}{(2m)!(2(m+1))!} \frac{w^{2m}(k)^{2m+1}}{(\frac{n\pi}{2})^{2m+1}}$$
$$+ \sum_{m=1}^{\infty} (-1)^m \; (\beta)^{2m} \; (2m) \; \frac{2^{2m}(2^{2m}-1)B_{2m}}{(2m)!(2m-1)!} \; \frac{w^{2m-1}(k)^{2m}}{(\frac{n\pi}{2})^{2m+1}}$$

Remark 7. *We remark that* 0 *is a solution to the dispersion relation:*

$$e^{-4ik_{1,n}w} = \frac{(k_{1,n}+k\beta)^2}{(-k_{1,n}+k\beta)^2}$$

So we further denote $k_{1,0} = 0$.

Asymptotic of $g(k^2 - k_{1,n}^2; 0, 0)$

We start by deriving the asymptotic expansion of $g(k^2 - k_{1,n}^2; 0, 0)$ for $n \neq 0$. We deduce from (2.3.7) the following equality:

$$g(\lambda^2; x_2, y_2) =$$
$$\frac{1}{2i\lambda(e^{-2i\lambda h}-1)} \{ \frac{\lambda + k\beta}{\lambda - k\beta} e^{i\lambda(x_2+y_2)} + e^{-2i\lambda h} e^{i\lambda|x_2-y_2|} + e^{-i\lambda|x_2-y_2|}$$
$$+ \frac{(\lambda - k\beta)}{(\lambda + k\beta)} e^{-2i\lambda h} e^{-i\lambda(x_2+y_2)} \}$$

Hence

$$\begin{aligned} g(\lambda^2; 0, 0) &= \frac{1}{2i\lambda(e^{-2i\lambda h}-1)} \left(\frac{\lambda + k\beta}{\lambda - k\beta} + e^{-2i\lambda h} + 1 + \frac{(\lambda - k\beta)}{(\lambda + k\beta)} e^{-2i\lambda h} \right) \\ &= \frac{1}{i(e^{-2i\lambda h}-1)} \left(e^{-2i\lambda h} \frac{1}{(\lambda + k\beta)} + \frac{1}{\lambda - k\beta} \right) \end{aligned}$$

$$g(k^2 - k_{1,n}^2; 0, 0) =$$
$$\frac{1}{i(e^{-2i\sqrt{k^2-k_{1,n}^2}h}-1)} \left(\frac{e^{-2i\sqrt{k^2-k_{1,n}^2}h}}{(\sqrt{k^2-k_{1,n}^2}+k\beta)} + \frac{1}{\sqrt{k^2-k_{1,n}^2}-k\beta} \right)$$

Now, we fix the branch cut defining the complex square root used in the previous expression:

$$\forall z \in \mathbb{C} \setminus i\mathbb{R}^+ \quad \sqrt{z} = e^{\ln|z| + i\arg(z)}$$

Where, $\arg(z)$ is the continuous determination of the argument in the complex plane minus the non-negative imaginary axis defined as follows:

$$\begin{array}{rcccl} \arg & : & \mathbb{C}\setminus i\mathbb{R}^+ & \to & (\frac{-3\pi}{2},\frac{\pi}{2}) \\ & & z & \mapsto & t \quad \textit{such that} \quad |z|\,e^{it}=z \end{array}$$

So, according to this determination of the square root we have: $\sqrt{-1}=-i$ and $\sqrt{1}=1$.

We remark that $\mathrm{Re}(k^2-k_{1,n}(w)^2)\neq 0$.

Then

$$\sqrt{k^2-k_{1,n}(w)^2}=-i\sqrt{k_{1,n}(w)^2-k^2}$$

and consequently

$$g(k^2-k_{1,n}^2;0,0)=$$
$$\frac{1}{i(e^{-2\sqrt{(k_{1,n}^2-k^2)}h}-1)}\left(e^{-2\sqrt{(k_{1,n}^2-k^2)}h}\frac{1}{(-i\sqrt{k_{1,n}^2-k^2}+k\beta)}+\frac{1}{-i\sqrt{k_{1,n}^2-k^2}-k\beta}\right)$$

In order to calculate $g(k^2-k_{1,n}^2;0,0)$, we need to consider $\sqrt{k_{1,n}(w)^2-k^2}$. We have from (2.4.2) that for $n\neq 0$:

$$k_{1,n}(w)=\frac{n\pi}{2w}+\sum_{p=1}^{\infty}C_p\ w^{p-1}\ k^p$$

So, the square of $k_{1,n}(w)$ has the following asymptotic expansion

$$\begin{aligned} k_{1,n}(w)^2 &= \left(\frac{n\pi}{2w}+\sum_{p=1}^{\infty}C_p\ w^{p-1}\ k^p\right)^2 \\ &= (\frac{n\pi}{2w})^2+(\frac{n\pi C_1k}{w})+(C_1k)^2+(n\pi C_2k^2)+O(w) \end{aligned}$$

Hence

$$\begin{aligned} k_{1,n}(w)^2-k^2 &= (\frac{n\pi}{2w})^2+(\frac{n\pi C_1k}{w})-k^2+(C_1k)^2+(n\pi C_2k^2)+O(w) \\ &= (\frac{n\pi}{2w})^2\left(1+4\frac{C_1k}{n\pi}w+4\frac{-k^2+(C_1k)^2+n\pi C_2k^2}{(n\pi)^2}w^2+O(w^3)\right) \end{aligned}$$

A forward calculation gives

$$\sqrt{k_{1,n}(w)^2-k^2} = (\frac{n\pi}{2w})\left(1+2\frac{C_1k}{n\pi}w+\frac{16k^2(-{C_1}^2-1+C_1+n\pi C_2)}{8(n\pi)^2}w^2+O(w^3)\right)$$

Then, $\forall p \in \mathbb{N}$

$$e^{-2\sqrt{k_{1,n}(w)^2-k^2}h} = e^{-2h\frac{n\pi}{2w}}O(1) = o(w^p),$$

and consequently

$$e^{-2\sqrt{(k_{1,n}^2-k^2)}h}\frac{1}{(i\sqrt{k_{1,n}^2-k^2}+k\beta)} = o(w^p)O(w) = o(w^p),$$

and

$$\frac{1}{i(e^{-2\sqrt{(k_{1,n}^2-k^2)}h}-1)} = -\frac{1}{i}\frac{1}{1-o(w^p)} = -\frac{1}{i}+o(w^p).$$

On the other hand

$$\frac{1}{-i\sqrt{k_{1,n}^2-k^2}-k\beta} =$$

$$= \frac{-2w}{in\pi} - 4k\frac{C_1-i\beta}{i(n\pi)^2}w^2 + 2k^2\frac{6{C_1}^2+2-2C_1-2n\pi C_2-8iC_1\beta-4\beta^2}{i(n\pi)^3}w^3 + O(w^4)$$

Therefore

$$g(k^2-k_{1,n}^2;0,0) =$$
$$\frac{-2}{n\pi}w - 4k\frac{C_1-i\beta}{(n\pi)^2}w^2 + 2k^2\frac{6{C_1}^2+2-2C_1-2n\pi C_2-8iC_1\beta-4\beta^2}{(n\pi)^3}w^3 + O(w^4)$$

We finally deduce from (2.4.2) that:

$$C_1 = \frac{2i\beta}{n\pi} \quad and \quad C_2 = \frac{-16\beta^2}{(n\pi)^3}$$

and the expansion of $g(k^2-k_{1,n}^2;0,0)$ is

$$g(k^2-k_{1,n}^2;0,0) =$$
$$\frac{-2}{n\pi}w - 4k\frac{2i\beta-i\beta n\pi}{(n\pi)^3}w^2 + 2k^2\left(\frac{8\beta^2}{(n\pi)^5}+\frac{16\beta^2-4i\beta}{(n\pi)^4}+\frac{2-4\beta^2}{(n\pi)^3}\right)w^3 + O(w^4) \tag{2.4.3}$$

Asymptotic of $v_n(wx)$

We deduce from (2.3.5) that

$$v_n(wx) = \cos(wk_{1,n}x + \frac{n\pi}{2})$$

In order to derive the asymptotic expansion of $v_n(wx)$, we will use the already known expansion of $k_{1,n}$. From (2.4.2), we have that for $n \neq 0$:

$$wk_n(w) = \frac{n\pi}{2} + \sum_{p=1}^{\infty} C_p \; w^p \; k^p$$

Hence

$$v_n(wx) = cos(\frac{n\pi}{2} + \frac{n\pi}{2}x + x\sum_{p=1}^{\infty} C_p \; w^p \; k^p) = \cos(\frac{n\pi}{2}(1+x) + x\sum_{p=1}^{\infty} C_p \; w^p \; k^p)$$

After a long calculation, we find for $n \neq 0$:

$$\begin{aligned} v_n(wx) &= \cos(\frac{n\pi}{2}(1+x)) - \sin(\frac{n\pi}{2}(1+x))xC_1(wk) \\ -\sin(\frac{n\pi}{2}(1+x))xC_2(wk)^2 - \frac{1}{2}\cos(\frac{n\pi}{2}(1+x))x^2{C_1}^2(wk)^2 &+ o((wk)^2). \end{aligned} \tag{2.4.4}$$

Asymptotic of $v_n(wx)v_n(wy)$

Let

$$\begin{aligned} R_n(x,y) &= \cos(\frac{n\pi}{2}(1+x))\cos(\frac{n\pi}{2}(1+y)) \\ T_n(x,y) &= \cos(\frac{n\pi}{2}(1+x))\sin(\frac{n\pi}{2}(1+y)) \\ Q_n(x,y) &= \sin(\frac{n\pi}{2}(1+x))\sin(\frac{n\pi}{2}(1+y)). \end{aligned}$$

Using the previous asymptotic expansion (2.4.4), we obtain that for $n \neq 0$:

$$v_n(wx)v_n(wy) = \begin{cases} R_n(x,y) - \frac{2\beta iy}{n\pi}T_n(x,y)(wk) - \frac{2\beta ix}{n\pi}T_n(x,y)(wk) \\ -\frac{4\beta^2 xy}{(n\pi)^2}Q_n(x,y)xy(wk)^2 + \frac{2\beta^2 y^2}{(n\pi)^2}R_n(x,y)(wk)^2 \\ +\frac{16\beta^2 y}{(n\pi)^3}T_n(x,y)(wk)^2 + \frac{2\beta^2 x^2}{(n\pi)^2}R_n(x,y)(wk)^2 \\ +\frac{16\beta^2 x}{(n\pi)^3}T_n(x,y)(wk)^2 + o((wk)^2). \end{cases} \tag{2.4.5}$$

Asymptotic of $\int_{-w}^{w} {v_n}^2(x)dx$

We first recall that for $n \neq 0$:

$$\begin{aligned}
\int_{-w}^{w} {v_n}^2(x)dx &= \int_{-w}^{w} \cos^2(k_{1,n}x + \frac{n\pi}{2})dx \\
&= \frac{1}{4}\int_{-w}^{w} e^{2i(k_{1,n}x+\frac{n\pi}{2})} + e^{-2i(k_{1,n}x+\frac{n\pi}{2})}dx \\
&= w + \frac{(e^{2i(k_{1,n}w)} - e^{-2i(k_{1,n}w)})(e^{in\pi} + e^{-in\pi})}{8ik_{1,n}} \\
&= w + \frac{\cos(n\pi)\sin(2k_{1,n}w)}{2k_{1,n}} \\
&= w + \frac{(-1)^n \sin(2k_{1,n}w)}{2k_{1,n}}.
\end{aligned}$$

Again, we recall (2.4.2), for $n \neq 0$: $wk_n(w) = \dfrac{n\pi}{2} + \displaystyle\sum_{p=1}^{\infty} C_p\ w^p\ k^p$.

Thus

$$\sin(2k_{1,n}w) = \sin(n\pi + 2\sum_{p=1}^{\infty} C_p\ w^p\ k^p) = (-1)^n \sin(2\sum_{p=1}^{\infty} C_p\ w^p\ k^p)$$

Therefore

$$\int_{-w}^{w} {v_n}^2(x)dx = w + \frac{\sin(2\sum_{p=1}^{\infty} C_p\ w^p\ k^p)}{2k_{1,n}}$$

Hence

$$\frac{\sin(2\sum_{p=1}^{\infty} C_p\ w^p\ k^p)}{2k_{1,n}} = \frac{w}{n\pi}\frac{\sin(2\sum_{p=1}^{\infty} C_p\ w^p\ k^p)}{1 + \frac{2}{n\pi}\sum_{p=1}^{\infty} C_p\ w^p\ k^p}$$

On the other hand

$$\sin(2\sum_{p=1}^{\infty} C_p\ w^p\ k^p) = 2C_1(wk) + 2C_2(wk)^2 + o((wk)^2)$$

$$\frac{1}{1 + \frac{2}{n\pi}\sum_{p=1}^{\infty} C_p\ w^p\ k^p} = 1 - \frac{2}{n\pi}C_1(wk) + \frac{2}{n\pi}(\frac{2}{n\pi}{C_1}^2 - C_2)(wk)^2 + o((wk)^2)$$

Therefore

$$\frac{\sin(2\sum_{p=1}^{\infty} C_p\ w^p\ k^p)}{1 + \frac{2}{n\pi}\sum_{p=1}^{\infty} C_p\ w^p\ k^p} = 2C_1(wk) + (2C_2 - \frac{4}{n\pi}{C_1}^2)(wk)^2 + o((wk)^2)$$

Consequently

$$\frac{\sin(2\sum_{p=1}^{\infty} C_p\ w^p\ k^p)}{2k_{1,n}} = w\left(\frac{2}{n\pi}C_1(wk) + \frac{2}{n\pi}(C_2 - \frac{2}{n\pi}{C_1}^2)(wk)^2 + o((wk)^2)\right)$$

And so

$$\int_{-w}^{w} {v_n}^2(x)dx = w\left(1+\frac{2}{n\pi}C_1(wk)+\frac{2}{n\pi}(C_2-\frac{2}{n\pi}{C_1}^2)(wk)^2+o((wk)^2)\right)$$

Then, for $n \neq 0$ the following equality

$$\frac{1}{\int_{-w}^{w} {v_n}^2(x)dx} = \frac{1}{w}\left(1-\frac{2}{n\pi}C_1(wk)+o((wk)^2)\right)$$

holds. Finally, we obtain

$$\frac{1}{\int_{-w}^{w} {v_n}^2(x)dx} = \frac{1}{w}\left(1-\frac{4\beta i}{n\pi^2}(wk)+o((wk)^2)\right) \tag{2.4.6}$$

Asymptotic of $\dfrac{g(k^2-k_{1,n}^2;0,0)}{\int_{-w}^{w} {v_n}^2(x)dx}$

We first deduce from (2.3.7) that

$$g(k^2-k_{1,n}^2;0,0) =$$
$$w\left(\frac{-2}{n\pi}-4k\frac{2i\beta-i\beta n\pi}{(n\pi)^3}w+2k^2\left(\frac{8\beta^2}{(n\pi)^5}+\frac{16\beta^2-4i\beta}{(n\pi)^4}+\frac{2-4\beta^2}{(n\pi)^3}\right)w^2+O(w^3)\right)$$

and from (2.4.6), we obtain

$$\frac{1}{\int_{-w}^{w} {v_n}^2(x)dx} = \frac{1}{w}\left(1-\frac{4\beta i}{n\pi^2}(wk)+o((wk)^2)\right)$$

So by multiplying the precedent terms, we find that for $n \neq 0$:

$$\begin{aligned}\frac{g(k^2-k_{1,n}^2;0,0)}{\int_{-w}^{w} {v_n}^2(x)dx} &= \frac{-2}{n\pi}+\frac{4i\beta}{(n\pi)^2}wk \\ &+2\left(\frac{8\beta^2}{(n\pi)^5}+\frac{16\beta^2-4i\beta}{(n\pi)^4}+\frac{2-4\beta^2}{(n\pi)^3}\right)(wk)^2+o(w^2)\end{aligned} \tag{2.4.7}$$

Asymptotic of $\dfrac{v_n(wx)v_n(wy)g(k^2-k_{1,n}^2;0,0)}{\int_{-w}^{w} {v_n}^2(x)dx}$

By multiplying (2.4.5) and (2.4.7), we find

$$\frac{v_n(wx)v_n(wy)g(k^2-k_{1,n}^2;0,0)}{\int_{-w}^{w} {v_n}^2(x)dx} = \tag{2.4.8}$$

$$\begin{cases} \dfrac{-2}{n\pi}R_n(x,y)+\dfrac{4i\beta}{(n\pi)^2}R_n(x,y)(wk)+\dfrac{4\beta iy}{(n\pi)^2}T_n(x,y)(wk) \\ +\dfrac{4\beta ix}{(n\pi)^2}T_n(y,x)(wk)+\dfrac{8\beta^2xy}{(n\pi)^3}Q_n(x,y)xy(wk)^2-\dfrac{4\beta^2y^2}{(n\pi)^3}R_n(x,y)(wk)^2 \\ -\dfrac{32\beta^2y}{(n\pi)^4}T_n(x,y)(wk)^2-\dfrac{4\beta^2x^2}{(n\pi)^3}R_n(x,y)(wk)^2-\dfrac{32\beta^2x}{(n\pi)^4}T_n(y,x)(wk)^2 \\ +2\left(\frac{8\beta^2}{(n\pi)^5}+\frac{16\beta^2-4i\beta}{(n\pi)^4}+\frac{2-4\beta^2}{(n\pi)^3}\right)R_n(x,y)(wk)^2 \\ +\frac{8\beta^2y}{(n\pi)^3}T_n(x,y)(wk)^2+\frac{8\beta^2x}{(n\pi)^3}T_n(y,x)(wk)^2+o(w^2) \end{cases}$$

Asymptotic of $G_i(wx_1,0;wy_1,0)$

Recall the expression

$$G_i(wx_1,0;wy_1,0)=\sum_{n=0}^{\infty}\frac{v_n(wx_1)v_n(wy_1)}{\int_{-w}^{w}v_n^2}g(k^2-k_{1,n}^2;0,0)$$

$$=\frac{v_0(wx_1)v_0(wy_1)}{\int_{-w}^{w}v_0^2}g(k^2-k_{1,0}^2;0,0)+\sum_{n=1}^{\infty}\frac{v_n(wx_1)v_n(wy_1)}{\int_{-w}^{w}v_n^2}g(k^2-k_{1,n}^2;0,0)$$

A first calculation gives

$$\frac{v_0(wx_1)v_0(wy_1)}{\int_{-w}^{w}v_0^2}g(k^2-k_{1,0}^2;0,0)=$$

$$\frac{1}{2wi(e^{-2ikh}-1)}\left(e^{-2ikh}\frac{1}{(k+k\beta)}+\frac{1}{k-k\beta}\right)$$

Then

$$G_i(wx_1,0;wy_1,0) =$$

$$\begin{cases} \frac{1}{2wi(e^{-2ikh}-1)}\left(e^{-2ikh}\frac{1}{(k+k\beta)}+\frac{1}{k-k\beta}\right) \\ +\sum_{n=1}^{\infty}\frac{-2}{n\pi}R_n(x,y)+\sum_{n=1}^{\infty}\frac{4i\beta}{(n\pi)^2}R_n(x,y)(wk) \\ +\sum_{n=1}^{\infty}\frac{4\beta iy}{(n\pi)^2}T_n(x,y)(wk)+\sum_{n=1}^{\infty}\frac{4\beta ix}{(n\pi)^2}T_n(x,y)(wk) \\ +\sum_{n=1}^{\infty}\frac{8\beta^2xy}{(n\pi)^3}Q_n(x,y)xy(wk)^2-\sum_{n=1}^{\infty}\frac{4\beta^2y^2}{(n\pi)^3}R_n(x,y)(wk)^2 \\ -\sum_{n=1}^{\infty}\frac{32\beta^2y}{(n\pi)^4}T_n(x,y)(wk)^2-\sum_{n=1}^{\infty}\frac{4\beta^2x^2}{(n\pi)^3}R_n(x,y)(wk)^2 \\ -\sum_{n=1}^{\infty}\frac{32\beta^2x}{(n\pi)^4}T_n(y,x)(wk)^2+\sum_{n=1}^{\infty}\frac{16\beta^2}{(n\pi)^5}R_n(x,y)(wk)^2 \\ +\sum_{n=1}^{\infty}\frac{32\beta^2-8i\beta}{(n\pi)^4}R_n(x,y)(wk)^2+\sum_{n=1}^{\infty}\frac{4-8\beta^2}{(n\pi)^3}R_n(x,y)(wk)^2 \\ +\sum_{n=1}^{\infty}\frac{8\beta^2y}{(n\pi)^3}R_n(x,y)(wk)^2+\sum_{n=1}^{\infty}\frac{8\beta^2x}{(n\pi)^3}R_n(y,x)(wk)^2+o(w^2) \end{cases}$$

Using the following equalities

$$\sum_{n=1}^{\infty}\frac{\cos(\frac{n\pi}{2}(1+x))\cos(\frac{n\pi}{2}(1+y))}{(n\pi)} =$$
$$\frac{1}{\pi}\left(-\ln(2)-\frac{1}{2}\ln(\left|\sin(\pi\frac{x+y+2}{4})\sin(\pi\frac{x-y}{4})\right|)\right)$$

$$\sum_{n=1}^{\infty}\frac{\cos(\frac{n\pi}{2}(1+x))\cos(\frac{n\pi}{2}(1+y))}{(n\pi)^2} =$$
$$\frac{1}{6}+\frac{1}{32}\left((x+y+2)^2+(x-y)^2\right)-\frac{1}{8}\left(x+y+2+|x-y|\right)$$

$$\sum_{n=1}^{\infty}\frac{\cos(\frac{n\pi}{2}(1+x))\cos(\frac{n\pi}{2}(1+y))}{(n\pi)^4} = \frac{-1}{768}x^4-\frac{1}{184}x^2-\frac{1}{128}x^2y^2-\frac{1}{8}\frac{(x-y)}{|x-y|}(\frac{x^3}{3}-x^2y)$$

$$\sum_{n=1}^{\infty}\frac{\sin(\frac{n\pi}{2}(1+x))\cos(\frac{n\pi}{2}(1+y))}{(n\pi)^3} = \frac{1}{96}x^3+\frac{1}{48}x+\frac{1}{32}xy^2+\frac{1}{2}\frac{(x-y)}{|x-y|}(\frac{x^2}{2}-xy)$$

we obtain

$$G_i(wx_1,0;wy_1,0) =$$

$$\begin{cases} \frac{1}{2wi(e^{-2ikh}-1)}\left(e^{-2ikh}\frac{1}{(k+k\beta)}+\frac{1}{k-k\beta}\right) \\ +\frac{2}{\pi}\left(\ln(2)+\frac{1}{2}\ln(\left|\sin(\pi\frac{x+y+2}{4})\sin(\pi\frac{x-y}{4})\right|)\right) \\ +4i\beta\left(\frac{1}{6}+\frac{1}{32}\left((x+y+2)^2+(x-y)^2\right)-\frac{1}{8}\left(x+y+2+|x-y|\right)\right)(wk) \\ +\sum_{n=1}^{\infty}\frac{4\beta iy}{(n\pi)^2}T_n(x,y)(wk)+\sum_{n=1}^{\infty}\frac{4\beta ix}{(n\pi)^2}T_n(x,y)(wk) \\ +\sum_{n=1}^{\infty}\frac{8\beta^2xy}{(n\pi)^3}Q_n(x,y)xy(wk)^2-\sum_{n=1}^{\infty}\frac{4\beta^2y^2}{(n\pi)^3}R_n(x,y)(wk)^2 \\ -\sum_{n=1}^{\infty}\frac{32\beta^2y}{(n\pi)^4}T_n(x,y)(wk)^2-\sum_{n=1}^{\infty}\frac{4\beta^2x^2}{(n\pi)^3}R_n(x,y)(wk)^2 \\ -\sum_{n=1}^{\infty}\frac{32\beta^2x}{(n\pi)^4}T_n(x,y)(wk)^2+\sum_{n=1}^{\infty}\frac{16\beta^2}{(n\pi)^5}R_n(x,y)(wk)^2 \\ +(32\beta^2-8i\beta)\left(\frac{-1}{768}x^4-\frac{1}{184}x^2-\frac{1}{128}x^2y^2-\frac{1}{8}\frac{(x-y)}{|x-y|}\right)(wk)^2 \\ +\sum_{n=1}^{\infty}\frac{4-8\beta^2}{(n\pi)^3}R_n(x,y)(wk)^2 \\ +8\beta^2y\left(\frac{1}{96}y^3+\frac{1}{48}y+\frac{1}{32}yx^2+\frac{1}{2}\frac{(y-x)}{|x-y|}(\frac{y^2}{2}-xy)\right)(wk)^2 \\ +8\beta^2x\left(\frac{1}{96}x^3+\frac{1}{48}x+\frac{1}{32}xy^2+\frac{1}{2}\frac{(x-y)}{|x-y|}(\frac{x^2}{2}-xy)\right)(wk)^2+o(wk^2) \end{cases}$$

We further denote

$$e(k,\beta)=\frac{1}{2i(e^{-2ikh}-1)}\left(e^{-2ikh}\frac{1}{(k+k\beta)}+\frac{1}{k-k\beta}\right) \tag{2.4.9}$$

Let

$$a_1(\beta,x,y)=4i\beta\left(\frac{1}{6}+\frac{1}{32}\left((x+y+2)^2+(x-y)^2\right)-\frac{1}{8}\left(x+y+2+|x-y|\right)\right)$$
$$+\sum_{n=1}^{\infty}\frac{4\beta iy}{(n\pi)^2}R_n(x,y)+\sum_{n=1}^{\infty}\frac{4\beta ix}{(n\pi)^2}T_n(x,y)$$

$$a_2(\beta,x,y) = \tag{2.4.10}$$

$$\begin{cases} \sum_{n=1}^{\infty}\frac{8\beta^2xy}{(n\pi)^3}Q_n(x,y)xy - \sum_{n=1}^{\infty}\frac{4\beta^2y^2}{(n\pi)^3}R_n(x,y) - \sum_{n=1}^{\infty}\frac{32\beta^2y}{(n\pi)^4}T_n(x,y) \\ -\sum_{n=1}^{\infty}\frac{4\beta^2x^2}{(n\pi)^3}R_n(x,y) - \sum_{n=1}^{\infty}\frac{32\beta^2x}{(n\pi)^4}T_n(x,y) + \sum_{n=1}^{\infty}\frac{16\beta^2}{(n\pi)^5}R_n(x,y) \\ +(32\beta^2-8i\beta)\left(\frac{-1}{768}x^4 - \frac{1}{184}x^2 - \frac{1}{128}x^2y^2 - \frac{1}{8}\frac{(x-y)}{|x-y|}\right) \\ +\sum_{n=1}^{\infty}\frac{4-8\beta^2}{(n\pi)^3}R_n(x,y) + 8\beta^2y\left(\frac{1}{96}y^3 + \frac{1}{48}y + \frac{1}{32}yx^2 + \frac{1}{2}\frac{(y-x)}{|x-y|}(\frac{y^2}{2} - xy)\right) \\ +8\beta^2x\left(\frac{1}{96}x^3 + \frac{1}{48}x + \frac{1}{32}xy^2 + \frac{1}{2}\frac{(x-y)}{|x-y|}(\frac{x^2}{2} - xy)\right) \end{cases}$$

So, we can rewrite G_i as follows

$$\begin{aligned} G_i(wx_1,0;wy_1,0) &= \frac{e(k,\beta)}{w} + \frac{2}{\pi}\left(\ln(2) + \frac{1}{2}\ln(\left|\sin(\pi\frac{x+y+2}{4})sin(\pi\frac{x-y}{4})\right|\right) \\ &\quad +a_1(\beta,x,y)(wk) + a_2(\beta,x,y)(wk)^2 + o((wk)^2) \end{aligned} \tag{2.4.11}$$

2.4.2 Asymptotic of G_e

From (2.3.1) we have that:
$G_e(x_1,x_2;y_1,y_2)$

$$= \frac{1}{4\pi}\int_{-\infty}^{+\infty}\left(-\frac{\sqrt{\xi^2-k^2}-ik\beta}{\sqrt{\xi^2-k^2}+ik\beta}\frac{e^{-\sqrt{\xi^2-k^2}(x_2+y_2)}}{\sqrt{\xi^2-k^2}} - \frac{e^{-\sqrt{\xi^2-k^2}|x_2-y_2|}}{\sqrt{\xi^2-k^2}}\right)e^{-i(x_1-y_1)\xi}d\xi.$$

Then
$G_e(wx_1,0;wy_1,0)$

$$= \frac{1}{4\pi}\int_{-\infty}^{+\infty}\left(-\frac{\sqrt{\xi^2-k^2}-ik\beta}{\sqrt{\xi^2-k^2}+ik\beta}\frac{1}{\sqrt{\xi^2-k^2}} - \frac{1}{\sqrt{\xi^2-k^2}}\right)e^{-i(wx_1-wy_1)\xi}d\xi$$

$$= \frac{1}{4\pi}\int_{-\infty}^{+\infty}-\frac{1}{\sqrt{\xi^2-k^2}}\frac{2\sqrt{\xi^2-k^2}}{\sqrt{\xi^2-k^2}+ik\beta}e^{-i(wx_1-wy_1)\xi}d\xi$$

$$= \frac{1}{4\pi}\int_{-\infty}^{+\infty}\frac{-2}{\sqrt{\xi^2-k^2}+ik\beta}e^{-i(wx_1-wy_1)\xi}d\xi$$

Operating the change of variables $\xi = k\zeta$, we get

$$G_e(wx_1,0;wy_1,0) = \frac{1}{4\pi}\int_{-\infty}^{+\infty}\frac{-2}{\sqrt{\zeta^2-1}+i\beta}e^{-iwk(x_1-y_1)\zeta}d\zeta$$

We further denote

$$\alpha = wk\left|(x_1-y_1)\right|.$$

Then

$$G_e(wx_1,0;wy_1,0)=\frac{1}{4\pi}\int_{-\infty}^{+\infty}\frac{-2}{\sqrt{\zeta^2-1}+i\beta}e^{-i\alpha\zeta}d\zeta$$

Assuming $x_1<y_1$ snd applying the change of variables $\chi=-\zeta$, we find

$$G_e(wx_1,0;wy_1,0)=\frac{-1}{\pi}\int_{0}^{+\infty}\frac{\cos(\alpha\zeta)}{\sqrt{\zeta^2-1}+i\beta}d\zeta$$

To derive the asymptotic expansion of G_e we first calculate the leading terms in the integral defining the Green function. We first have

$$\frac{1}{\sqrt{\zeta^2-1}+i\beta}=\frac{1}{|\zeta|}\frac{1}{\sqrt{1-\frac{1}{\zeta^2}}+i\frac{\beta}{|\zeta|}}$$

Hence

$$\sqrt{1-\frac{1}{\zeta^2}}=1-\frac{1}{2\zeta^2}-\frac{1}{8\zeta^4}+o(\frac{1}{\zeta^4})$$

Then

$$\sqrt{1-\frac{1}{\zeta^2}}+i\frac{\beta}{\zeta}=1+i\frac{\beta}{\zeta}-\frac{1}{2\zeta^2}-\frac{1}{8\zeta^4}+o(\frac{1}{\zeta^4})$$

Therefore

$$\begin{aligned}\frac{1}{\sqrt{1-\frac{1}{\zeta^2}}+i\frac{\beta}{\zeta}} &= \frac{1}{1+i\frac{\beta}{\zeta}-\frac{1}{2\zeta^2}-\frac{1}{8\zeta^4}+o(\frac{1}{\zeta^4})}\\ &= 1-\frac{i\beta}{\zeta}+\frac{1-2\beta^2}{2\zeta^2}+i(\beta^3-\beta)\frac{1}{\zeta^3}+O(\frac{1}{\zeta^4})\end{aligned}$$

Consequently

$$\frac{1}{\sqrt{\zeta^2-1}+i\beta}=\frac{1}{\zeta}-\frac{i\beta}{\zeta^2}+(\frac{1}{2}-\beta^2)\frac{1}{\zeta^3}+i(\beta^3-\beta)\frac{1}{\zeta^4}+O(\frac{1}{\zeta^5})=\sum_{p=1}^{\infty}a_p(\beta)\frac{1}{\zeta^p},$$

which gives

$$\int_0^{+\infty}\frac{\cos(\alpha\zeta)}{\sqrt{\zeta^2-1}+i\beta}d\zeta=\sum_{p=1}^{3}a_p(\beta)\int_1^{+\infty}\frac{\cos(\alpha\zeta)}{\zeta^p}d\zeta$$

$$+\int_0^{+\infty}\left(\frac{1}{\sqrt{\zeta^2-1}+i\beta}-\sum_{p=1}^{3}a_p(\beta)\frac{1}{\zeta^p}1_{\{\zeta>1\}}(\zeta)\right)\cos(\alpha\zeta)d\zeta$$

$$= \int_0^{+\infty} \left(\frac{1}{\sqrt{\zeta^2-1}+i\beta} + (-\frac{1}{\zeta} + \frac{i\beta}{\zeta^2} - (\frac{1}{2}-\beta^2)\frac{1}{\zeta^3})1_{\{\zeta>1\}} \right) \cos(\alpha\zeta)d\zeta$$
$$+ \int_1^{+\infty} \frac{\cos(\alpha\zeta)}{\zeta} d\zeta - i\beta \int_1^{+\infty} \frac{\cos(\alpha\zeta)}{\zeta^2} d\zeta + (\frac{1}{2}-\beta^2) \int_1^{+\infty} \frac{\cos(\alpha\zeta)}{\zeta^2} d\zeta$$

$$= \int_0^{+\infty} \left(\frac{1}{\sqrt{\zeta^2-1}+i\beta} + (-\frac{1}{\zeta} + \frac{i\beta}{\zeta^2} - (\frac{1}{2}-\beta^2)\frac{1}{\zeta^3})1_{\{\zeta>1\}} \right) d\zeta$$
$$- \frac{1}{2} \int_0^{+\infty} \left(\frac{\zeta^2}{\sqrt{\zeta^2-1}+i\beta} + (-\zeta + i\beta - \frac{(\frac{1}{2}-\beta^2)}{\zeta})1_{\{\zeta>1\}} \right) d\zeta\alpha^2 + O(\alpha^4) +$$
$$\int_1^{+\infty} \frac{\cos(\alpha\zeta)}{\zeta} d\zeta - i\beta \int_1^{+\infty} \frac{\cos(\alpha\zeta)}{\zeta^2} d\zeta + (\frac{1}{2}-\beta^2) \int_1^{+\infty} \frac{\cos(\alpha\zeta)}{\zeta^2} d\zeta$$

We have $\int_1^{+\infty} \frac{\cos(\alpha\zeta)}{\zeta} d\zeta = \int_\alpha^{+\infty} \frac{\cos(\zeta)}{\zeta} d\zeta = -C_i(\alpha)$
with $C_i(\alpha)$ is the cosine integral, so we obtain the following expansion:
$$\int_1^{+\infty} \frac{\cos(\alpha\zeta)}{\zeta} d\zeta = -\gamma - \ln(\alpha) - \sum_{n=1}^{\infty} (-1)^n \frac{\alpha^{2n}}{(2n)!(2n)}$$
where γ is the Euler–Mascheroni constant.

More generally the following expansion of the exponential integral holds

$$\int_1^{+\infty} \frac{e^{-i\alpha\zeta}}{\zeta} d\zeta = -\gamma - i\frac{\pi}{2} - \ln(\alpha) - \sum_{n=1}^{\infty} \frac{(-i\alpha)^n}{(n)!(n)}$$

By differentiating the latter expression with respect to α, we find that :
$$\int_1^{+\infty} \frac{e^{-i\alpha\zeta}}{\zeta^2} d\zeta = \frac{1}{3} + i(\gamma + i\frac{\pi}{2})\alpha + i(\ln(\alpha) - \alpha) + i\sum_{n=1}^{\infty} (-i)^n \frac{\alpha^{n+1}}{(n+1)!n}$$
So,
$$\int_1^{+\infty} \frac{\cos(\alpha\zeta)}{\zeta^2} d\zeta = \frac{1}{3} - \frac{\pi}{2}\alpha + i\sum_{n=1}^{\infty} (-i)^{(2n-1)} \frac{\alpha^{2n}}{(2n)!(2n-1)}$$

and
$$\int_1^{+\infty} \frac{e^{-i\alpha\zeta}}{\zeta^3} d\zeta = \frac{1}{4} - \frac{1}{3}i\alpha + \frac{(\gamma + i\frac{\pi}{2})}{2}\alpha^2 - \frac{1}{2}\alpha^2 - \frac{1}{4}\alpha^2 + \frac{\alpha^2}{2}\ln(\alpha) + \sum_{n=1}^{\infty} (-i)^n \frac{\alpha^{n+2}}{(n+2)!n}$$
so,
$$\int_1^{+\infty} \frac{\cos(\alpha\zeta)}{\zeta^3} d\zeta = \frac{1}{4} + (\frac{\gamma}{2} - \frac{3}{4})\alpha^2 + \frac{\alpha^2}{2}\ln(\alpha) + \sum_{n=1}^{\infty} (-1)^n \frac{\alpha^{2n+2}}{(2n+2)!(2n)}$$

Finally, we find

$$\int_0^{+\infty} \frac{\cos(\alpha\zeta)}{\sqrt{\zeta^2-1}+i\beta} d\zeta =$$

$$\int_0^{+\infty} \left(\frac{1}{\sqrt{\zeta^2-1}+i\beta} - (\frac{1}{\zeta} + \frac{i\beta}{\zeta^2} - (\frac{1}{2}-\beta^2)\frac{1}{\zeta^3})1_{\{\zeta>1\}} \right) d\zeta$$

$$-\gamma + \frac{(\frac{1}{2}-\beta^2)}{4} - \frac{i\beta}{3} + i\beta\frac{\pi}{2}\alpha - \ln(\alpha) + (\frac{-1}{8} - \frac{i\beta}{2} + \frac{\gamma}{4} + \frac{3}{4}\beta^2 - \frac{\gamma}{2}\beta^2)\alpha^2$$

$$-\frac{1}{2}\int_0^{+\infty} \left(\frac{\zeta^2}{\sqrt{\zeta^2-1}+i\beta} + (-\zeta + i\beta - \frac{(\frac{1}{2}-\beta^2)}{\zeta})1_{\{\zeta>1\}} \right) d\zeta\alpha^2$$

$$+(\frac{1}{2}-\beta^2)\frac{\alpha^2}{2}\ln(\alpha) + O(\alpha^4)$$

Therefore

$$G_e(wx_1, 0; wy_1, 0) =$$

$$\frac{-1}{\pi}\int_0^{+\infty} \left(\frac{1}{\sqrt{\zeta^2-1}+i\beta} + (-\frac{1}{\zeta} + \frac{i\beta}{\zeta^2} - (\frac{1}{2}-\beta^2)\frac{1}{\zeta^3})1_{\{\zeta>1\}} \right) d\zeta$$

$$+\frac{\gamma}{\pi} - \frac{(\frac{1}{2}-\beta^2)}{4\pi} + \frac{i\beta}{3\pi} - \frac{i\beta}{2}\alpha$$

$$+\frac{\ln(\alpha)}{\pi} - \frac{1}{\pi}(\frac{-1}{8} - \frac{i\beta}{2} + \frac{\gamma}{4} + \frac{3}{4}\beta^2 - \frac{\gamma}{2}\beta^2)\alpha^2$$

$$+\frac{1}{2\pi}\int_0^{+\infty} \left(\frac{\zeta^2}{\sqrt{\zeta^2-1}+i\beta} + (-\zeta + i\beta - \frac{(\frac{1}{2}-\beta^2)}{\zeta})1_{\{\zeta>1\}} \right) d\zeta\alpha^2$$

$$-\frac{1}{\pi}(\frac{1}{2}-\beta^2)\frac{\alpha^2}{2}\ln(\alpha) + O(\alpha^4)$$

$$= \frac{-1}{\pi}\int_0^{+\infty} \left(\frac{1}{\sqrt{\zeta^2-1}+i\beta} + (-\frac{1}{\zeta} + \frac{i\beta}{\zeta^2} - (\frac{1}{2}-\beta^2)\frac{1}{\zeta^3})1_{\{\zeta>1\}} \right) d\zeta$$

$$+\frac{\gamma}{\pi} - \frac{(\frac{1}{2}-\beta^2)}{4\pi} + \frac{i\beta}{3\pi} - \frac{i\beta}{2}wk\,|x_1-y_1| + \frac{\ln(k)}{\pi} + \frac{\ln(|x_1-y_1|)}{\pi}$$

$$+\frac{\ln(w)}{\pi} - \frac{1}{\pi}\left(\frac{-1}{8} - \frac{i\beta}{2} + \frac{\gamma}{4} + \frac{3}{4}\beta^2 - \frac{\gamma}{2}\beta^2\right)(x_1-y_1)^2k^2w^2$$

$$+\frac{1}{2\pi}\int_0^{+\infty} \left(\frac{\zeta^2}{\sqrt{\zeta^2-1}+i\beta} + (-\zeta + i\beta - \frac{(\frac{1}{2}-\beta^2)}{\zeta})1_{\{\zeta>1\}} \right) d\zeta(x_1-y_1)^2k^2w^2$$

$$-\frac{1}{\pi}(\frac{1}{2}-\beta^2)\frac{(x_1-y_1)^2k^2w^2}{2}\ln(k\,|x_1-y_1|) - \frac{1}{\pi}(\frac{1}{2}-\beta^2)\frac{(x_1-y_1)^2k^2w^2}{2}\ln(w)$$

$$+O(w^4)$$

Denote

$$\delta(\beta) = \frac{-1}{\pi}\int_0^{+\infty}\left(\frac{1}{\sqrt{\zeta^2-1}+i\beta} + (-\frac{1}{\zeta}+\frac{i\beta}{\zeta^2}-(\frac{1}{2}-\beta^2)\frac{1}{\zeta^3})1_{\{\zeta>1\}}\right)d\zeta + \frac{\gamma}{\pi} - \frac{(\frac{1}{2}-\beta^2)}{4\pi} + \frac{i\beta}{3\pi} \quad (2.4.12)$$

$$b_2(\beta,k,x,y) = -\frac{1}{\pi}\left(\frac{-1}{8}-\frac{i\beta}{2}+\frac{\gamma}{4}+\frac{3}{4}\beta^2-\frac{\gamma}{2}\beta^2\right)(x_1-y_1)^2 + \frac{1}{2\pi}\int_0^{+\infty}\left(\frac{\zeta^2}{\sqrt{\zeta^2-1}+i\beta} + (-\zeta+i\beta-\frac{(\frac{1}{2}-\beta^2)}{\zeta})1_{\{\zeta>1\}}\right)d\zeta(x_1-y_1)^2 - \frac{1}{\pi}(\frac{1}{2}-\beta^2)\frac{(x_1-y_1)^2}{2}\ln(k\,|x_1-y_1|) \quad (2.4.13)$$

Then G_e can be rewritten as follows

$$G_e(wx_1,0;wy_1,0) = \delta(\beta) + \frac{\ln(|x_1-y_1|)}{\pi} - \frac{i\beta}{2}|x_1-y_1|(wk) + \frac{\ln(wk)}{\pi} + b_2(\beta,k,x,y)(wk)^2 - \frac{1}{\pi}(\frac{1}{2}-\beta^2)\frac{(x_1-y_1)^2}{2}k^2w^2\ln(w) + O(w^4) \quad (2.4.14)$$

2.4.3 Asymptotic of $S(w,k)$

From the previous asymptotic expansions (2.4.14) and (2.4.11), we obtain the following result.

Theorem 8. *Let $0 < w < w_0$, the kernel of $S(w,k)$ has the following expansion*

$$G_i(wx_1,0;wy_1,0) + G_e(wx_1,0;wy_1,0) = \theta_w + s_1 + s_2w + s_3w^2\ln(w) + s_4$$

where

$$\begin{cases} \theta_w(k) &= \frac{e(k,\beta)}{w} + \delta(\beta) + \frac{\ln(wk)}{\pi} \\ s_1(x_1,y_1) &= \frac{1}{\pi}\ln|4(x_1-y_1)\sin(\frac{\pi(x_1+y_1+2)}{4})\sin(\frac{\pi(x_1-y_1)}{4})| \\ s_2(k,x_1,y_1) &= -\frac{i\beta}{2}|x_1-y_1|k + a_1(\beta,x,y)k \\ s_3(k,x_1,y_1) &= -\frac{1}{\pi}(\frac{1}{2}-\beta^2)\frac{(x_1-y_1)^2}{2}k^2 \\ s_4(w,k,x_1,y_1) &= a_2(\beta,x_1,y_1)(wk)^2 + b_2(\beta,k,x_1,y_1)(wk)^2 + o((wk)^2) \end{cases}$$

The functions $e, a_2, \delta(\beta)$ *and* b_2 *are given respectively in* (2.4.9), (2.4.10), (2.4.12) *and* (2.4.13).

We then have the following asymptotic behavior of $S(w,k)$.

Corollary 9. *The operator valued function* $S(w,k)$ *verifies*

$$S(w,k) = \Theta_w(k) + S_1 + wS_2(k) + w^2 \ln(w) S_3(k) + w^2 S_4(w,k)$$

where:
$\Theta_w(k)\phi(x) = \theta_w(k) \int_{-1}^{1} \phi(y)dy$
$S_1\phi(x) = \int_{-1}^{1} s_1(x,y)\phi(y)dy$
$S_2(k)\phi(x) = \int_{-1}^{1} s_2(k,x,y)\phi(y)dy$
$S_3(k)\phi(x) = \int_{-1}^{1} s_3(k,x,y)\phi(y)dy$
$S_4(w,k)\phi(x) = \int_{-1}^{1} s_4(w,k,x,y)\phi(y)dy$
The asymptotic expansion is uniform with respect to k *within a compact set of the complex plane.*

2.4.4 Asymptotic of resonant frequencies

We derive in this section the asymptotic expansion of the resonant frequencies. We will show that they converge to the zeros of the function $e(k,\beta)$ when w tends to zero.

Define the $k_n(0)$ to be the zero of the function $e(k,\beta)$, that is $e(k_n(0)\beta) = 0$, ordered with respect to their real values and imaginary value of the real parts coincide.

Let

$$L(w,k) = S_1 + wS_2(k) + w^2 \ln(w) S_3(k) + w^2 S_4(w,k)$$

$L(w,k)$ is invertible for w small enough. Using the Neumann series, its inverse can be written as:

$$L^{-1}(w,k) = S_1^{-1} + \sum_{p=1}^{\infty} \left(-S_1^{-1}(S_2(k) + w\ln(w)S_3(k) + wS_4(w,k))\right)^p S_1^{-1} w^p$$

Fix w_0 small enough. For $w < w_0$ the following expression holds:

$$S^{-1}(w,k) = L^{-1}(w,k) - \frac{L^{-1}(w,k)1}{\Theta_w(k)L^{-1}(w,k)1 + 1}\Theta_w(k)L^{-1}(w,k)$$

The resonances $k_n(w)$ in $D_{\frac{\pi}{w_0}}$, are exactly the zeros of the function:

$$f_w(k) := \Theta_w(k)L^{-1}(w,k)1 + 1 := \theta_w(k)\langle 1, L^{-1}(w,k)1\rangle + 1$$

where
$$\theta_w(k) = \frac{e(k,\beta)}{w} + \delta(\beta) + \frac{ln(w)}{\pi} + \frac{ln(k)}{\pi}$$

We observe that

$$\langle 1, L^{-1}(w,k)1\rangle = \langle 1, S_1^{-1}1\rangle - \langle 1, S_1^{-1}S_2(k)S_1^{-1}1\rangle w + o(w)$$
$$\langle 1, \partial_k L^{-1}(w,k)1\rangle = O(w)$$

We further denote note

$$q_0 = \langle 1, S_1^{-1}1\rangle \tag{2.4.15}$$
$$q_1(k) = -\langle 1, S_1^{-1}S_2(k)S_1^{-1}1\rangle. \tag{2.4.16}$$

Therefore, the function $\frac{\partial_k f_w(k)}{f_w(k)}$ tends to $\frac{\partial_k e(k,\beta)}{e(k,\beta)}$ when w goes to zero, uniformly on every compact far from the isolated zeros and poles pf the function $e(k,\beta)$.

For $r_n > 0$ small enough, we have

$$\frac{1}{2i\pi}\int_{|k-k_n(0)|=r_n} \frac{\partial_k e(k,\beta)}{e(k,\beta)}dk = 1$$

Moreover, as $\lim_{w\to 0} \frac{\partial_k f_w(k)}{f_w(k)} = \frac{\partial_k e(k,\beta)}{e(k,\beta)}$ uniformly with respect to k on the circle $|k - k_n(0)| = r_n$, we deduce

$$\lim_{w\to 0} \frac{1}{2i\pi}\int_{|k-k_n(0)|=r_n} \frac{\partial_k f_w(k)}{f_w(k)}dk = 1$$

Recall that the zeros of $e(k,\beta)$ are noted $k_n(0)$ and those of $f_w(k)$ are noted $k_n(w)$. Then

$$k_n(w) - k_n(0) = -\frac{1}{2i\pi}\int_{|k-k_n(0)|=r_n} (k - k_n(0))\frac{\partial_k f_w(k)}{f_w(k)}dk$$

From the explicit form of the function $\theta_w(k)$ we have

$$f_w(k) = \frac{1}{w}\left(e(k,\beta)q_0 + \frac{q_0}{\pi}w\ln(w) + (\delta(\beta)q_0 + \frac{ln(k)}{\pi}q_0 + e(k,\beta)q_1 + 1)w + o(w)\right)$$

$$\partial_k f_w(k) = \frac{1}{w}\left(\partial_k e(k,\beta)q_0 + (\partial_k e(k,\beta)q_1 + \frac{q_0}{\pi k} + \partial_k q_1(k)e(k,\beta))w + o(w)\right)$$

The asymptotic expansion of $(f_w(k))^{-1}$ is as follows

$$(f_w(k))^{-1} = \frac{w}{e(k,\beta)q_0}\left(1 - \frac{1}{\pi e(k,\beta)} w\ln(w) - (\frac{\delta(\beta) + \frac{ln(k)}{\pi}}{e(k,\beta)} + \frac{q_1}{q_0} + \frac{1}{e(k,\beta)q_0})w + o(w)\right)$$

Therefore

$$\begin{aligned}\frac{\partial_k f_w(k)}{f_w(k)} &= \frac{\partial_k e(k,\beta)}{e(k,\beta)} - \frac{\partial_k e(k,\beta)}{\pi e(k,\beta)^2} w\ln(w) \\ &+(-\frac{\delta(\beta)\partial_k e(k,\beta)}{e(k,\beta)^2} - \frac{\partial_k e(k,\beta)\ln(k)}{\pi e(k,\beta)^2} \frac{-q_1(k)\partial_k e(k,\beta)}{e(k,\beta)q_0} \\ &-\frac{\partial_k e(k,\beta)}{q_0 e(k,\beta)^2} + \frac{q_1(k)\partial_k e(k,\beta)}{e(k,\beta)q_0} + \frac{1}{e(k,\beta)\pi k} + \frac{\partial_k q_1(k)}{q_0})w + o(w)\end{aligned}$$

On the other hand, we have

$$\begin{aligned}&\int_{|k-k_n(0)|=r_n} (k-k_n(0))\frac{\partial_k e(k,\beta)}{e(k,\beta)}dk = 0 \\ &\int_{|k-k_n(0)|=r_n} (k-k_n(0))\frac{\partial_k e(k,\beta)}{e(k,\beta)^2}dk = \frac{2i\pi}{\partial_k e(k_n(0),\beta)} \\ &\int_{|k-k_n(0)|=r_n} (k-k_n(0))\frac{1}{e(k,\beta)k}dk = 0 \\ &\int_{|k-k_n(0)|=r_n} (k-k_n(0))\frac{q_1(k)\partial_k e(k,\beta)}{e(k,\beta)}dk = 0 \\ &\int_{|k-k_n(0)|=r_n} (k-k_n(0))\partial_k q_1(k)dk = 0 \\ &\int_{|k-k_n(0)|=r_n} (k-k_n(0))\frac{\partial_k e(k,\beta)\ln(k)}{e(k,\beta)^2}dk = 2i\pi\frac{\ln(k_n(0))}{\partial_k e(k_n(0),\beta)}\end{aligned}$$

Using the previous equalities, we find

$$\begin{aligned}\int_{|k-k_n(0)|=r_n} (k-k_n(0))\frac{\partial_k f_w(k)}{f_w(k)}dk &= -\frac{2i}{\partial_k e(k_n(0),\beta)} w\ln(w) \\ -\left(\delta(\beta)\frac{2i\pi}{\partial_k e(k_n(0),\beta)} + 2i\frac{\ln(k_n(0))}{\partial_k e(k_n(0),\beta)} + \frac{2i\pi}{q_0\partial_k e(k_n(0),\beta)}\right) w + o(w)\end{aligned}$$

Therefore

$$k_n(w) = k_n(0) + \frac{1}{\pi \partial_k e(k_n(0),\beta)} w \ln(w)$$
$$+ \left(\delta(\beta) \frac{1}{\partial_k e(k_n(0),\beta)} + \frac{\ln(k_n(0))}{\pi \partial_k e(k_n(0),\beta)} + \frac{1}{q_0 \partial_k e(k_n(0),\beta)} \right) w + o(w)$$

Hence

$$k_n(w) = k_n(0) + \frac{1}{\pi \partial_k e(k_n(0),\beta)} w \ln(w)$$
$$+ \frac{1}{\partial_k e(k_n(0),\beta)} \left(\delta(\beta) + \frac{\ln(k_n(0))}{\pi} + \frac{1}{q_0} \right) w + o(w)$$

Recall the expression (2.4.9)

$$e(k,\beta) = \frac{1}{2i(e^{-2ikh}-1)} \left(e^{-2ikh} \frac{1}{(k+k\beta)} + \frac{1}{k-k\beta} \right)$$

A simple calculation gives

$$\partial_k e(k,\beta) =$$
$$\frac{h}{k(e^{-2ikh}-1)^2} \left(e^{-2ikh} \frac{1}{(1+\beta)} + \frac{1}{1-\beta} \right)$$
$$+ \frac{1}{2ik^2(e^{-2ikh}-1)} \left(e^{-2ikh} \frac{2ih+1}{(1+\beta)} + \frac{1}{1-\beta} \right)$$

$$\partial_k e(k,\beta) = \frac{e^{-2ikh}(1-\beta)(2ih + (2ih+1)(e^{-2ikh}-1)) + (1+\beta)(2ihk + (e^{-2ikh}-1))}{2ik^2(e^{-2ikh}-1)^2(1-\beta^2)}$$

We resume the previous asymptotic expansions in the following main theorem.

Theorem 10. *Let $k_n(0)$ be a fixed zero of the function $e(k,\beta)$ given by* (2.4.9)*, that is, it satisfies the dispersion equation*

$$e^{-2ikh} = \frac{\beta-1}{\beta+1}. \tag{2.4.17}$$

There exists $w_0 > 0$ small enough such that for $0 < w < w_0$, the unique resonance $k_n(w)$ located near $k_n(0)$ has the following asymptotic expansion

$$k_n(w) = k_n(0) + \frac{A(\beta)}{\pi} w \ln(w) + A(\beta) \left(\delta(\beta) + \frac{\ln(k_n(0))}{\pi} + \frac{1}{q_0} \right) w + o(w),$$

where $\delta(\beta)$ is given in (2.4.12)*, and $A(\beta)$ is defined by*

$$A(\beta) =$$
$$\frac{2ik_n(0)^2(e^{-2ik_n(0)h}-1)^2(1-\beta^2)}{e^{-2ik_n(0)h}(1-\beta)(2ih + (2ih+1)(e^{-2ik_n(0)h}-1)) + (1+\beta)(2ihk_n(0) + (e^{-2ik_n(0)h}-1))}$$

In particular, as w tends to zero, the imaginary part of resonance $k_n(w)$ behaves as

$$
\begin{aligned}
Im(k_n(w)) = Im(k_n(0)) + \frac{1}{\pi} Im(\frac{1}{\partial_k e(k_n(0),\beta)}) w \ln(w) \\
+Im(\frac{1}{\partial_k e(k_n(0),\beta)} \left(Re(\delta(\beta)) + \frac{Re(\ln(k_n(0)))}{\pi} + \frac{1}{q_0} \right)) w \\
+Re(\frac{1}{\partial_k e(k_n(0),\beta)} \left(Im(\delta(\beta)) + \frac{Im(\ln(k_n(0)))}{\pi} + \frac{1}{q_0} \right)) w + o(w).
\end{aligned}
$$

Chapter 3

Asymptotic of resonances of a periodic array of metallic subwavelength cavities

Sommaire

3.1 Introduction **64**

3.2 Position of the problem **65**

3.2.1 Description of the geometry and notations 65

3.2.2 Formulation of the problem 66

3.2.3 Quasi-periodicity 67

3.2.4 The radiation condition 68

3.2.5 The periodic problem 73

3.3 Wellposedness of the problem **73**

3.3.1 θ-periodic functional spaces 74

3.3.2 Truncation of the domain 76

3.3.3 The variational formulation 77

3.3.4 Characterization of singular frequencies 79

3.4 Reduction of the problem to an integral equation **80**

3.4.1 The Green function in Ω_i 80

3.4.2 The Green function in Ω_e 81

3.4.3 Integral representation 82

3.5 Asymptotics **85**

3.5.1 The case d is independent of w 85

3.5.2 The case $d = mw$ 101

3.1 Introduction

Metallic surfaces containing subwavelength cavities have been studied intensively for the last two decades, and that is due to their exceptional optical properties. These exceptional properties can be resumed in the enhancement and the localization of the electromagnetic field inside the cavities. In fact, at the resonance frequency, the electromagnetic fields can be enhanced locally by several orders of magnitude, first due to the multiple back and forth reflections between the cavity's walls, and secondly due to interaction of the incident electromagnetic field with independent surface plasmon modes on the surface of the metal. These amazing features could find application in many domains like imaging, microscopy, spectroscopy and communication. In this chapter, we study a particular case of a periodic array of subwavelength metallic rectangular cavities.

Due to geometrical considerations and to the choice of a time harmonic incident field [5], the scattering problem can be reduced to a Helmholtz equation in an unbounded planar domain. Using the Green formula we reformulate the Helmholtz equation in the whole domain as a system of integral equations defined on the aperture of the cavity in the unit periodic cell. Rescaling the integral equation, and using the explicit spectral expression of the periodic Green function, we determine the asymptotic expansion of the integral operator. Using an operator version of the Rouché theorem, we are able to derive finally the asymptotic expansion of the resonant frequencies $k_n(w)$ of our system.

The outline of the chapter is as follows. Section 2 describes the physical problem. In section 3, we study the well posedness of the associated scattering problem through a classical variational formulation.

In section 4, an integral representation of the solution to the diffraction problem is derived. We reduce the Helmholtz equation in the unbounded diffraction domain to a linear system of integral equations on the aperture of the single cavity in the unit periodic cell (Lemma 3.4.3). By rescaling the obtained integral equation we show that the resonances are exactly the zeros of a given operator valued function $S(w, k)$.

Section 5 is devoted to the asymptotic expansion of $S(w, k)$ and the resonant frequencies $k_n(w)$ as the width of the cavity w tends to 0. We consider two asymptotic regimes: the first is the case where the period of the array d is fixed and is independent on w, and the second case is when d depends linearly on w, that is, $d = mw$ for some constant $m > 0$ The asymptotic expansions of the associated integral operator $S(w, k)$ are provided Corollaries 21 and 29. Using the generalized Rouché Theorem and the asymptotic expansion of the integral operators we obtain the asymptotic behavior of the

resonant frequencies for two different regimes in Theorems 26 and 33.

3.2 Position of the problem

3.2.1 Description of the geometry and notations

Let (e_1, e_2, e_3) be an orthonormal basis of $\mathbb{R}^3$. The device is made by a perfectly conducting metal and consists on a periodic array of metallic cavities of the same width w. It is invariant in the x_3 direction and periodic in the x_1 direction with period $d > 0$.

The scattering domain is the air above the optical device, characterized by a constant electric permittivity ε and a magnetic permeability μ. It has the form $\Omega \times \mathbb{R}$.

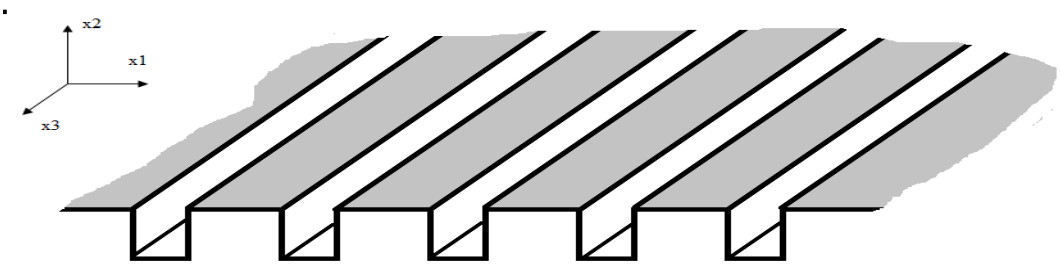

Figure 3.1: The grating of stripes Ω

Its cross-section Ω as shown in Figure 2 consists of the union of the upper-half plane $\Omega_e = \mathbb{R}^2_+$ and the set of the open cavities $\Omega_i = \cup_{j\in\mathbb{Z}}]jd - w/2, jd + w/2[\times] - h, 0]$.

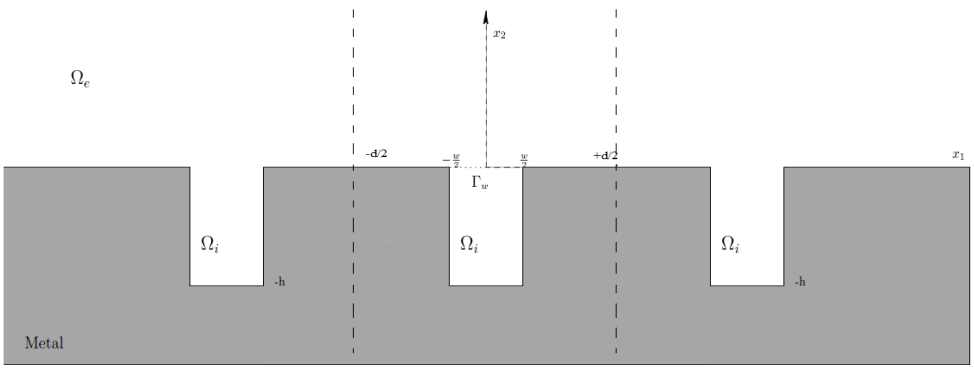

Figure 3.2: The diffracting domain Ω

We likewise define the unit cell of the grid $U \times \mathbb{R}$ by

$$U =]-\frac{d}{2}, \frac{d}{2}[\times\mathbb{R}$$

and introduce the following notations:
$O = \Omega \cap U$, $O_e = \Omega_e \cap O$, $O_i = \Omega_i \cap O$, $\Gamma_w = (-w/2, w/2)$, and $\overline{\partial O} = \{X \in \partial\Omega; -\frac{d}{2} \leq x_1 \leq \frac{d}{2}\}$.

3.2.2 Formulation of the problem

Assume Ω is filled with a homogeneous dielectric material of magnetic permeability μ, and electric permittivity ε. The time-dependent, linear Maxwell equations take the form

$$\begin{aligned} \text{curl}\,\mathbf{E} + \mu\frac{\partial \mathbf{H}}{\partial t} &= 0 \quad \text{in } \Omega \times \mathbb{R} \times \mathbb{R}_+ \\ \text{curl}\,\mathbf{H} - \varepsilon\frac{\partial \mathbf{E}}{\partial t} &= 0 \quad \text{in } \Omega \times \mathbb{R} \times \mathbb{R}_+ \end{aligned}$$

where $\mathbf{E} \in \mathbb{R}^3$ and $\mathbf{H} \in \mathbb{R}^3$ respectively denote the electric and magnetic fields. In this chapter we only consider time-harmonic solutions, i.e., special solutions of the form

$$\mathbf{E}(x,t) = \text{Re}(E(x)e^{-i\omega t}) \quad \text{and} \quad \mathbf{H}(x,t) = \text{Re}(H(x)e^{-i\omega t})$$

where ω denotes the time pulsation and the complex fields $E(x)$ and $H(x)$ satisfy

$$\text{curl}\,E - i\omega\mu H = 0 \tag{3.2.1}$$

$$\text{curl}\,H + i\omega\varepsilon E = 0 \tag{3.2.2}$$

We assume that the surface of the device is a perfect conductor, so that E satisfies the following boundary condition on $\partial\Omega \times \mathbb{R}$

$$\text{curl}\,E \times \mathbf{n} = \mathbf{0}$$

where $\mathbf{n} = (n, 0)$. Here n denotes is the outward normal vector to $\partial\Omega$.

As in [3], we focus on the transverse magnetic polarization (TM), where the total magnetic field is transverse to the invariant dimension. In this case, $H = (0, 0, H_3(x_1, x_2))$ and the x_3-component of the total magnetic field verifies the Helmholtz equation

$$\begin{cases} \Delta H_3(X) + k^2 H_3(X) = 0 & X \in \Omega, \\ \partial_n H_3 = 0 & X \in \partial\Omega, \end{cases} \tag{3.2.3}$$

with $k = \omega\sqrt{\varepsilon\mu}$.
We assume that the metal is illuminated under the incidence angle β by a

harmonic incident plane wave, and we denote by $\mathbf{k_i} = \mathbf{k_1 e_1} + \mathbf{k_2 e_2}$ its wave vector, that is

$$H^{inc}(x_1, x_2) = H_0^{inc} e^{k_1 x_1 + k_2 x_2},$$

and

$$k = \|\mathbf{k_i}\| = \sqrt{k_1^2 + k_2^2},$$

Let θ be the unique real verifying

$$k_1 = k\cos(\beta) = \theta + \frac{2p_0\pi}{d}, \quad \theta \in \left]-\frac{\pi}{d}, \frac{\pi}{d}\right] \tag{3.2.4}$$

We consider the diffraction of (time harmonic) incident fields E^{inc}, H^{inc} by the surface $\partial\Omega$. Then

$$\begin{aligned} E &= E^{inc} + E^s, \\ H &= H^{inc} + H^s, \end{aligned}$$

where E and H are the total electric and magnetic fields, and E^s, H^s are the diffracted electric and magnetic fields. Since H^{inc} verifies the Helmholtz equation, so from (3.2.3) and taking into account the linearity of the Δ operator, we can show that

$$\begin{cases} \Delta H_3^s(X) + k^2 H_3^s(X) = 0 & X \in \Omega, \\ \partial_n H_3^s = f & X \in \partial\Omega. \end{cases} \tag{3.2.5}$$

where $f = -\partial_n H_3^{inc}$.

Since the scattering domain is unbounded, we require that the scattered fields (E^s, H^s) satisfy a radiation condition that fixes the behavior of the solution at infinity.

We further denote H,H^{inc} and H^s the third components of the total, incident and scattered fields respectively.

3.2.3 Quasi-periodicity

Regarding the periodicity of the domain the incident field H^{inc} satisfies

$$H^{inc}(x_1 + pd, x_2) = H^{inc}(x_1, x_2) e^{i\theta pd}, \quad \forall (x_1, x_2) \in \Omega, \ \forall p \in \mathbb{Z} \tag{3.2.6}$$

In fact, if we assume that H is a solution of (3.2.3). Then, by the periodicity of the domain Ω, every field $H^{(p)}$ of the form

$$H^{(p)}(x_1, x_2) = H(x_1 + pd, x_2) e^{i\theta pd}$$

for $p \in \mathbb{Z}$ is a solution of the same problem. Of course, the associated diffracted field$(H^{(p)})^s$ has the same behavior for $|x_2| \to +\infty$ as H^s, and

there is no physical criterion to eliminate some of these solutions. In order to avoid to have infinitely many solutions, we will search solutions that are $\theta-$periodic, that is

$$H(x_1 + pd, x_2) = H(x_1, x_2)e^{i\theta pd}, \quad \forall (x_1, x_2) \in \Omega, \ \forall p \in \mathbb{Z}.$$

The $\theta-$periodicity condition will allow us now to write a radiation condition in the x_2-direction. Indeed, if the diffracted field H^s is $\theta-$periodic, it means that the function

$$H_{per}(x_1, x_2) = H^s(x_1, x_2)e^{-i\theta x_1}$$

is periodic. If we suppose furthermore that $d < \lambda = \dfrac{2\pi}{k}$ then we get $\theta = k_1 = k\cos(\beta)$.

3.2.4 The radiation condition

The radiation condition that we consider has been used in [28] and [29].

Let $L_0 > 0$, the Fourier decomposition of H_{per} for $x_2 > L_0$ leads to the so-called $\theta-$periodic Fourier decomposition of H^s:

$$H^s(x_1, x_2) = \sum_{p\in\mathbb{Z}} H_p^s(x_2)e^{i(\theta+\theta_p)x_1}, \tag{3.2.7}$$

where $\theta_p = \dfrac{2\pi p}{d}$ and $H_p^s(x_2) = \displaystyle\int_0^d H^s(x_1, x_2)e^{-i(\theta+\theta_p)x_1}dx_1$.
Since H^s satisfies

$$\Delta H^s(X) + k^2 H^s(X) = 0, X \in \Omega,$$

the Fourier coefficient H_p^s must solve the following differential equation:

$$\frac{d^2 H_p^s}{dx_2^2} + (k^2 - (\theta + \theta_p)^2)H_p^s = 0. \tag{3.2.8}$$

This 1d-equation has two linearly independent solutions but only one of them is physically admissible.

Classical radiation condition

Here, we deal with the physically significant case where ω is positive, which in turn implies that k is also positive and hence $k^2 - (\theta + \theta_p)^2$ is real. The following radiation conditions are developed in [29].

Let

$$
\begin{aligned}
Z^+(k) &= \{p \in \mathbb{Z}; (\theta+\theta_p)^2 - k^2 > 0\}, \\
Z^0(k) &= \{p \in \mathbb{Z}; (\theta+\theta_p)^2 - k^2 = 0\}, \\
Z^-(k) &= \{p \in \mathbb{Z}; (\theta+\theta_p)^2 - k^2 < 0\}.
\end{aligned} \tag{3.2.9}
$$

Then, the radiation conditions consist on:

1. For $p \in Z^+(k)$, we choose the exponentially decreasing solution

$$H_p^s(x_2) = H_p^s(L_0) e^{-\sqrt{(\theta+\theta_p)^2-k^2}(x_2-L_0)}.$$

2. For $p \in Z^0(k)$, we choose the constant solution

$$H_p^s(x_2) = H_p^s(L_0)$$

3. For $p \in Z^-(k)$, we choose the solution which satisfies the outgoing Sommerfeld radiation condition

$$H_p^s(x_2) = H_p^s(L_0) e^{i\sqrt{k^2-(\theta+\theta_p)^2}(x_2-L_0)}.$$

Finally, the diffracted field H^s has the following expression for $x_2 > L_0$:

$$H^s(x_1, x_2) = \sum_{p\in\mathbb{Z}} H_p^s(L_0) e^{\alpha_p(k)(x_2-L_0)} e^{i(\theta+\theta_p)x_1}, \tag{3.2.10}$$

where α_p is given by :

$$\alpha_p(k) = \begin{cases} -\sqrt{(\theta+\theta_p)^2 - k^2} & \text{if} \quad p \in Z^+(k) \\ 0 & \text{if} \quad p \in Z^0(k) \\ i\sqrt{(\theta+\theta_p)^2 - k^2} & \text{if} \quad p \in Z^-(k) \end{cases}$$

We notice that $Z^0(k)$ and $Z^-(k)$ are finite sets, so that the previous series expansion contains only a finite number of non decreasing terms.

Generalized radiation conditions

The radiation condition stated first deals with real positive frequencies. In order to apply the complex integration contour method needed in the asymptotic expansion of resonances we will deal with solutions to the problem (3.2.5) with complex frequency k.

The continuation of the problem to the complex domain requires to fix the branch cut of the complex square root function.

We further extend $\theta(k)$ to the complex domain by $\theta(k) = k_1 = k\cos(\beta)$ where β is the incident angle.

We first need to define the square root of $(\theta + \theta_p)^2 - k^2$

$$\begin{aligned}(\theta + \theta_p)^2 - k^2 &= -\sin^2(\beta)k^2 + \frac{4\pi p}{d}\cos(\beta)k + \frac{4\pi^2 p^2}{d^2} \\ &= -\sin^2(\beta)(k - k_{1,p})(k - k_{2,p})\end{aligned}$$

where

$$k_{1,p} = \frac{2\pi p}{d\sin^2(\beta)}(\cos(\beta) + 1) \quad \text{and} \quad k_{2,p} = \frac{2\pi p}{d\sin^2(\beta)}(\cos(\beta) - 1).$$

We define the square root of $((\theta + \theta_p)^2 - k^2)$ as the product of $(-\sin^2(\beta))^{\frac{1}{2}}$, $(k - k_{1,p})^{\frac{1}{2}}$ and $(k - k_{2,p})^{\frac{1}{2}}$ using the following choice of the determination of the complex square root function:

$$\forall z \in \mathbb{C}, \quad z^{\frac{1}{2}} = |z|^{\frac{1}{2}} e^{i\arg(z)/2} \quad \text{where} \quad \arg(z) \in \left]\frac{\pi}{2}, \frac{5\pi}{2}\right[$$

The previous square root is defined using the analytic branch of argument in the whole complex plane minus the positive imaginary axis. We then obtain

$$((\theta + \theta_p)^2 - k^2)^{\frac{1}{2}} = i|\sin(\beta)|(k - k_{1,p})^{\frac{1}{2}}(k - k_{2,p})^{\frac{1}{2}} \tag{3.2.11}$$

It's clear that the term $((\theta + \theta_p)^2 - k^2)^{\frac{1}{2}}$ is defined and analytic with respect to k in the region $\mathbb{C} \setminus (\{k_{1,p} + i\mathbb{R}^+\} \cup \{k_{2,p} + i\mathbb{R}^+\})$. Consequently, the expression (3.2.7) is defined and analytic on the region D that occupies the whole complex plane minus all the axis $\{k_{1,p} + i\mathbb{R}^+\}$ and $\{k_{2,p} + i\mathbb{R}^+\}$ for all $p \in \mathbb{Z}$ (see Figure 3.2.4).

$$D = \mathbb{C} \setminus \bigcup_{p\in\mathbb{Z}, i\in\{1,2\}} \{k_{i,p} + i\mathbb{R}^+\} \tag{3.2.12}$$

The generalized radiation condition consist of choosing one admissible solution to (3.2.8). So we write $H_p^s(x_2)$ as $H_p^s(L_0)e^{\alpha_p(k)(x_2 - L_0)}$ where

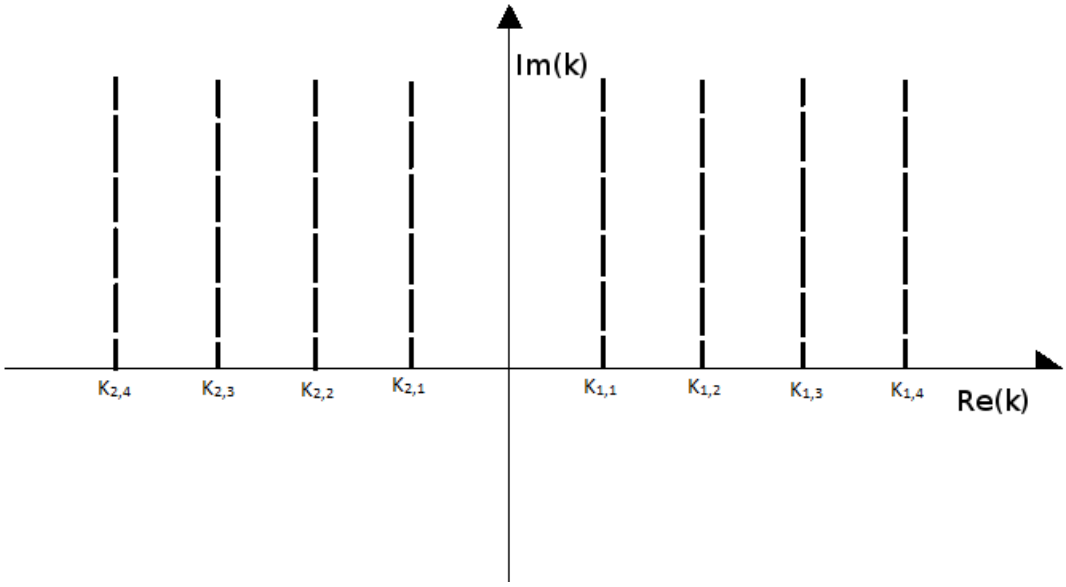

Figure 3.3: The Domain D

$$\alpha_p(k) = \begin{cases} ((\theta+\theta_p)^2 - k^2)^{\frac{1}{2}} & \text{if} \quad \mathrm{Re}(((\theta+\theta_p)^2 - k^2)^{\frac{1}{2}}) < 0, \\ ((\theta+\theta_p)^2 - k^2)^{\frac{1}{2}} & \text{if} \quad \mathrm{Re}(((\theta+\theta_p)^2 - k^2)^{\frac{1}{2}}) = 0 \\ & \text{and} \quad \mathrm{Im}(((\theta+\theta_p)^2 - k^2)^{\frac{1}{2}}) > 0, \\ -((\theta+\theta_p)^2 - k^2)^{\frac{1}{2}} & \text{if} \quad \mathrm{Re}(((\theta+\theta_p)^2 - k^2)^{\frac{1}{2}}) = 0 \\ & \text{and} \quad \mathrm{Im}(((\theta+\theta_p)^2 - k^2)^{\frac{1}{2}}) < 0, \\ -((\theta+\theta_p)^2 - k^2)^{\frac{1}{2}} & \text{if} \quad \mathrm{Re}(((\theta+\theta_p)^2 - k^2)^{\frac{1}{2}}) > 0. \end{cases}$$

Now, we study the sign of $\mathrm{Re}(((\theta+\theta_p)^2-k^2)^{\frac{1}{2}})$. we deduce from (3.2.11) the following

$$\mathrm{Re}(((\theta+\theta_p)^2 - k^2)^{\frac{1}{2}}) = -|\sin(\beta)|\mathrm{Im}((k-k_{1,p})^{\frac{1}{2}}(k-k_{2,p})^{\frac{1}{2}}).$$

The term $\mathrm{Im}((k-k_{1,p})^{\frac{1}{2}}(k-k_{2,p})^{\frac{1}{2}})$ is equal to zero for k in the interval $]-\infty, k_{2,p}[\cup]k_{1,p}, +\infty[$.

$\mathrm{Im}((k-k_{1,p})^{\frac{1}{2}}(k-k_{2,p})^{\frac{1}{2}})$ is positive if k is in the region $\{\mathrm{Im}(k) > 0 \quad \text{and} \quad \mathrm{Re}(k) \in]-\infty, k_{2,p}[\cup]k_{1,p}, +\infty[\}$ and negative if $\mathrm{Im}(k) < 0$ or $(\mathrm{Im}(k) > 0$ and $\mathrm{Re}(k) \in]k_{2,p}, k_{1,p}[)$.

Then

$$\begin{cases} \mathrm{Re}(((\theta+\theta_p)^2-k^2)^{\frac{1}{2}})>0 & \text{if} \quad \mathrm{Im}(k)<0 \\ & \text{or } (\mathrm{Im}(k)>0 \text{ and } \mathrm{Re}(k)\in]k_{2,p},k_{1,p}[) \\ \mathrm{Re}(((\theta+\theta_p)^2-k^2)^{\frac{1}{2}})<0 & \text{if} \quad \mathrm{Im}(k)>0 \\ & \text{and } \mathrm{Re}(k)\in]-\infty,k_{2,p}[\cup]k_{1,p},+\infty[\\ \mathrm{Re}(((\theta+\theta_p)^2-k^2)^{\frac{1}{2}})=0 & \text{if} \quad k\in]-\infty,k_{2,p}[\cup]k_{1,p},+\infty[\end{cases}$$

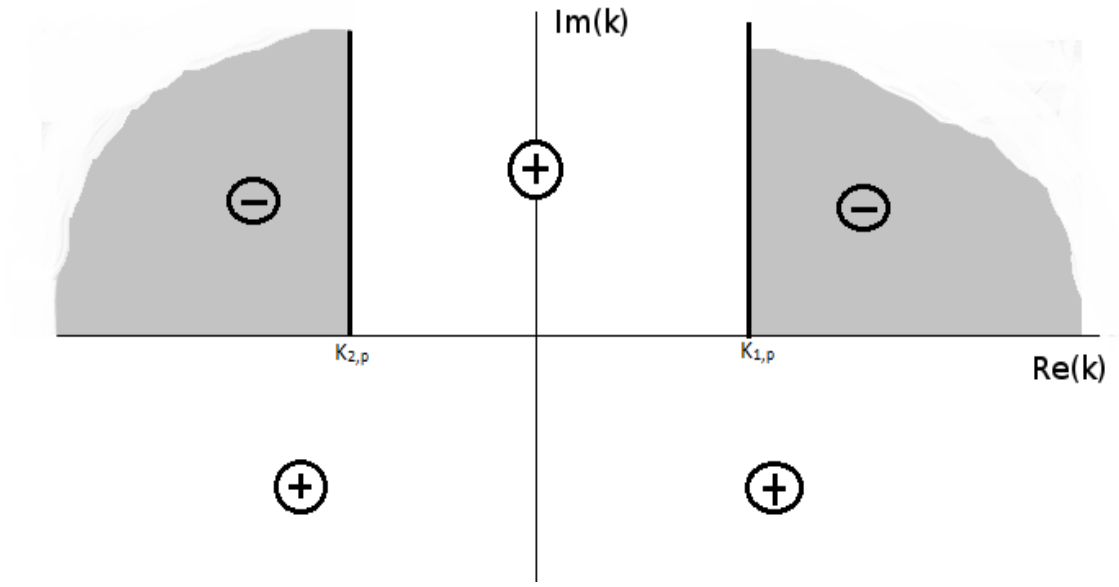

Figure 3.4: The sign of $Re(((\theta+\theta_p)^2-k^2)^{\frac{1}{2}})$

When $\mathrm{Re}(((\theta+\theta_p)^2-k^2)^{\frac{1}{2}})=0$ which is equivalent to $k\in]-\infty,k_{2,p}[\cup]k_{1,p},+\infty[$, the sign of $\mathrm{Im}(((\theta+\theta_p)^2-k^2)^{\frac{1}{2}})$ is as follows:

$$\begin{cases} \mathrm{Im}(((\theta+\theta_p)^2-k^2)^{\frac{1}{2}})>0 & \text{if} \quad k>k_{1,p} \\ \mathrm{Im}(((\theta+\theta_p)^2-k^2)^{\frac{1}{2}})<0 & \text{if} \quad k<k_{2,p} \end{cases}$$

Finally, we have the expression of $\alpha_p(k)$:

$$\alpha_p(k)=\begin{cases} ((\theta+\theta_p)^2-k^2)^{\frac{1}{2}} & \text{if } \ k>k_{1,p} \ \text{ or } \mathrm{Im}(k)>0 \text{ and } \mathrm{Re}(k)\in]-\infty,k_{2,p}[\cup]k_{1,p},+\infty[\\ -((\theta+\theta_p)^2-k^2)^{\frac{1}{2}} & \text{otherwise} \end{cases} \tag{3.2.13}$$

Hence the generalized radiation conditions are equivalent to write for $x_2>L_0$:

$$H^s(x_1,x_2)=\sum_{p\in\mathbb{Z}} H_p^s(L_0)e^{\alpha_p(k)(x_2-L_0)}e^{i(\theta+\theta_p)x_1}, \tag{3.2.14}$$

where $\alpha_p(k)$ is given by (3.2.13).

Remark 11. *From the expression of $\alpha_p(k)$, we remark that $\forall k \in \mathbb{C}$, $\exists M(k)$ such that $\forall p > M(k)$, $\alpha_p(k) = -((\theta+\theta_p)^2 - k^2)^{\frac{1}{2}}$. So we define $M(k)$ by*

$$M(k) = \min\{p \in \mathbb{Z}, \alpha_p(k) = -((\theta+\theta_p)^2 - k^2)^{\frac{1}{2}}\} \tag{3.2.15}$$

3.2.5 The periodic problem

Let $H_{per}(x_1, x_2)$ be defined by:

$$H^s(x_1, x_2) = e^{i\theta x_1} H_{per}(x_1, x_2). \tag{3.2.16}$$

Consequently, $H_{per}(x_1, x_2)$ is a periodic function with respect to x_1 of period d.

Lemma 3.2.1. *The x_1-periodic field H_{per} solves the following boundary value problem:*

$$\begin{cases} \Delta_\theta H_{per}(X) + k^2 H_{per}(X) = 0 & X \in O_e \cup O_i \\ \dfrac{\partial H_{per}}{\partial_\theta n}(x_1; x_2) = f & (x_1, x_2) \in \overline{\partial O} \end{cases} \tag{3.2.17}$$

where $\Delta_\theta = (\partial_{x_1} + i\theta)^2 + \partial_{x_2}^2$, $\dfrac{\partial}{\partial_\theta n} = (\partial_{x_1} + i\theta, \partial_{x_2})^T.n$ *and* $\overline{\partial O} = \{X \in \partial\Omega; -\frac{d}{2} \leq x_1 \leq \frac{d}{2}\}$.

Proof. We substitute the expression (3.2.16) in (3.2.3), and we use the formula $\Delta e^{i\theta x_1} = e^{i\theta x_1}\Delta_\theta$. By considering the fact that H_p is periodic, we find the result.

□

Remark 12. *The previous lemma, allows us to reduce the problem* (3.2.5) *defined in the whole Ω to the problem* (3.2.17) *defined in the unit cell O. The problem* (3.2.17) *is more suitable for the integral equation representation method developed in chapter two.*

3.3 Wellposedness of the problem

In this part we will prove the wellposedness of the problem (3.2.3) on $\mathbb{C}$ except for a discrete family of values which are the resonance frequencies.
We will first consider the case where $k \in \mathbb{R}$ and use the classical radiation condition (3.2.10) to prove the wellposedness of the problem. Then we extend the solution to the whole complex plane $\mathbb{C}$ using a clever integral

representation and the Steinberg Theorem.

Since we look for $\theta-$periodic solution, the problem can be rewritten on a unique cell of the grating. Let us consider the following problem (verified by the total field):

P_O-problem:

$$\Delta H(X) + k^2 H(X) = 0, X \in O \tag{3.3.1}$$
$$\frac{\partial H}{\partial n}(x_1; x_2) = 0, (x_1, x_2) \in \overline{\partial O} \tag{3.3.2}$$
$$H(\frac{d}{2}; x_2) = H(-\frac{d}{2}; x_2)e^{i\theta d} \tag{3.3.3}$$
$$\frac{\partial H}{\partial n}(\frac{d}{2}; x_2) = \frac{\partial H}{\partial n}(-\frac{d}{2}; x_2)e^{i\theta d} \tag{3.3.4}$$
$$H^s = H - H^{ins} \text{ has the form (3.2.10) for } x_2 > L_0 \tag{3.3.5}$$

Thanks to conditions (3.3.3) and (3.3.4), every solution of the cell problem can be extended by pseudo-periodicity to a solution to the diffraction problem (3.2.3) in the whole plan.

For $L > L_0$, we set

$$\begin{aligned} O_L &= \{X \in O; x_2 < L\} \\ \Gamma_L &= \{X \in O; x_2 = L\} \end{aligned}$$

Now we will set an equivalent problem set in the bounded domain O_L, where a boundary condition on Γ_L is introduced. This condition will be derived from the expression (3.2.10) of the diffracted field for $x_2 > L_0$.

Before doing that, let us define some useful functional spaces that have been already extensively studied in [30, 31], and recall some Green formulas.

3.3.1 θ-periodic functional spaces

We consider the following spaces:

1. $\mathcal{C}_\theta^\infty(\mathbb{R}^2)$ is the set of all functions which are $\mathcal{C}^\infty(\mathbb{R}^2)$, satisfy (3.2.6) and vanish for large x_2.

2. $\mathcal{C}_\theta^\infty(O)$(resp $\mathcal{C}_\theta^\infty(O_L)$) is the set of restrictions to O (resp O_L) of all functions of $\mathcal{C}_\theta^\infty(\mathbb{R}^2)$.

3. $\mathcal{H}^1_\theta(O)$(resp $\mathcal{H}^1_\theta(O_L)$) is the smallest closed subspace of $\mathcal{H}^1(O)$(resp $\mathcal{H}^1(O_L)$) which contains $\mathcal{C}^\infty_\theta(O)$(resp $\mathcal{C}^\infty_\theta(O_L)$).

The following Green formula holds for $i = 1$or 2:

$$\forall u, v \in \mathcal{H}^1_\theta(O), \int_O \frac{\partial u}{\partial x_i}\bar{v}dx = -\int_O u\frac{\partial \bar{v}}{\partial x_i}dx + \int_{\partial \bar{O}} u\bar{v}n_i d\gamma$$

where $n = (n_1, n_2)$ is the outward normal to $\partial\bar{O}$. We also have

$$\forall u, v \in \mathcal{H}^1_\theta(O), \int_O -\Delta u\bar{v}dx = \int_O \nabla u\nabla\bar{v}dx - \int_{\overline{\partial O}} \frac{\partial u}{\partial n}\bar{v}d\gamma \tag{3.3.6}$$

Notice that these formulas involve no term on the lateral boundaries $\{x_1 = -\frac{d}{2}\}$ and $\{x_1 = \frac{d}{2}\}$ of O. Likewise, we have

$$\forall u, v \in \mathcal{H}^1_\theta(O_L), \int_{O_L} \frac{\partial u}{\partial x_i}\bar{v}dx = -\int_{O_L} u\frac{\partial \bar{v}}{\partial x_i}dx + \int_{\overline{\partial O}\cup\Gamma_L} u\bar{v}n_i d\gamma \tag{3.3.7}$$

$$\forall u, v \in \mathcal{H}^1_\theta(O_L), \int_{O_L} -\Delta u\bar{v}dx = \int_{O_L} \nabla u\nabla\bar{v}dx - \int_{\overline{\partial O}\cup\Gamma_L} \frac{\partial u}{\partial n}\bar{v}d\gamma \tag{3.3.8}$$

We also introduce the following space:

$$\mathcal{H}^{\frac{1}{2}}_\theta(\Gamma_L) = \left\{ v = \sum_{p\in\mathbb{Z}} v_p(L)e^{i(\theta+\theta_p)x_1}; \sum_{p\in\mathbb{Z}}(1+(\theta+\theta_p))^{\frac{1}{2}}|v_p(L)|^2 < +\infty \right\}$$

$\mathcal{H}^{\frac{1}{2}}_\theta(\Gamma_L)$ is a closed subspace of the usual Sobolev space $\mathcal{H}^{\frac{1}{2}}(\Gamma_L)$, and the norm

$$|v|^2_{\frac{1}{2},\theta} = d\sum_{p\in\mathbb{Z}}(1+(\theta+\theta_p))^{\frac{1}{2}}|v_p(L)|^2$$

is equivalent on $\mathcal{H}^{\frac{1}{2}}_\theta(\Gamma_L)$ to the classical $\mathcal{H}^{\frac{1}{2}}$-norm. The dual space of $\mathcal{H}^{\frac{1}{2}}_\theta(\Gamma_L)$ is

$$\mathcal{H}^{-\frac{1}{2}}_\theta(\Gamma_L) = \left\{ v = \sum_{p\in\mathbb{Z}} v_p(L)e^{i(\theta+\theta_p)x_1}; \sum_{p\in\mathbb{Z}}(1+(\theta+\theta_p))^{-\frac{1}{2}}|v_p(L)|^2 < +\infty \right\}$$

and the associated norm is

$$|v|^2_{-\frac{1}{2},\theta} = d\sum_{p\in\mathbb{Z}}(1+(\theta+\theta_p))^{-\frac{1}{2}}|v_p(L)|^2$$

$\mathcal{H}^{\frac{1}{2}}_\theta(\Gamma_L)$ is exactly the space of the traces on Γ_L of all functions of $\mathcal{H}^1_\theta(O_L)$.

The duality product between $\mathcal{H}^{\frac{1}{2}}_\theta(\Gamma_L)$and $\mathcal{H}^{-\frac{1}{2}}_\theta(\Gamma_L)$ is given by

$$\langle u, v\rangle_{\theta,\Gamma_L} = d\sum_{p\in\mathbb{Z}} u_p(L)\bar{v}_p(L)$$

3.3.2 Truncation of the domain

If H is solution of P_O -problem ,then by (3.2.10),H satisfies on Γ_L, the following boundary condition:

$$\frac{\partial H}{\partial n} = -T(k,\theta)H \ , \ \text{on} \ \ \Gamma_L \tag{3.3.9}$$

where the operator $T(k,\theta)$ is defined as follows:

$$\begin{array}{llll} T(k,\theta) \ : & \mathcal{H}_\theta^{\frac{1}{2}}(\Gamma_L) & \to & \mathcal{H}_\theta^{-\frac{1}{2}}(\Gamma_L) \\ & \displaystyle\sum_{p\in\mathbb{Z}} v_p(L)e^{i(\theta+\theta_p)x_1} & \mapsto & \displaystyle\sum_{p\in\mathbb{Z}} \mu_p(k,\theta)v_p(L)e^{i(\theta+\theta_p)x_1} \end{array}$$

where

$$\mu_p(k,\theta) = \begin{cases} \sqrt{(\theta+\theta_p)^2 - k^2} & \text{if} \quad p \in Z^+(k,\theta) \\ 0 & \text{if} \quad p \in Z^0(k,\theta) \\ i\sqrt{k^2 - (\theta+\theta_p)^2} & \text{if} \quad p \in Z^-(k,\theta) \end{cases}$$

One can check easily that $T(k,\theta)$ is continuous. Consider now the following truncated problem:

P_{O_L}-problem: Find $H \in \mathcal{H}_\theta^1(O_L)$ such that

$$\Delta H(X) + k^2 H(X) = 0, X \in O_L, \tag{3.3.10}$$

$$\frac{\partial H}{\partial n}(x_1;x_2) = 0, (x_1,x_2) \in \overline{\partial O}, \tag{3.3.11}$$

$$\frac{\partial H}{\partial n}(\frac{d}{2};x_2) = \frac{\partial H}{\partial n}(-\frac{d}{2};x_2)e^{i\theta d}, \tag{3.3.12}$$

$$\frac{\partial H}{\partial n} = \frac{\partial H^{inc}}{\partial n} - T(k,\theta)(H - H^{inc}) \ \ on \ \ \Gamma_L, \tag{3.3.13}$$

Proposition 13. *If H is a solution of P_O such that $\tilde{H} = H_{|O_L} \in \mathcal{H}_\theta^1(O_L)$, then $\tilde{H}$ is a solution of P_{O_L}. Conversely, if $\tilde{H}$ is a solution of P_{O_L}, it can be extended to a solution H of P_O.*

Proof. The first part of the proof is obvious. Conversely, if $\tilde{H}$ is a solution of P_{O_L}, then

$$H = \begin{cases} \tilde{H} & \text{if} \quad x_2 < L \\ \displaystyle\sum_{p\in\mathbb{Z}} \tilde{H}_p(L_0)e^{-\mu_p(k,\theta)(x_2-L_0)}e^{i(\theta+\theta_p)x_1} & \text{if} \quad x_2 > L \end{cases}$$

This function is clearly continuous through $x_2 = L$. Moreover the continuity of the normal derivative is obtained thanks to the boundary condition (3.3.13), and one can check easily that H is a solution to P_O.

□

3.3.3 The variational formulation

The problem P_{O_L} has the following variational formulation:

$$\begin{cases} \text{Find} \quad H \in \mathcal{H}^1_\theta(O_L) \quad \text{such that} \\ a(H,v) = l(v) \quad \forall v \in \mathcal{H}^1_\theta(O_L) \end{cases} \tag{3.3.14}$$

where the forms $a(H,v)$ and $l(v)$ are defined by

$$a(H,v) = \int_{O_L} \left(\nabla H.\nabla \bar{v} - k^2 H\bar{v}\right) dx + \langle T(k,\theta)H, v\rangle_{\theta,\Gamma_L}$$

$$l(v) = \langle \frac{\partial H^{inc}}{\partial n} + T(k,\theta)H^{inc}, v\rangle_{\theta,\Gamma_L}$$

We now establish a Freedholm decomposition for formulation (3.3.14). The following identity holds

$$a(H,v) = b(H,v) + c(H,v) \tag{3.3.15}$$

where

$$b(H,v) = \int_{O_L} (\nabla H.\nabla \bar{v} + H\bar{v})\, dx + \langle T(k,\theta)H, v\rangle_{\theta,\Gamma_L}$$

and

$$c(H,v) = -(k^2+1)\int_{O_L} (H\bar{v})\, dx$$

Since $b(H,v)$ and $c(H,v)$ are continuous sesquilinear forms on $\mathcal{H}^1_\theta(O_L)$, we can define two bounded operators B and C of $\mathcal{H}^1_\theta(O_L)$ by the identities

$$(BH,v)_{\mathcal{H}^1_\theta(O_L)} = b(H,v) \;\text{ and }\; (CH,v)_{\mathcal{H}^1_\theta(O_L)} = c(H,v)\; \forall H,v \in \mathcal{H}^1_{\theta(O_L)}.$$

Lemma 3.3.1. *The operator B is an automorphism of $\mathcal{H}^1_\theta(O_L)$ and the operator C is compact on $\mathcal{H}^1_\theta(O_L)$*

Proof. By definition of $T(k,\theta)$, we have

$$\forall u \in \mathcal{H}^1_\theta(O_L),\;\; \mathrm{Re}(\langle T(k,\theta)u, u\rangle_{\theta,\Gamma_L}) = d \sum_{p\in Z^+(k,\theta)} \sqrt{(\theta+\theta_p)^2 - k^2}\, |v_p(L)|^2 \geq 0$$

and consequently $b(.,.)$ is coercive on $\mathcal{H}^1_\theta(O_L)$,

$$\forall u \in \mathcal{H}^1_\theta(O_L),\;\; \mathrm{Re}(b(u,u)) \geq \int_{O_L} \left(|\nabla u|^2 + |u|^2\right) dx$$

This proves that B is an automorphism of $\mathcal{H}^1_\theta(O_L)$. The fact that C is compas is a direct consequence of the compact embedding of $\mathcal{H}^1_\theta(O_L)$ into $L^2(O_L)$ □

Let us denote by y the unique element of $\mathcal{H}^1_\theta(O_L)$ such that

$$(y,v)_{\mathcal{H}^1_\theta(O_L)} = l(v), \quad \forall v \in H^1_\theta(O_L)$$

Then, the problem P_{O_L} can be formulated as follows:

$$\text{Find } u \in \mathcal{H}^1_\theta(O_L) \text{ such that } Bu + Cu = y.$$

By Lemma 3.3.1 and by the Freedholm alternative, the existence of a solution will follow from the study of the homogeneous problem:

$$\text{Find } u \in \mathcal{H}^1_\theta(O_L) \textit{ such that } Bu + Cu = 0.$$

which has the following equivalent form

$$\text{Find } \ u \in \mathcal{H}^1_\theta(O_L) \textit{ such that } a(u,v) = 0 \ \ \forall v \in \mathcal{H}^1_\theta(O_L). \tag{3.3.16}$$

Lemma 3.3.2. *Let u be a solution of* (3.3.16)*. Then $u_p(L) = 0$, $\forall p \in Z^-(k,\theta)$.*

Proof. It follows directly from the identity $\mathrm{Im}(a(u,u)) = 0$. □

Lemma 3.3.2 means that a solution of the homogeneous problem is either exponentially decreasing or tends to a constant function for large x_2.

Theorem 14. *Problem P_{O_L} has at least one solution and the set of solutions is at most a finite-dimensional affine space.*

Proof. This result is based on the Freedholm alternative. If (3.3.16) has only the trivial solution, then (3.3.14) has a unique solution.
Suppose now that (3.3.16) has non-trivial solutions, and let us denote by V the set of these solutions. Then, by Freedholm alternative $\dim(V) < +\infty$ and problem (3.3.14) has a solution if and only if

$$l(v) = 0 \quad \forall v \in V. \tag{3.3.17}$$

Let us prove (3.3.17). We have that

$$l(v) = \langle \frac{\partial H_3^{inc}}{\partial n} + T(k,\theta)H^{inc}, v\rangle_{\theta,\Gamma_L}$$

and

$$H^{inc}(x_1,x_2) = H_0^{inc} e^{k_1x_1+k_2x_2} = H_0^{inc} e^{(\theta+\theta_{p_0})x_1} e^{k_2x_2}$$

Hence

$$\frac{\partial H^{inc}}{\partial n} = ik_2 H^{inc} \ \ on\ \Gamma_L.$$

We have that $k_2^2 = k^2 - k_1^2 = k^2 - (\theta + \theta_{p_0})^2 \geq 0$. Then $p_0 \in Z^-(k,\theta)$ or $p_0 \in Z^0(k,\theta)$ and

$$T(k,\theta)H^{inc} = \mu_p(k,\theta)H^{inc} = i\sqrt{k^2 - (\theta + \theta_{p_0})^2}H^{inc} = i|k_2|H^{inc}$$

which implies

$$l(v) = i(|k_2| + k_2)\langle H^{inc}, v\rangle_{\theta,\Gamma_L}.$$

If $p_0 \in Z^0(k,\theta)$ then $k_2 = 0$, and if $p_0 \in Z^-(k,\theta)$, then by lemma (3.3.2) $\langle H^{inc}, v\rangle_{\theta,\Gamma_L} = 0 \ \ \forall v \in V$, and consequently (3.3.17) is proved. □

3.3.4 Characterization of singular frequencies

We further call k a singular frequency for the problem P_O, if (3.3.16) has non-trivial solutions.

Define

$$\begin{array}{rcccc} T_R(k,\theta) & : & \mathcal{H}_\theta^{\frac{1}{2}}(\Gamma_L) & \to & \mathcal{H}_\theta^{-\frac{1}{2}}(\Gamma_L) \\ & & \sum_{p\in\mathbb{Z}} v_p(L)e^{i(\theta+\theta_p)x_1} & \mapsto & \sum_{p\in Z^+(k,\theta)} \mu_p(k,\theta)v_p(L)e^{i(\theta+\theta_p)x_1} \end{array}$$

and set

$$a_R(H,v) = \int_{O_L} \nabla H.\nabla\bar{v}dx + \langle T_R(k,\theta)H, v\rangle_{\theta,\Gamma_L}, \ \ \forall v \in \mathcal{H}_\theta^1(O_L).$$

Lemma 3.3.3. *If H is a non trivial solution of* (3.3.16)*, then it is a solution of*

$$H \neq 0, \qquad a_R(H,v) = k^2 \int_{O_L} H\bar{v}dx, \quad \forall v \in \mathcal{H}_\theta^1(O_L). \tag{3.3.18}$$

Proof. It is a direct consequence of lemma 3.3.2. □

The converse statement is false. Indeed, a solution u of (3.3.18) is a solution of (3.3.16) if and only if $u_p(L) = 0$ for $p \in Z^-(k,\theta)$.

In fact, we introduced the problem (3.3.18) because $a_R(.,.)$ is hermitian while $a(.,.)$ is not.

Let us consider the following eigenvalue problem:

$$\begin{cases} \text{Find } \ \lambda \text{ such that there exists } \ \ H \in \mathcal{H}_\theta^1(O_L), \ H \neq 0, \text{satsifying} \\ a_R(H,v) = \lambda \displaystyle\int_{O_L} H\bar{v}dx, \quad \forall v \in \mathcal{H}_\theta^1(O_L). \end{cases}$$

(3.3.19)

Since $a_R(H,v) + \int_{O_L} H\bar{v}dx$ is coercive on $\mathcal{H}^1_\theta(O_L)$, the study of problem (3.3.19) is forward (cf. [32]), and we can state the following proposition.

Proposition 15. *The eigenvalues of problem* (3.3.16) *form a sequence* $(\lambda_m(k))_{m\geq 1}$ *which tends to* $+\infty$ *and one has the following characterisation:*

$$\lambda_m(k) = \min_{E\in E_m(\mathcal{H}^1_\theta(O_L))} \sup_{u\in E, u\neq 0} \frac{a_R(u,u)}{\int_{O_L}|u|^2dx} \tag{3.3.20}$$

where $E_m(\mathcal{H}^1_\theta(O_L))$ *denotes the set of all m-dimensional subspaces of* $\mathcal{H}^1_\theta(O_L))$.

A direct consequence of the previous proposition is the following corollary.

Corollary 16. *Problem* (3.3.18) *has solutions if and only if k solves for some* $m \geq 1$ *the equation*

$$\lambda_m(k) = k^2. \tag{3.3.21}$$

Theorem 17. *Problem* P_O *is well posed for every value of* $k \in \mathbb{R}^+$ *except for the values* $k = k_m(\theta, L)$ *the unique solution to the equation* (3.3.21). *Moreover, the sequence* $(k_m(\theta,L))_{m\geq 1}$ *tends to infinity as* $m \to +\infty$.

Proof. To prove that the equation (3.3.21) has one and only one solution, it suffices to check that the function $k \to \lambda_m(k)$ is continuous and non-increasing. The monotonicity is given by the expression (3.3.20). The proof is detailed in (cf. [33]). □

3.4 Reduction of the problem to an integral equation

3.4.1 The Green function in Ω_i

Let G_i be the Green function defined by

$$\begin{cases} \Delta_{-\theta}G_i(x_1,x_2;y_1,y_2) + k^2G_i(x_1,x_2;y_1,y_2) = \delta(x_1-y_1, x_2-y_2), & X \in O_i \\ \dfrac{\partial G_i}{\partial_{-\theta}n}(X;Y) = 0, & X \in \overline{\partial O_i} \end{cases}$$

Lemma 3.4.1. *The Green function* G_i *is given by*

$$G_i(x_1,x_2;y_1,y_2) = \frac{4e^{i\theta(x_1-y_1)}}{hw}\sum_{m,n=0}^{+\infty}\frac{\cos(\frac{m\pi}{w}(x_1+\frac{w}{2}))\cos(\frac{m\pi}{w}(y_1+\frac{w}{2}))}{k^2-(\frac{m\pi}{w})^2-(\frac{n\pi}{h})^2}\cos(\frac{n\pi}{h}(x_2+h))\cos(\frac{n\pi}{h}(y_2+h)) \tag{3.4.1}$$

Proof. We obtain the result by combining the Green function derived in [5] and by using the formula $e^{i\theta(x_1-y_1)}\Delta = \Delta_{-\theta}e^{i\theta(x_1-y_1)}$.

□

3.4.2 The Green function in Ω_e

Let G_e be the Green function defined by

$$\Delta_{-\theta} G_e(x_1, x_2; y_1, y_2) + k^2 G_e(x_1, x_2; y_1, y_2) = \delta^p(x_1 - y_1, x_2 - y_2), \ X \in \Omega_e \tag{3.4.2}$$

$$G_e \text{ is periodic in } x_1 \text{ and } y_1 \tag{3.4.3}$$

$$\frac{\partial G_e}{\partial x_2}(x_1, x_2 = 0; y_1, y_2) = 0 \tag{3.4.4}$$

$$G_e \text{ verifies the radiation conditions } (3.2.14) \tag{3.4.5}$$

where $\delta^p(x_1 - y_1, x_2 - y_2) = \dfrac{1}{d} \displaystyle\sum_{l \in \mathbb{Z}} e^{\frac{-i2\pi l}{d}(x_1 - y_1)} \otimes \delta_{x_2 - y_2}$

Lemma 3.4.2. *The expression of G_e is given by the two following equivalent sums:*

$$G_e(x_1, x_2; y_1, y_2) = \frac{1}{2d} \sum_{l=-\infty}^{+\infty} \frac{1}{\alpha_l} e^{-i\frac{2\pi l}{d}(x_1 - y_1)} \left(e^{\alpha_l |x_2 - y_2|} + e^{\alpha_l |x_2 + y_2|} \right) \tag{3.4.6}$$

$$G_e(x_1, x_2; y_1, y_2) = -\frac{i}{4} \sum_{l=-\infty}^{+\infty} e^{i\theta(x_1 - y_1 + ld)} \{ H_0^{(1)}(k|x_1 - y_1 + ld, x_2 - y_2|) + H_0^{(1)}(k|x_1 - y_1 + ld, x_2 + y_2|) \} \tag{3.4.7}$$

where $H_0^{(1)}$ is the Hankel function of the first kind of order zero, $|x_1 - y_1, x_2 - y_2| = \sqrt{(x_1 - y_1)^2 + (x_2 - y_2)^2}$ and $\alpha_l(k)$ is defined by (3.2.13).

Proof. We develop the solution of (3.4.2) in Fourier basis, and we compute the coefficients of this expansion. We find

$$\frac{1}{2d} \sum_{l=-\infty}^{+\infty} \frac{1}{\alpha_l} e^{-i\frac{2\pi l}{d}(x_1 - y_1)} e^{\alpha_l |x_2 - y_2|}.$$

By eliminating the case where $\alpha_l = 0$ (see [29]) by the method of images we obtain the expression (3.4.6) of G_e.

On the other hand, from [5], and using the formula $e^{i\theta(x_1 - y_1)}\Delta = \Delta_{-\theta} e^{i\theta(x_1 - y_1)}$, we find

$$\tilde{G}_e = -\frac{i}{4} e^{i\theta(x_1-y_1)} \left(H_0^{(1)}(k|x_1-y_1, x_2-y_2|) - H_0^{(1)}(k|x_1-y_1, x_2+y_2| \right)$$

satisfies

$$\begin{cases} \Delta_{-\theta}\tilde{G}_e(x_1,x_2;y_1,y_2) + k^2\tilde{G}_e(x_1,x_2;y_1,y_2) = \delta(x_1-y_1, x_2-y_2), & X \in O_e \\ \dfrac{\partial \tilde{G}_e}{\partial x_2}(x_1, x_2 = 0; y_1, y_2) = 0, & x_1 \in [-\dfrac{d}{2}, \dfrac{d}{2}] \end{cases}$$

We then periodize it in the whole Ω_e using the Fourier series expansion, and obtain

$$G_e(x_1,x_2;y_1,y_2) = \sum_{l,l'=-\infty}^{+\infty} c_{l,l'} e^{i\frac{2l\pi}{d}x_1} e^{i\frac{2l'\pi}{d}y_1}$$

with $c_{l,l'}$ is the Fourier coefficient of $\tilde{G}_e$ given by

$$c_{l,l'} = \frac{1}{d^2} \int_{-\frac{d}{2}}^{\frac{d}{2}} \int_{-\frac{d}{2}}^{\frac{d}{2}} \tilde{G}_e(x_1,x_2;y_1,y_2) e^{i\frac{-2l\pi}{d}x_1} e^{i\frac{2l'\pi}{d}y_1}$$

Finally by the Poisson summation formula, we find that

$$G_e(x_1,x_2;y_1,y_2) = \sum_{l,l'=-\infty}^{+\infty} \tilde{G}_e(x_1+ld, x_2; y_1-l'd, y_2)$$

□

Remark 18. *The Green functions G_i and G_e have different spacial singularities. In fact G_i is singular when X tends to Y whereas G_e is singular when $(x_1-y_1)=0$ or $|x_1-y_1| = pd$.*

3.4.3 Integral representation

Lemma 3.4.3. *Let $Y = (y_1,y_2) \in O_e \cup O_i$, a regular solution H of the problem* (3.2.17) *admits the following integral representations in O_i and O_e*

$$\int_{-\frac{w}{2}}^{\frac{w}{2}} \left(G_e(x_1,0;y_1,0) + G_i(x_1,0;y_1,0)\right) \frac{\partial H_{per}}{\partial x_2}(x_1,0)dx_1 = F(y_1,y_2) \tag{3.4.8}$$

where

$$F(y_1,y_2) = \int_{-\frac{d}{2}}^{-\frac{w}{2}} G_e(x_1,0;y_1,y_2) f(x_1,0)dx_1$$

$$+ \int_{\frac{w}{2}}^{\frac{d}{2}} G_e(x_1,0;y_1,y_2) f(x_1,0)dx_1 - \int_{\partial O_i \setminus \Gamma_w} G_i(x_1,0;y_1,y_2) f(x_1,x_2)dx_1.$$

Proof. We multiply the equation (3.2.17) by G_i and we integrate over O_i. By Green formula we find

$$H_{per}(y_1,y_2)\chi_{\Omega_i}(y_1,y_2)+2i\theta\int_{O_i}\left(\partial_{x_1}G_i(X,Y)H_{per}(X)+\partial_{x_1}H_{per}(X)G_i(X,Y)\right)dX$$
$$-\int_{\partial O_i}\frac{\partial G_i}{\partial n}(X,Y)H_{per}(X)d\sigma(X)+\int_{\partial O_i}\frac{\partial H_{per}}{\partial n}(X)G_i(X,Y)d\sigma(X)=0$$

which is equivalent to:

$$H_{per}(y_1,y_2)\chi_{\Omega_i}(y_1,y_2)+\int_{\partial O_i}\frac{\partial H_{per}}{\partial_\theta n}(X)G_i(X,Y)d\sigma(X)-\int_{\partial O_i}\frac{\partial G_i}{\partial_{-\theta} n}(X,Y)H_{per}(X)=0$$

After taking into account the boundary conditions satisfied by the different functions, we obtain

$$\begin{aligned}H_{per}(y_1,y_2)\chi_{\Omega_i}(y_1,y_2)&=-\int_{-\frac{w}{2}}^{\frac{w}{2}}G_i(x_1,0;y_1,y_2)\frac{\partial H_{per}}{\partial x_2}(x_1,0)dx_1\\&-\int_{\partial O_i\setminus\Gamma_w}G_i(x_1,0;y_1,y_2)f(x_1,x_2)dx_1\end{aligned}\tag{3.4.9}$$

We apply the same method in $O_e\cup\{x_2<L\}$, and get

$$\begin{aligned}H_{per}(y_1,y_2)\chi_{\Omega_e}(y_1,y_2)&=\int_{-\frac{w}{2}}^{\frac{w}{2}}G_e(x_1,0;y_1,y_2)\frac{\partial H_{per}}{\partial x_2}(x_1,0)dx_1\\&-\int_{\frac{d}{2}}^{-\frac{d}{2}}\frac{\partial H_{per}}{\partial x_2}(x_1,L)G_e(x_1,L;y_1,y_2)dx_1+\int_{\frac{d}{2}}^{-\frac{d}{2}}\frac{\partial G_e}{\partial x_2}(x_1,L;y_1,y_2)H_{per}(x_1,L)dx_1\\&-\int_{-\frac{d}{2}}^{-\frac{w}{2}}G_e(x_1,0;y_1,y_2)f(x_1,0)dx_1-\int_{\frac{w}{2}}^{\frac{d}{2}}G_e(x_1,0;y_1,y_2)f(x_1,0)dx_1\end{aligned}$$

From the radiation condition, we have

$$G_e(x_1,x_2;y_1,y_2)=\frac{1}{2d}\sum_{l\in\mathbb{Z}}\frac{1}{\alpha_l}e^{-i\frac{2\pi l}{d}(x_1-y_1)}\left(e^{\alpha_l|x_2-y_2|}+e^{\alpha_l|x_2+y_2|}\right)$$

and

$$H_{per}(x_1,x_2)=\sum_{l\in\mathbb{Z}}H_{per,l}(L_0)e^{\alpha_l(x_2-L_0)}e^{i\frac{2\pi l}{d}x_1}$$

So

$$-\int_{\frac{d}{2}}^{-\frac{d}{2}}\frac{\partial H_{per}}{\partial x_2}(x_1,L)G_e(x_1,L;y_1,y_2)dx_1+\int_{\frac{d}{2}}^{-\frac{d}{2}}\frac{\partial G_e}{\partial x_2}(x_1,L;y_1,y_2)H_{per}(x_1,L)dx_1=0$$

We deduce the following integral representation

$$H_{per}(y_1,y_2)\chi_{\Omega_e}(y_1,y_2) = \int_{-\frac{w}{2}}^{\frac{w}{2}} G_e(x_1,0;y_1,y_2)\frac{\partial H_{per}}{\partial x_2}(x_1,0)dx_1$$
$$-\int_{-\frac{d}{2}}^{-\frac{w}{2}} G_e(x_1,0;y_1,y_2)f(x_1,0)dx_1 - \int_{\frac{w}{2}}^{\frac{d}{2}} G_e(x_1,0;y_1,y_2)f(x_1,0)dx_1. \tag{3.4.10}$$

We take the limit $y_2 \to 0$ and we add (3.4.9) and (3.4.10), we obtain the wanted result.

$$\int_{-\frac{w}{2}}^{\frac{w}{2}} \left(G_e(x_1,0;y_1,0) + G_i(x_1,0;y_1,0)\right)\frac{\partial H_{per}}{\partial x_2}(x_1,0)dx_1 =$$
$$\int_{-\frac{d}{2}}^{-\frac{w}{2}} G_e(x_1,0;y_1,y_2)f(x_1,0)dx_1 + \int_{\frac{w}{2}}^{\frac{d}{2}} G_e(x_1,0;y_1,y_2)f(x_1,0)dx_1$$
$$-\int_{\partial O_i\setminus\Gamma_w} G_i(x_1,0;y_1,y_2)f(x_1,x_2)dx_1$$

□

We now rescale rescale the integral equation (3.4.8) to obtain

$$\int_{-\frac{1}{2}}^{\frac{1}{2}} \left(G_e(wx_1,0;wy_1,0) + G_i(wx_1,0;wy_1,0)\right)\frac{\partial H_{per}}{\partial x_2}(wx_1,0)dx_1 = F(y_1,0), \tag{3.4.11}$$

for all $y \in]-\frac{1}{2},\frac{1}{2}[$: Let $S(w,k)$ be an integral operator from $\widetilde{H}^{-\frac{1}{2}}(-\frac{1}{2},\frac{1}{2})$ to $H^{\frac{1}{2}}(-\frac{1}{2},\frac{1}{2})$, defined by

$$S(w,k)\phi(y_1) := \int_{-\frac{1}{2}}^{\frac{1}{2}} \left(G_e(wx_1,0;wy_1,0) + G_i(wx_1,0;wy_1,0)\right)\phi(x_1)dx_1. \tag{3.4.12}$$

Then, $\dfrac{\partial H_{per}}{\partial x_2}(wx_1,0)$ satisfies the following integral equation

$$S(w,k)\frac{\partial H_{per}}{\partial x_2}(w.,0) = F(y_1,0), \quad y_1 \in]-\frac{1}{2},\frac{1}{2}[. \tag{3.4.13}$$

Following the same analysis developed in [5], based on the radiation condition and Green formulas, we can prove that the scattering resonances of the gratings are exactly the poles of the operator valued function $k \to S^{-1}(w,k)$ (or the zeros of the function $k \to S(w,k)$).

3.5 Asymptotics

Here we first derive the asymptotic expansion of the operator $S(w,k)$ as w tends to zero. Then using complex contour techniques we determine the asymptotic expansion of the resonances. We consider two asymptotic regimes: the first is the case where the period of the array d is fixed and is independent on w, and the second case is when d depends on w linearly, that is $d = mw$ for some constant $m > 0$.

3.5.1 The case d is independent of w

Asymptotic of G_i

$$G_i(wx_1, 0; wy_1, 0) = e^{i\theta w(x_1-y_1)} \frac{4}{hw} \sum_{m,n=0}^{+\infty} \frac{\cos(m\pi(x_1+\frac{1}{2}))\cos(m\pi(y_1+\frac{1}{2}))}{k^2 - (\frac{m\pi}{w})^2 - (\frac{n\pi}{h})^2}$$

We deduce from [5], the following asymptotic expansion

$$\begin{aligned}
&G_i(wx_1, 0; wy_1, 0) = \frac{e(k)}{w} + ie(k)\theta(x_1-y_1) + \frac{2\ln(2)}{\pi} \\
&+ \frac{1}{\pi}\ln(|\sin(\frac{\pi}{2}(x_1-y_1))\sin(\frac{\pi}{2}(x_1+y_1+1))|) \\
&- \frac{2}{h}\left(\frac{1}{6} + \frac{1}{8}((x_1+y_1+1)^2 + (x_1-y_1)^2) - \frac{1}{4}(x_1+y_1+2+|x_1-y_1|)\right) w \\
&+ i\left(\frac{2\ln(2)}{\pi} + \frac{1}{\pi}\ln(|\sin(\frac{\pi}{2}(x_1-y_1))\sin(\frac{\pi}{2}(x_1+y_1+1))|)\right)\theta(x_1-y_1)w \\
&- e(k)\theta^2(x_1-y_1)^2 w + O(w^2)
\end{aligned}$$

where

$$e(k) = -(\frac{1}{hk} + \cot(hk))\frac{2}{k} = \frac{4}{h}\sum_{n=0}^{\infty} \frac{1}{k^2 - (\frac{n\pi}{h})^2}. \tag{3.5.1}$$

Asymptotic of G_e

$$G_e(wx_1, 0; wy_1, 0) = \frac{1}{d}\sum_{l=-\infty}^{+\infty} \frac{1}{\alpha_l} e^{-i\frac{2\pi l w}{d}(x_1-y_1)} \tag{3.5.2}$$

The latter function series is divergent when $x_1 = y_1$ or $w = 0$. In fact, in this case, the general term of the series is $\frac{1}{d}\frac{1}{\alpha_l}$ which is equivalent to $-\frac{1}{2\pi|l|}$ as $|l| \to +\infty$. If $x_1 \neq y_1$, the series is simply convergent by Abel Theorem.

Extraction of the singularities and expansion of G_e

$$G_e(wx_1,0;wy_1,0)=\frac{1}{d}\sum_{l=-M}^{M}\frac{1}{\alpha_l}e^{-i\frac{2\pi l w}{d}(x_1-y_1)}+W(w(x_1-y_1)) \quad (3.5.3)$$

$$G_e(wx_1,0;wy_1,0)=\frac{1}{d\alpha_0}+\frac{1}{d}\sum_{p=0}^{\infty}\sum_{l=1}^{M-1}(\frac{(-1)^p}{\alpha_l}+\frac{1}{\alpha_{-l}})(i\frac{2\pi l}{d})^p(x_1-y_1)^p w^p$$
$$+W(w(x_1-y_1))$$

where $M=M(k)$ defined in (3.2.15) and W is the function defined on $\mathbb{R}\backslash\{0\}$ by:

$$W(X)=\sum_{l=M}^{+\infty}w_l(X)$$

with

$$w_l(X)=\frac{1}{d}\left(\frac{1}{\alpha_l}e^{-i\frac{2\pi l}{d}X}+\frac{1}{\alpha_{-l}}e^{i\frac{2\pi l}{d}X}\right)$$

To extract the singularity of G_e which is also that of W, we will proceed with a development of $w_l(X)$ when l is big ($l>M(k)$)

$$\begin{aligned}\alpha_l(k,\theta) &= -\sqrt{(\theta+\frac{2\pi l}{d})^2-k^2}\\ &= -\sqrt{\theta^2-k^2+\frac{4\theta\pi}{d}l+\frac{(2\pi)^2}{d^2}l^2}\\ &= -\frac{2\pi}{d}l\sqrt{1+\frac{\theta d}{\pi}\frac{1}{l}+\frac{(\theta^2-k^2)d^2}{(2\pi)^2}\frac{1}{l^2}}\end{aligned}$$

Then

$$\begin{aligned}\frac{1}{\alpha_l} &= -\frac{d}{2\pi}\frac{1}{l}(1+\frac{\theta d}{\pi}\frac{1}{l}+\frac{(\theta^2-k^2)d^2}{(2\pi)^2}\frac{1}{l^2})^{-\frac{1}{2}}\\ &= -\frac{d}{2\pi}\frac{1}{l}+\frac{\theta d^2}{8\pi^2}\frac{1}{l^2}-\frac{(2\theta^2+k^2)d^3}{16\pi^3}\frac{1}{l^3}-\frac{(129\theta^3-144\theta k^2)d^4}{48(2\pi)^4}\frac{1}{l^4}+O(\frac{1}{l^5})\end{aligned}$$

On the other hand

$$\frac{1}{\alpha_l}=-\sum_{n=1}^{+\infty}\frac{a_n}{l^n} \quad \text{and} \quad \frac{1}{\alpha_{-l}}=\sum_{n=1}^{+\infty}\frac{a_n}{(-l)^n}$$

Hence

$$
\begin{aligned}
W(X) &= \sum_{l=M}^{+\infty} w_l(X) \\
&= \frac{1}{d}\sum_{l=M}^{+\infty} \frac{e^{-i\frac{2\pi l}{d}X}}{\alpha_l} + \frac{1}{d}\sum_{l=M}^{+\infty} \frac{e^{i\frac{2\pi l}{d}X}}{\alpha_{-l}} \\
&= -\frac{1}{d}\sum_{n=1}^{4} a_n \sum_{l=M}^{+\infty} \frac{e^{-i\frac{2\pi l}{d}X}}{l^n} - \frac{1}{d}\sum_{l=M}^{+\infty} (\frac{1}{\alpha_l} - \sum_{n=1}^{4} \frac{a_n}{l^n}) e^{-i\frac{2\pi l}{d}X} \\
&+ \frac{1}{d}\sum_{n=1}^{4} a_n \sum_{l=M}^{+\infty} \frac{e^{i\frac{2\pi l}{d}X}}{(-l)^n} + \frac{1}{d}\sum_{l=M}^{+\infty} (\frac{1}{\alpha_{-l}} - \sum_{n=1}^{4} \frac{a_n}{(-l)^n}) e^{i\frac{2\pi l}{d}X}
\end{aligned}
$$

Denote

$$
\beta_l = (\frac{1}{\alpha_l} - \sum_{n=1}^{4} \frac{a_n}{l^n}) \quad \text{and} \quad \beta_l = O(\frac{1}{l^5})
$$

Then, we can rewrite $W(X)$ as follows:

$$
\begin{aligned}
W(X) &= -\frac{1}{d}\sum_{n=1}^{4} a_n \sum_{l=M}^{+\infty} \frac{e^{-i\frac{2\pi l}{d}X}}{l^n} - \frac{1}{d}\sum_{l=M}^{+\infty} \beta_l e^{-i\frac{2\pi l}{d}X} + \frac{1}{d}\sum_{n=1}^{4} a_n \sum_{l=M}^{+\infty} \frac{e^{i\frac{2\pi l}{d}X}}{(-l)^n} \\
&+ \frac{1}{d}\sum_{l=M}^{+\infty} \beta_{-l} e^{i\frac{2\pi l}{d}X} \\
&= -\frac{1}{d}\sum_{n=1}^{4} a_n \sum_{l=M}^{+\infty} \frac{e^{-i\frac{2\pi l}{d}X}}{l^n} + \frac{1}{d}\sum_{n=1}^{4} a_n \sum_{l=M}^{+\infty} \frac{e^{i\frac{2\pi l}{d}X}}{(-l)^n} \\
&- \frac{1}{d}\sum_{l=M}^{+\infty}\sum_{p=0}^{+\infty} \beta_l \frac{(-i\frac{2\pi l}{d})^p}{p!} X^p + \frac{1}{d}\sum_{l=M}^{+\infty}\sum_{p=0}^{+\infty} \beta_{-l} \frac{(i\frac{2\pi l}{d})^p}{p!} X^p \\
&= -\frac{1}{d} a_1 \sum_{l=M}^{+\infty} \frac{e^{-i\frac{2\pi l}{d}X}}{l} - \frac{1}{d} a_2 \sum_{l=M}^{+\infty} \frac{e^{-i\frac{2\pi l}{d}X}}{l^2} - \frac{1}{d} a_3 \sum_{l=M}^{+\infty} \frac{e^{-i\frac{2\pi l}{d}X}}{l^3} \\
&- \frac{1}{d} a_4 \sum_{l=M}^{+\infty} \frac{e^{-i\frac{2\pi l}{d}X}}{l^4} - \frac{1}{d} a_1 \sum_{l=M}^{+\infty} \frac{e^{i\frac{2\pi l}{d}X}}{l} + \frac{1}{d} a_2 \sum_{l=M}^{+\infty} \frac{e^{i\frac{2\pi l}{d}X}}{l^2} \\
&- \frac{1}{d} a_3 \sum_{l=M}^{+\infty} \frac{e^{i\frac{2\pi l}{d}X}}{l^3} + \frac{1}{d} a_4 \sum_{l=M}^{+\infty} \frac{e^{i\frac{2\pi l}{d}X}}{l^4} - \frac{1}{d}\sum_{p=0}^{3}\sum_{l=M}^{+\infty} \frac{(-i\frac{2\pi l}{d})^p}{p!} \beta_l X^p \\
&- \frac{1}{d}\sum_{l=M}^{+\infty}\sum_{p=4}^{+\infty} \beta_l \frac{(-i\frac{2\pi l}{d})^p}{p!} X^p + \frac{1}{d}\sum_{p=0}^{3}\sum_{l=M}^{+\infty} \frac{(i\frac{2\pi l}{d})^p}{p!} \beta_{-l} X^p \\
&+ \frac{1}{d}\sum_{l=M}^{+\infty}\sum_{p=4}^{+\infty} \beta_{-l} \frac{(i\frac{2\pi l}{d})^p}{p!} X^p
\end{aligned}
$$

We deduce from some known sums given in [34], which are valid for $0 < X < 2\pi$, the following equalities

$$\sum_{l=1}^{+\infty} \frac{e^{ilX}}{l} = -\ln(1-e^{iX}) = -\ln(2\sin\frac{X}{2}) + i\frac{\pi - X}{2}$$
$$\sum_{l=1}^{+\infty} \frac{e^{-ilX}}{l} = -\ln(1-e^{-iX}) = -\ln(2\sin\frac{X}{2}) - i\frac{\pi - X}{2}$$
$$\sum_{l=1}^{+\infty} \frac{e^{ilX}}{l^2} = \frac{\pi^2}{6} - \frac{X}{4}(2\pi - X) - i(X\ln(X) - X - \frac{X^3}{72} - \frac{X^5}{14400} - ...)$$
$$\sum_{l=1}^{+\infty} \frac{e^{-ilX}}{l^2} = \frac{\pi^2}{6} - \frac{X}{4}(2\pi - X) + i(X\ln(X) - X - \frac{X^3}{72} - \frac{X^5}{14400} - ...)$$
$$\sum_{l=1}^{+\infty} \frac{e^{ilX}}{l^3} = \sum_{n=1}^{+\infty} \frac{1}{n^3} + i(\frac{\pi^2}{6}X - \frac{\pi}{4}X^2 + \frac{X^3}{12}) + (\frac{X^2}{2}\ln(X) - \frac{3}{4}X^2 - \frac{X^4}{288} + ...)$$
$$\sum_{l=1}^{+\infty} \frac{e^{-ilX}}{l^3} = \sum_{n=1}^{+\infty} \frac{1}{n^3} - i(\frac{\pi^2}{6}X - \frac{\pi}{4}X^2 + \frac{X^3}{12}) + (\frac{X^2}{2}\ln(X) - \frac{3}{4}X^2 - \frac{X^4}{288} + ...)$$
$$\sum_{l=1}^{+\infty} \frac{e^{ilX}}{l^4} = \sum_{l=1}^{+\infty} \frac{1}{l^4} + i(\sum_{n=1}^{+\infty} \frac{1}{n^3})X - (\frac{\pi^2}{12}X^2 - \frac{\pi}{12}X^3 + \frac{X^4}{48}) + i(\frac{X^3}{6}\ln(X)$$
$$- \frac{5}{12}X^3 - \frac{X^5}{1440} + ...)$$
$$\sum_{l=1}^{+\infty} \frac{e^{-ilX}}{l^4} = \sum_{l=1}^{+\infty} \frac{1}{l^4} - i(\sum_{n=1}^{+\infty} \frac{1}{n^3})X - (\frac{\pi^2}{12}X^2 - \frac{\pi}{12}X^3 + \frac{X^4}{48}) - i(\frac{X^3}{6}\ln(X)$$
$$- \frac{5}{12}X^3 - \frac{X^5}{1440} + ...)$$

Consequently

$$
\begin{aligned}
W(X) = & -\frac{1}{d}a_1(\sum_{l=1}^{+\infty}\frac{e^{-i\frac{2\pi l}{d}X}}{l}+\sum_{l=1}^{+\infty}\frac{e^{i\frac{2\pi l}{d}X}}{l})+\frac{1}{d}a_1\sum_{l=1}^{M-1}\frac{1}{l}(e^{-i\frac{2\pi l}{d}X}+e^{i\frac{2\pi l}{d}X}) \\
& +\frac{1}{d}a_2(\sum_{l=1}^{+\infty}\frac{e^{i\frac{2\pi l}{d}X}}{l^2}-\sum_{l=1}^{+\infty}\frac{e^{-i\frac{2\pi l}{d}X}}{l^2})-\frac{1}{d}a_2\sum_{l=1}^{M-1}\frac{1}{l^2}(e^{i\frac{2\pi l}{d}X}-e^{-i\frac{2\pi l}{d}X}) \\
& -\frac{1}{d}a_3(\sum_{l=1}^{+\infty}\frac{e^{-i\frac{2\pi l}{d}X}}{l^3}+\sum_{l=1}^{+\infty}\frac{e^{i\frac{2\pi l}{d}X}}{l^3})+\frac{1}{d}a_3\sum_{l=1}^{M-1}\frac{1}{l^3}(e^{-i\frac{2\pi l}{d}X}+e^{i\frac{2\pi l}{d}X}) \\
& +\frac{1}{d}a_4(\sum_{l=1}^{+\infty}\frac{e^{i\frac{2\pi l}{d}X}}{l^4}-\frac{1}{d}a_4\sum_{l=1}^{+\infty}\frac{e^{-i\frac{2\pi l}{d}X}}{l^4})-\frac{1}{d}a_4\sum_{l=1}^{M-1}\frac{1}{l^4}(e^{i\frac{2\pi l}{d}X}e^{-i\frac{2\pi l}{d}X}) \\
& -\frac{1}{d}\sum_{p=0}^{3}\sum_{l=M}^{+\infty}\frac{(-i\frac{2\pi l}{d})^p}{p!}\beta_l X^p-\frac{1}{d}\sum_{l=M}^{+\infty}\sum_{p=4}^{+\infty}\beta_l\frac{(-i\frac{2\pi l}{d})^p}{p!}X^p \\
& +\frac{1}{d}\sum_{p=0}^{3}\sum_{l=M}^{+\infty}\frac{(i\frac{2\pi l}{d})^p}{p!}\beta_{-l}X^p+\frac{1}{d}\sum_{l=M}^{+\infty}\sum_{p=4}^{+\infty}\beta_{-l}\frac{(i\frac{2\pi l}{d})^p}{p!}X^p
\end{aligned}
$$

$$
\begin{aligned}
= & -\frac{1}{d}a_1(\sum_{l=M}^{+\infty}\frac{e^{-i\frac{2\pi l}{d}|X|}}{l}+\sum_{l=M}^{+\infty}\frac{e^{i\frac{2\pi l}{d}|X|}}{l})+\frac{1}{d}a_2\frac{X}{|X|}(\sum_{l=M}^{+\infty}\frac{e^{i\frac{2\pi l}{d}|X|}}{l^2}-\sum_{l=M}^{+\infty}\frac{e^{-i\frac{2\pi l}{d}|X|}}{l^2}) \\
& -\frac{1}{d}a_3(\sum_{l=M}^{+\infty}\frac{e^{-i\frac{2\pi l}{d}|X|}}{l^3}+\sum_{l=M}^{+\infty}\frac{e^{i\frac{2\pi l}{d}|X|}}{l^3})+\frac{1}{d}a_4\frac{X}{|X|}(\sum_{l=M}^{+\infty}\frac{e^{i\frac{2\pi l}{d}|X|}}{l^4}-\frac{1}{d}a_4\sum_{l=M}^{+\infty}\frac{e^{-i\frac{2\pi l}{d}|X|}}{l^4}) \\
& +\frac{1}{d}\sum_{l=1}^{M-1}(\frac{a_1}{l}+\frac{a_3}{l^3})(e^{-i\frac{2\pi l}{d}X}+e^{i\frac{2\pi l}{d}X})-\frac{1}{d}\sum_{l=1}^{M-1}(\frac{a_2}{l^2}+\frac{a_4}{l^4})(e^{i\frac{2\pi l}{d}X}-e^{-i\frac{2\pi l}{d}X}) \\
& -\frac{1}{d}\sum_{p=0}^{3}\sum_{l=M}^{+\infty}\frac{(-i\frac{2\pi l}{d})^p}{p!}\beta_l X^p-\frac{1}{d}\sum_{l=M}^{+\infty}\sum_{p=4}^{+\infty}\beta_l\frac{(-i\frac{2\pi l}{d})^p}{p!}X^p \\
& +\frac{1}{d}\sum_{p=0}^{3}\sum_{l=M}^{+\infty}\frac{(i\frac{2\pi l}{d})^p}{p!}\beta_{-l}X^p+\frac{1}{d}\sum_{l=M}^{+\infty}\sum_{p=4}^{+\infty}\beta_{-l}\frac{(i\frac{2\pi l}{d})^p}{p!}X^p
\end{aligned}
$$

$$
\begin{aligned}
&= \frac{2}{d}a_1 \ln(2\sin\frac{\pi|X|}{d}) - \frac{2i}{d}a_2\frac{X}{|X|}\{\frac{2\pi}{d}|X|\ln|X| + \frac{2\pi}{d}\ln(\frac{2\pi}{d})|X| \\
&- \frac{2\pi}{d}|X| - \frac{\pi^3|X|^3}{9d^3} - \frac{(2\pi)^5}{d^5}\frac{|X|^5}{14400} - ...\} - \frac{2}{d}a_3\{\sum_{n=1}^{\infty}\frac{1}{n^3} + \frac{2\pi^2}{d^2}X^2\ln|X| \\
&+ \frac{2\pi^2}{d^2}\ln(\frac{2\pi}{d})X^2 - \frac{3\pi^2}{d^2}X^2 - \frac{\pi^4}{18d^4}X^4 + ...\} + \frac{2i}{d}a_4\frac{X}{|X|}\{\frac{2\pi}{d}\sum_{n=1}^{+\infty}\frac{1}{n^3}|X| \\
&+ \frac{4\pi^3}{3d^3}|X|^3\ln|X| + \frac{4\pi^3}{3d^3}\ln(\frac{2\pi}{d})|X|^3 - \frac{10\pi^3}{3d^3}|X|^3 - \frac{(2\pi)^5}{d^5}\frac{|X|^5}{1440} + ...\} \\
&+ \frac{2}{d}\sum_{p=0}^{\infty}\sum_{l=1}^{M-1}(\frac{a_1}{l} + \frac{a_3}{l^3})\frac{1}{(2p)!}(i\frac{2\pi l}{d})^{2p}X^{2p} \\
&- \frac{2}{d}\sum_{p=0}^{\infty}\sum_{l=1}^{M-1}(\frac{a_2}{l^2} + \frac{a_4}{l^4})\frac{1}{(2p+1)!}(i\frac{2\pi l}{d})^{2p+1}X^{2p+1} - \frac{1}{d}\sum_{p=0}^{3}\sum_{l=M}^{+\infty}\frac{(-i\frac{2\pi l}{d})^p}{p!}\beta_l X^p \\
&- \frac{1}{d}\sum_{l=M}^{+\infty}\sum_{p=4}^{+\infty}\beta_l\frac{(-i\frac{2\pi l}{d})^p}{p!}X^p + \frac{1}{d}\sum_{p=0}^{3}\sum_{l=M}^{+\infty}\frac{(i\frac{2\pi l}{d})^p}{p!}\beta_{-l}X^p \\
&+ \frac{1}{d}\sum_{l=M}^{+\infty}\sum_{p=4}^{+\infty}\beta_{-l}\frac{(i\frac{2\pi l}{d})^p}{p!}X^p
\end{aligned}
$$

$$
\begin{aligned}
&= \frac{2}{d}a_1 \ln(2\sin\frac{\pi|X|}{d}) - \frac{2i}{d}a_2 X\{\frac{2\pi}{d}\ln(|X|) + \frac{2\pi}{d}\ln(\frac{2\pi}{d}) - \frac{2\pi}{d} - \frac{\pi^3|X|^2}{9d^3} \\
&- \frac{(2\pi)^5}{d^5}\frac{|X|^4}{14400} - ...\} - \frac{2}{d}a_3\{\sum_{n=1}^{\infty}\frac{1}{n^3} + \frac{2\pi^2}{d^2}X^2\ln|X| + \frac{2\pi^2}{d^2}\ln(\frac{2\pi}{d})X^2 \\
&- \frac{3\pi^2}{d^2}X^2 - \frac{\pi^4}{18d^4}X^4 + ...\} + \frac{2i}{d}a_4 X\{\frac{2\pi}{d}\sum_{n=1}^{+\infty}\frac{1}{n^3} + \frac{4\pi^3}{3d^3}|X|^2\ln|X| \\
&+ \frac{4\pi^3}{3d^3}\ln(\frac{2\pi}{d})|X|^2 - \frac{10\pi^3}{3d^3}|X|^2 - \frac{(2\pi)^5}{d^5}\frac{|X|^4}{1440} + ...\} \\
&+ \frac{2}{d}\sum_{p=0}^{\infty}\sum_{l=1}^{M-1}(\frac{a_1}{l} + \frac{a_3}{l^3})\frac{1}{(2p)!}(i\frac{2\pi l}{d})^{2p}X^{2p} \\
&- \frac{2}{d}\sum_{p=0}^{\infty}\sum_{l=1}^{M-1}(\frac{a_2}{l^2} + \frac{a_4}{l^4})\frac{1}{(2p+1)!}(i\frac{2\pi l}{d})^{2p+1}X^{2p+1} \\
&- \frac{1}{d}\sum_{p=0}^{3}\sum_{l=M}^{+\infty}\frac{(-i\frac{2\pi l}{d})^p}{p!}\beta_l X^p - \frac{1}{d}\sum_{l=M}^{+\infty}\sum_{p=4}^{+\infty}\beta_l\frac{(-i\frac{2\pi l}{d})^p}{p!}X^p \\
&+ \frac{1}{d}\sum_{p=0}^{3}\sum_{l=M}^{+\infty}\frac{(i\frac{2\pi l}{d})^p}{p!}\beta_{-l}X^p + \frac{1}{d}\sum_{l=M}^{+\infty}\sum_{p=4}^{+\infty}\beta_{-l}\frac{(i\frac{2\pi l}{d})^p}{p!}X^p
\end{aligned}
$$

We then get

$$
\begin{aligned}
W(X) = {} & C_0 + \frac{1}{\pi}\ln(2\sin\frac{\pi|X|}{d}) + i\frac{\theta}{2\pi}X\ln|X| + \frac{i\theta}{2\pi}\{\ln(\frac{2\pi}{d}) \\
& + \frac{d^2}{32\pi^2}(43\theta^2 - 48k^2)\sum_{n=1}^{\infty}\frac{1}{n^3} - 1 + \sum_{l=1}^{M-1}(\frac{i\theta}{2\pi l} - \frac{i(129\theta^3 - 144\theta k^2)d^2}{24(2\pi)^3 l^3}) \\
& + \frac{1}{d}\sum_{l=1}^{+\infty}(i\frac{2\pi l}{d})(\beta_l + \beta_{-l})\}X - \frac{1}{4\pi}(2\theta^2 + k^2)X^2\ln|X| \\
& + \frac{(2\theta^2 + k^2)}{8\pi}\{-\frac{1}{2}\ln(\frac{2\pi}{d}) + 3 - \frac{1}{2}\sum_{l=1}^{M-1}(\frac{4\pi l}{d^2} + \frac{2\theta^2 + k^2}{2\pi l}) \\
& - \frac{1}{d}\sum_{l=1}^{+\infty}\frac{(i\frac{2\pi l}{d})^2}{2}(\beta_l - \beta_{-l})\}X^2 + \frac{i\theta}{96\pi}(43\theta^2 - 48k^2)X^3\ln|X| \\
& + i\theta\{-\frac{\pi}{36d^2} + \frac{1}{192\pi}(43\theta^2 - 48k^2) + \frac{1}{6}\sum_{l=1}^{M-1}(\frac{-2i\pi\theta l}{d^2} + \frac{i(129\theta^3 - 144\theta k^2)}{48\pi l}) \\
& + \frac{1}{d}\sum_{l=1}^{+\infty}\frac{(i\frac{2\pi l}{d})^3}{6}(\beta_l + \beta_{-l})\}X^3 + o(X^3)
\end{aligned}
$$

and C_0 can be computed as follows:

$$
C_0 = \frac{1}{d}\sum_{l=1}^{M-1}(\frac{1}{\alpha_l} - \frac{d}{2\pi l}) + \frac{1}{d}\sum_{l=1}^{M-1}(\frac{1}{\alpha_{-l}} - \frac{d}{2\pi l}) + \frac{1}{\pi}\sum_{l=1}^{M-1}\frac{1}{l}
$$

Consequently

$$
\begin{aligned}
&G_e(wx_1,0;wy_1,0)=\frac{1}{d\alpha_0(k)}+\frac{1}{d}\sum_{p=0}^{\infty}\sum_{l=1}^{M-1}(\frac{(-1)^p}{\alpha_l}+\frac{1}{\alpha_{-l}})(i\frac{2\pi l}{d})^p(x_1-y_1)^p w^p\\
&+W(w(x_1-y_1))\\
&=\frac{1}{id\sqrt{k^2-\theta^2}}+C+\frac{1}{\pi}\ln(2\sin(\frac{\pi}{d}w|x_1-y_1|))+i\frac{\theta}{2\pi}w(x_1-y_1)\ln(w|x_1-y_1|)\\
&+\frac{i\theta}{2\pi}\{\ln(\frac{2\pi}{d})+\frac{d^2}{32\pi^2}(43\theta^2-48k^2)\sum_{n=1}^{\infty}\frac{1}{n^3}-1\\
&+\sum_{l=1}^{M-1}(\frac{i\theta}{2\pi l}-\frac{i(129\theta^3-144\theta k^2)d^2}{24(2\pi)^3l^3})\}w(x_1-y_1)\\
&+\frac{i\theta}{2\pi}\{\frac{1}{d}\sum_{l=1}^{+\infty}(i\frac{2\pi l}{d})(\beta_l+\beta_{-l})+\sum_{l=1}^{M-1}\frac{i2\pi l}{d}(\frac{1}{\alpha_{-l}}-\frac{1}{\alpha_l})\}w(x_1-y_1)\\
&-\frac{1}{4\pi}(2\theta^2+k^2)w^2(x_1-y_1)^2\ln(w|x_1-y_1|)\\
&+\frac{(2\theta^2+k^2)}{8\pi}\{-\frac{1}{2}\ln(\frac{2\pi}{d})+3-\frac{1}{2}\sum_{l=1}^{M-1}(\frac{4\pi l}{d^2}+\frac{2\theta^2+k^2}{2\pi l})\}w^2(x_1-y_1)^2\\
&+\frac{(2\theta^2+k^2)}{8\pi}\{-\frac{1}{d}\sum_{l=1}^{+\infty}\frac{(i\frac{2\pi l}{d})^2}{2}(\beta_l-\beta_{-l})+\sum_{l=1}^{M-1}(\frac{i2\pi l}{d})^2(\frac{1}{\alpha_{-l}}+\frac{1}{\alpha_l})\}w^2(x_1-y_1)^2\\
&+\frac{i\theta}{96\pi}(43\theta^2-48k^2)w^3(x_1-y_1)^3\ln(w|x_1-y_1|)+i\theta\{-\frac{\pi}{36d^2}\\
&+\frac{1}{192\pi}(43\theta^2-48k^2)+\frac{1}{6}\sum_{l=1}^{M-1}(\frac{-2i\pi\theta l}{d^2}+\frac{i(129\theta^3-144\theta k^2)}{48\pi l})\}w^3(x_1-y_1)^3\\
&+i\theta\{\frac{1}{d}\sum_{l=1}^{+\infty}\frac{(i\frac{2\pi l}{d})^3}{6}(\beta_l+\beta_{-l})+\sum_{l=1}^{M-1}(\frac{i2\pi l}{d})^3(\frac{1}{\alpha_{-l}}-\frac{1}{\alpha_l})\}w^3(x_1-y_1)^3+o(w^3)
\end{aligned}
$$

where $C=C_0+\frac{1}{d}\sum_{l=1}^{M-1}\frac{1}{\alpha_l}+\frac{1}{\alpha_{-l}}$

$$
G_e(wx_1,0;wy_1,0)=\frac{1}{d\alpha_0(k)}+C+\frac{\ln(2)}{\pi}+\frac{1}{\pi}\ln(\frac{2\pi}{d})+\frac{1}{\pi}\ln(w)+\frac{1}{\pi}\ln(|x_1-
$$

$$
y_1|)+\frac{1}{\pi}\ln(\frac{d}{\pi w|x_1-y_1|}\sin(\frac{\pi}{d}w|x_1-y_1|))+i\frac{\theta}{2\pi}(x_1-y_1)w\ln(w)+\frac{i\theta}{2\pi}\{\ln(\frac{2\pi}{d})+
$$

$$
\frac{d^2(43\theta^2-48k^2)}{32\pi^2}\sum_{n=1}^{\infty}\frac{1}{n^3}-1+\sum_{l=1}^{M-1}(\frac{i\theta}{2\pi l}-\frac{i(129\theta^3-144\theta k^2)d^2}{24(2\pi)^3l^3})\}(x_1-y_1)w+
$$

$$
\frac{i\theta}{2\pi}\{\frac{1}{d}\sum_{l=1}^{+\infty}(i\frac{2\pi l}{d})(\beta_l+\beta_{-l})+\sum_{l=1}^{M-1}\frac{i2\pi l}{d}(\frac{1}{\alpha_{-l}}-\frac{1}{\alpha_l})+\ln|x_1-y_1|\}(x_1-y_1)w-
$$

$$\frac{1}{4\pi}(2\theta^2+k^2)(x_1-y_1)^2w^2\ln(w)+\frac{(2\theta^2+k^2)}{8\pi}\{-\frac{1}{2}\ln(\frac{2\pi}{d})+3-\frac{1}{2}\sum_{l=1}^{M-1}(\frac{4\pi l}{d^2}+\frac{2\theta^2+k^2}{2\pi l})\}(x_1-y_1)^2w^2+\frac{(2\theta^2+k^2)}{8\pi}\{-\frac{1}{d}\sum_{l=1}^{+\infty}\frac{(i\frac{2\pi l}{d})^2}{2}(\beta_l-\beta_{-l})+\sum_{l=1}^{M-1}(\frac{i2\pi l}{d})^2(\frac{1}{\alpha_{-l}}+\frac{1}{\alpha_l})-2\ln|x_1-y_1|\}(x_1-y_1)^2w^2+\frac{i\theta}{96\pi}(43\theta^2-48k^2)(x_1-y_1)^3w^3\ln(w)+i\theta\{-\frac{\pi}{36d^2}+\frac{(43\theta^2-48k^2)}{192\pi}+\frac{1}{6}\sum_{l=1}^{M-1}(\frac{-2i\pi\theta l}{d^2}+\frac{i(129\theta^3-144\theta k^2)}{48\pi l})\}(x_1-y_1)^3w^3+i\theta\{\frac{1}{d}\sum_{l=1}^{+\infty}\frac{(i\frac{2\pi l}{d})^3}{6}(\beta_l+\beta_{-l})+\sum_{l=1}^{M-1}(\frac{i2\pi l}{d})^3(\frac{1}{\alpha_{-l}}-\frac{1}{\alpha_l})+\frac{(43\theta^2-48k^2)}{96\pi}\ln|x_1-y_1|\}(x_1-y_1)^3w^3+o(w^3)$$

Simple calculation gives

$$\ln(\frac{d}{\pi w|x_1-y_1|}\sin(\frac{\pi}{d}w|x_1-y_1|))=-\frac{1}{6}\frac{\pi^2}{d^2}|x_1-y_1|^2w^2+O(w^4)$$

Hence

$$G_e(wx_1,0;wy_1,0)=\frac{1}{d\alpha_0(k)}+C+\frac{\ln(2)}{\pi}+\frac{1}{\pi}\ln(\frac{2\pi}{d})+\frac{1}{\pi}\ln(w)+\frac{1}{\pi}\ln(|x_1-y_1|)+i\frac{\theta}{2\pi}(x_1-y_1)w\ln(w)+\frac{i\theta}{2\pi}\{\ln(\frac{2\pi}{d})+\frac{d^2(43\theta^2-48k^2)}{32\pi^2}\sum_{n=1}^{\infty}\frac{1}{n^3}-1+\sum_{l=1}^{M-1}(\frac{i\theta}{2\pi l}-\frac{i(129\theta^3-144\theta k^2)d^2}{24(2\pi)^3l^3})\}(x_1-y_1)w+\frac{i\theta}{2\pi}\{\frac{1}{d}\sum_{l=1}^{+\infty}(i\frac{2\pi l}{d})(\beta_l+\beta_{-l})+\sum_{l=1}^{M-1}\frac{i2\pi l}{d}(\frac{1}{\alpha_{-l}}-\frac{1}{\alpha_l})+\ln|x_1-y_1|\}(x_1-y_1)w-\frac{1}{4\pi}(2\theta^2+k^2)(x_1-y_1)^2w^2\ln(w)+\frac{(2\theta^2+k^2)}{8\pi}\{-\frac{1}{2}\ln(\frac{2\pi}{d})+3-\frac{1}{2}\sum_{l=1}^{M-1}(\frac{4\pi l}{d^2}+\frac{2\theta^2+k^2}{2\pi l})-\frac{1}{6}\frac{\pi^2}{d^2}\}(x_1-y_1)^2w^2+\frac{(2\theta^2+k^2)}{8\pi}\{-\frac{1}{d}\sum_{l=1}^{+\infty}\frac{(i\frac{2\pi l}{d})^2}{2}(\beta_l-\beta_{-l})+\sum_{l=1}^{M-1}(\frac{i2\pi l}{d})^2(\frac{1}{\alpha_{-l}}+\frac{1}{\alpha_l})-2\ln|x_1-y_1|\}(x_1-y_1)^2w^2+\frac{i\theta}{96\pi}(43\theta^2-48k^2)(x_1-y_1)^3w^3\ln(w)+i\theta\{-\frac{\pi}{36d^2}+\frac{(43\theta^2-48k^2)}{192\pi}+\frac{1}{6}\sum_{l=1}^{M-1}(\frac{-2i\pi\theta l}{d^2}+\frac{i(129\theta^3-144\theta k^2)}{48\pi l})\}(x_1-y_1)^3w^3+i\theta\{\frac{1}{d}\sum_{l=1}^{+\infty}\frac{(i\frac{2\pi l}{d})^3}{6}(\beta_l+\beta_{-l})+\sum_{l=1}^{M-1}(\frac{i2\pi l}{d})^3(\frac{1}{\alpha_{-l}}-\frac{1}{\alpha_l})+\frac{(43\theta^2-48k^2)}{96\pi}\ln|x_1-y_1|\}(x_1-y_1)^3w^3+o(w^3).$$

Asymptotic of S(w,k)

Lemma 3.5.1. *The kernel of $S(w,k)$ has the following asymptotic expansion:*

$$G_e(wx_1,0;wy_1,0)+G_i(wx_1,0;wy_1,0)=\theta_w+s_1+s_2w\ln(w)+s_3w+s_4w^2\ln(w)+s_5w^2,$$

where

$$\begin{cases}
\theta_w(k)=\dfrac{1}{d\alpha_0(k)}+\dfrac{e(k)}{w}+\dfrac{\ln(w)}{\pi}+C+\dfrac{1}{\pi}\ln(\dfrac{8\pi}{d})\\
s_1(x_1,y_1)=\dfrac{1}{\pi}\ln(2|\sin(\dfrac{\pi}{2}(x_1-y_1))\sin(\dfrac{\pi}{2}(x_1+y_1+1))|)+\dfrac{1}{\pi}\ln(|x_1-y_1|)\\
+ie(k)\theta(x_1-y_1)\\
s_2(x_1,y_1)=i\dfrac{\theta}{2\pi}(x_1-y_1)\\
s_3(x_1,y_1)=-\dfrac{2}{h}\left(\dfrac{1}{6}+\dfrac{1}{8}((x_1+y_1+1)^2+(x_1-y_1)^2)-\dfrac{1}{4}(x_1+y_1+2+|x_1-y_1|)\right)\\
+i\left(\dfrac{2\ln(2)}{\pi}+\dfrac{1}{\pi}\ln(|\sin(\dfrac{\pi}{2}(x_1-y_1))\sin(\dfrac{\pi}{2}(x_1+y_1+1))|)\right)\theta(x_1-y_1)\\
+\frac{i\theta}{2\pi}\left(\ln(\frac{2\pi}{d})+\frac{d^2(43\theta^2-48k^2)}{32\pi^2}\sum_{n=1}^{\infty}\frac{1}{n^3}-1+\sum_{l=1}^{M-1}(\frac{i\theta}{2\pi l}-\frac{i(129\theta^3-144\theta k^2)d^2}{24(2\pi)^3l^3})\right)(x_1-y_1)\\
-e(k)\theta^2(x_1-y_1)^2+\dfrac{i\theta}{2\pi}\{\dfrac{1}{d}\sum_{l=1}^{+\infty}(i\dfrac{2\pi l}{d})(\beta_l+\beta_{-l})+\sum_{l=1}^{M-1}\dfrac{i2\pi l}{d}(\dfrac{1}{\alpha_{-l}}-\dfrac{1}{\alpha_l})\\
+\ln|x_1-y_1|\}(x_1-y_1)\\
s_4(x_1,y_1)=-\frac{1}{4\pi}(2\theta^2+k^2)(x_1-y_1)^2\\
s_5(w,x_1,y_1)=O(1)
\end{cases}$$

Let $H^{\frac{1}{2}}(-\frac{1}{2},\frac{1}{2})$ be the classical fractional Sobolev space and $\widetilde{H}^{-\frac{1}{2}}(-\frac{1}{2},\frac{1}{2})$ its dual. We define the following integral operators from $\widetilde{H}^{-\frac{1}{2}}(-\frac{1}{2},\frac{1}{2})$ to $H^{\frac{1}{2}}(-\frac{1}{2},\frac{1}{2})$:

$$\begin{cases}
\Theta(w,k)\phi(x) &:= \theta_w(k)\int_{-\frac{1}{2}}^{\frac{1}{2}}\phi(x)dx\\
S_1\phi(y) &:= \int_{-\frac{1}{2}}^{\frac{1}{2}}s_1(x,y)\phi(x)dx\\
S_2\phi(y) &:= \int_{-\frac{1}{2}}^{\frac{1}{2}}s_2(x,y)\phi(x)dx\\
S_3\phi(y) &:= \int_{-\frac{1}{2}}^{\frac{1}{2}}s_3(x,y)\phi(x)dx\\
S_4\phi(y) &:= \int_{-\frac{1}{2}}^{\frac{1}{2}}s_4(x,y)\phi(x)dx\\
S_5\phi(y) &:= \int_{-\frac{1}{2}}^{\frac{1}{2}}s_5(w,x,y)\phi(x)dx
\end{cases}$$

Theorem 19. *The linear operator S_1 is invertible near the zeros of $e(k)$.*

Proof. The operator S_1 can be split into two operators:

$$S_1 = S_0 + ie(k)\theta\tilde{S}_1$$

where

$$S_0\phi(y) = \int_{-\frac{1}{2}}^{\frac{1}{2}} \left(\frac{1}{\pi}\ln(2|\sin(\frac{\pi}{2}(x-y))\sin(\frac{\pi}{2}(x+y+1))|) + \frac{1}{\pi}\ln(|x_1-y_1|) \right)\phi(x)dx,$$

and $\tilde{S}_1\phi(y) = \int_{-\frac{1}{2}}^{\frac{1}{2}} (x-y)\phi(x)dx.$

In [5], it was proved that S_0 is invertible and $\tilde{S}_1$ is compact. Simple calculation gives

$$S_1 = S_0\left(I + ie(k)\theta {S_0}^{-1}\tilde{S}_1\right)$$

So near the zeros of $e(k)$, the norm of $ie(k)\theta {S_0}^{-1}\tilde{S}_1$ is small enough (< 1) and consequently $I + ie(k)\theta {S_0}^{-1}\tilde{S}_1$ is invertible.

□

Theorem 20. *The linear operators $S_j, j = 2, 3, 4, 5$ are compact .*

Proof. The proof is provided in [5]. □

Corollary 21. *$S(w,k)$ is bounded and satisfies the following asymptotic:*

$$S(w,k) = \Theta_w + S_1 + w\ln(w)S_2 + wS_3 + w^2\ln(w)S_4 + w^2S_5$$

We deduce from the previous corollary that $S(w,k)$ is a compact perturbation of the operator S_1 which is invertible. Therefore $S(w,k)$ is a Freedholm operator with index zero. Next we shall derive the asymptotic of its inverse and of its characteristic values as w tends to zero.

Theorem 22.

1. *The operator-valued function $S(w,k)$ is finitely meromorphic and of Freedholm type in D given by* (3.2.12).
2. *The operator-valued function $S(w,k)$ is invertible except at some discrete values.*
3. *The operator-valued function $S^{-1}(w,k)$ is finitely meromorphic on $\mathbb{C}\backslash\mathbb{R}_-$ and its poles are exactly the resonances of the scattering domain Ω.*

Proof. G_e is meromorphic in D. On the other hand, we deduce from the explicit expression of G_i that the kernel of the operator $S(w,k)$ is finitely meromorphic in D.

The integral representation shows that the uniqueness of the Helmholtz problem P_O is equivalent to the invertibility of $S(w,k)$. In theorem (17), we showed that the Helmholtz problem P_O is well-posed for every real value of k except some discrete sequence.

Finally, we deduce from the Steinberg Theorem that the operator-valued function $S(w,k)$ is invertible on $\mathbb{C}$ except some discrete points, the operator-valued function $S^{-1}(w,k)$ is finitely meromorphic on D, and its poles are exactly the resonances of Ω. $\square$

Define

$$L(w,k) = S_1 + w\ln(w)S_2 + wS_3 + w^2\ln(w)S_4 + w^2S_5.$$

Since S_1 is invertible near the zeros of $e(k)$ and $S_j, j = 2,3,4,5$ are compact, the operator $L(w,k)$ is Fredholm of index zero, and it is invertible for w small enough near the zeros of $e(k)$. Using the Neumann series, its inverse can be written as:

$$L^{-1}(w,k) = S_1^{-1} + \sum_{p=1}^{\infty}\left(-S_1^{-1}(\ln(w)S_2 + S_3 + w\ln(w)S_4 + wS_5)\right)^p S_1^{-1}w^p$$

Theorem 23. *Fix $w_0 > 0$ small enough . For $w < w_0$ the following expression holds near the zeros of $e(k)$:*

$$S^{-1}(w,k) = L^{-1}(w,k) - \frac{L^{-1}(w,k)1}{\Theta_w(k)L^{-1}(w,k)1 + 1}\Theta_w(k)L^{-1}(w,k).$$

The resonances of Ω, are exactly the zeros of the function

$$f_w(k) := \Theta_w(k)L^{-1}(w,k)1 + 1.$$

We further denote $\{k_n(w), n \in \mathbb{Z}\}$ the set of the zeros of $f_w(k)$.

Asymptotic of the resonances

Lemma 3.5.2. *The function $f_w(k)$ has the following asymptotic when w goes to zero*

$$\begin{aligned} f_w(k) = \frac{e(k)q_0}{w} + (\frac{q_0}{\pi} - q_1e(k))\ln(w) + (1 + C_1(k)q_0 - e(k)q_2) \\ -(C_1(k)q_1 + \frac{q_2}{\pi})w\ln(w) - \frac{q_1}{\pi}w\ln^2(w) - C_1(k)q_2w + o(w), \end{aligned}$$

where $C_1(k) = \dfrac{1}{d\alpha_0(k)} + C + \dfrac{1}{\pi}\ln(\dfrac{8\pi}{d})$,

and

$$\begin{cases} q_0 &= \langle 1, S_1^{-1}1\rangle \\ q_1 &= \langle 1, S_1^{-1}S_2S_1^{-1}1\rangle \\ q_2 &= \langle 1, S_1^{-1}S_3S_1^{-1}1\rangle \end{cases}$$

which are well defined as functions of k near the zeros of $e(k)$. Here $\langle , \rangle$ is the dual product between $\widetilde{H}^{-1/2}$ and $H^{1/2}$.

Proof. Recall $f_w(k) := \Theta_w(k)L^{-1}(w,k)1 + 1 = \theta_w(k)\langle 1, L^{-1}(w,k)1\rangle + 1$.

On the other hand

$$L^{-1}(w,k) = S_1^{-1} - S_1^{-1}S_2S_1^{-1}w\ln(w) - S_1^{-1}S_3S_1^{-1}w + o(w).$$

Hence

$$\partial_k L^{-1}(w,k) = \partial_k S_1^{-1} - \partial_k(S_1^{-1}S_2S_1^{-1})w\ln(w) + \partial_k(S_1^{-1}S_3S_1^{-1})w + o(w)$$

$$\langle 1, L^{-1}(w,k)1\rangle = \langle 1, S_1^{-1}1\rangle - \langle 1, S_1^{-1}S_2S_1^{-1}1\rangle w\ln(w) - \langle 1, S_1^{-1}S_3S_1^{-1}1\rangle w + o(w)$$

$$\langle 1, \partial_k L^{-1}(w,k)1\rangle = \langle 1, \partial_k S_1^{-1}1\rangle - \langle 1, \partial_k(S_1^{-1}S_2S_1^{-1})1\rangle w\ln(w) - \langle 1, \partial_k(S_1^{-1}S_3S_1^{-1})1\rangle w + o(w),$$

which imply

$$f_w(k) = \theta_w(k)\langle 1, L^{-1}(w,k)1\rangle + 1 = (\frac{e(k)}{w} + \frac{\ln(w)}{\pi} + C_1(k))(q_0 - q_1 w\ln(w) - q_2 w + o(w)) + 1.$$

where $C_1(k) = \dfrac{1}{d\alpha_0(k)} + C + \dfrac{1}{\pi}\ln(\dfrac{16\pi}{d})$.

Therefore

$$f_w(k) = \frac{e(k)q_0}{w} + (\frac{q_0}{\pi} - q_1 e(k))\ln(w) + (1 + C_1(k)q_0 - e(k)q_2) - (C_1(k)q_1 + \frac{q_2}{\pi})w\ln(w) - \frac{q_1}{\pi}w\ln^2(w) - C_1(k)q_2 w + o(w).$$

Consequently

$$\partial_k f_w(k) = \frac{\partial_k(e(k)q_0)}{w} + \partial_k(\frac{q_0}{\pi} - q_1 e(k))\ln(w) + \partial_k(1 + C_1(k)q_0 - e(k)q_2) - \partial_k(C_1(k)q_1 + \frac{q_2}{\pi})w\ln(w) - \frac{\partial_k q_1}{\pi}w\ln^2(w) - \partial_k(C_1(k)q_2)w + o(w).$$

□

Lemma 3.5.3. *$q_0(k) = \langle 1, S_1^{-1}1\rangle$ is different from zero.*

Proof. We begin with computing $\phi = S_1^{-1}1$. We have that $S_1\phi = 1$ which can be written as

$$S_0\phi + ie(k)\theta\langle\phi, x\rangle 1 - ie(k)\theta\langle\phi, 1\rangle x = 1$$

$$\Rightarrow \phi + ie(k)\theta\langle\phi, x\rangle {S_0}^{-1}1 - ie(k)\theta\langle\phi, 1\rangle {S_0}^{-1}x = {S_0}^{-1}1$$

$$\Rightarrow \phi = -ie(k)\theta\langle\phi, x\rangle {S_0}^{-1}1 + ie(k)\theta\langle\phi, 1\rangle {S_0}^{-1}x + {S_0}^{-1}1 \tag{3.5.4}$$

By multiplying the last equation by 1 and x respectively, we find the following system verified by $\langle\phi,1\rangle$ and $\langle\phi,x\rangle$:

$$\begin{cases} \langle\phi,1\rangle + ie(k)\theta\langle\phi,x\rangle\langle {S_0}^{-1}.1,1\rangle - ie(k)\theta\langle\phi,1\rangle\langle {S_0}^{-1}.x,1\rangle & = & \langle {S_0}^{-1}1,1\rangle \\ \langle\phi,x\rangle + ie(k)\theta\langle\phi,x\rangle\langle {S_0}^{-1}.1,x\rangle - ie(k)\theta\langle\phi,1\rangle\langle {S_0}^{-1}.x,x\rangle & = & \langle {S_0}^{-1}1,x\rangle \end{cases}$$

So by resolving the latter system, we can compute $\langle\phi,1\rangle$ and $\langle\phi,x\rangle$ and then compute ϕ by (3.5.4).
Therefore, we can determine $q_0(k) = \langle\phi,1\rangle$, and finally we obtain:

$$q_0(k) = \langle {S_0}^{-1}1,1\rangle \left(1 + e(k)^2\theta^2(\langle {S_0}^{-1}x,1\rangle^2 - \langle {S_0}^{-1}1,1\rangle\langle {S_0}^{-1}x,x\rangle)\right)^{-1}.$$

In [5], it was proven that $\langle {S_0}^{-1}1,1\rangle$ is different from zero. So, we conclude that $q_0(k)$ is different from zero.

□

Remark 24. *The poles of $q_0(k)$ are different from the zeros of $e(k)$. So near the zeros of $e(k)$, $q_0(k)$ is well defined, different from zero and has no poles.*

We denote $\{k_j(0), j \in J\}$ the set of all the zeros of $e(k)$ in $D_{\frac{\pi}{w_0}}$, the complex disc centered at zero and of radius $\frac{\pi}{w_0}$, that is

$$e(k_j(0)) \quad = \quad 0 \tag{3.5.5}$$

Theorem 25. *Let $k_n(0)$ be a fixed zero of the function $e(k)$, that verifies $k_n(0) < \frac{\pi}{w_0}$, and $r_n > 0$ be a fixed positive real such that the set $\{k_j(0), j \in J\} \cap B(k_n(0), r_n)$ is reduced to $k_n(0)$. Then, for $w < w_1 < w_0$ where w_1 is small enough, there exists a unique resonance $k_n(w)$ in $D_{r_n}(k_n(0))$.*

Proof. For k far from the zeros and poles of $e(k)$ and $q_0(k)$, we have

$$\frac{\partial_k f_w(k)}{f_w(k)} = \frac{\partial_k(e((k)q_0)}{e(k)q_0} + O(w).$$

Therefore, the function $\frac{\partial_k f_w(k)}{f_w(k)}$ tends to $\frac{\partial_k(e((k)q_0)}{e(k)q_0}$ when w goes to zero, uniformly on every compact far from the isolated zeros and poles of $e(k)$ and $q_0(k)$.

We note that $q_0(k)$ is not zero and has no poles near the zeros of $e(k)$, the zeros of $e(k)$ are simple and intertwined with its poles $\frac{(n-1)\pi}{h} < k_n(0) < \frac{n\pi}{h}$. So, there exists $r_n > 0$ small enough such that

$$\frac{1}{2i\pi}\int_{|k-k_n(0)|=r_n} \frac{\partial_k(e((k)q_0)}{e(k)q_0} dk = 1.$$

Moreover, as $\lim_{w\to 0} \frac{\partial_k f_w(k)}{f_w(k)} = \frac{\partial_k(e((k)q_0)}{e(k)q_0}$ uniformly with respect to k on the circle $|k - k_n(0)| = r_n$, we see that

$$\lim_{w\to 0} \frac{1}{2i\pi}\int_{|k-k_n(0)|=r_n} \frac{\partial_k f_w(k)}{f_w(k)} dk = 1,$$

and it follows from the Rouché theorem that $\frac{1}{2i\pi}\int_{|k-k_n(0)|=r_n}\frac{\partial_k f_w(k)}{f_w(k)}dk = 1$, for w small enough. Thus, there exists a unique resonance $k_n(w)$ in the complex disc $|k-k_n(0)| < r_n$. □

Theorem 26. *Let $k_n(0)$ a fixed zero of the function $e(k)$, that verifies $k_n(0) < \frac{\pi}{w_0}$. Then, for $w < w_0$, the unique resonance $k_n(w)$ located near $k_n(0)$ has the following asymptotic expansion:*

$$k_n(w) = k_n(0) + \frac{1}{\pi\partial_k e(k_n(0))}w\ln(w) + \frac{1+C_1(k_n(0))q_0(k_n(0))}{q_0(k_n(0))\partial_k e(k_n(0))}w + o(w)$$

In particular, as w goes to zero, its imaginary part behaves like:

$$Im(k_n(w)) = \\ -\frac{1}{\partial_k e(k_n(0))}\left(\frac{Im(q_0(k_n(0))}{Re(q_0(k_n(0))^2 + Im(q_0(k_n(0))^2} - Im(C_1(k_n(0)))\right)w + o(w)$$

Proof. Since $k_n(0)$ is a simple pole of the operator-valued function, the generalized Rouché theorem yield :

$$k_n(w) - k_n(0) = -\frac{1}{2i\pi}tr[\int_{|k-k_n(0)|=r_n}(k-k_n(0))S^{-1}(w,k)\frac{\partial_k S(w,k)}{\partial k}dk]$$

which reduces to

$$k_n(w) - k_n(0) = -\frac{1}{2i\pi}\int_{|k-k_n(0)|=r_n}(k-k_n(0))\frac{\partial_k f_w(k)}{f_w(k)}dk.$$

We have

$$\frac{1}{f_w(k)} = w\left(\frac{1}{e(k)q_0} - \frac{\frac{q_0}{\pi} - q_1 e(k)}{(e(k)q_0)^2}w\ln(w) - \frac{1+C_1(k)q_0 - e(k)q_2}{(e(k)q_0)^2}w + o(w)\right)$$

Hence

$$\begin{aligned}\frac{\partial_k f_w(k)}{f_w(k)} &= \frac{\partial_k(e((k)q_0)}{e(k)q_0} + \{\partial_k(\frac{q_0}{\pi} - q_1 e(k))w\ln(w) + \partial_k(C_1(k)q_0 - e(k)q_2)w\} \\ &\quad * \{-\frac{\frac{q_0}{\pi} - q_1 e(k)}{(e(k)q_0)^2}w\ln(w) - \frac{1+C_1(k)q_0 - e(k)q_2}{(e(k)q_0)^2}w\} \\ &= \frac{\partial_k(e((k)q_0)}{e(k)q_0} + \{\frac{\partial_k(\frac{q_0}{\pi} - q_1 e(k))}{e(k)q_0} - \frac{(\frac{q_0}{\pi} - q_1 e(k))\partial_k(e(k)q_0)}{(e(k)q_0)^2}\}w\ln(w) \\ &\quad + \{\frac{\partial_k(C_1(k)q_0 - e(k)q_2)}{e(k)q_0} - \frac{(1+C_1(k)q_0 - e(k)q_2)\partial_k(e(k)q_0)}{(e(k)q_0)^2}\}w + o(w)\end{aligned}$$

Consequently

$$k_n(w) - k_n(0) = -\frac{1}{2i\pi}\int_{|k-k_n(0)|=r_n}(k-k_n(0))\frac{\partial_k(e((k)q_0)}{e(k)q_0}dk$$

$$-\frac{1}{2i\pi}\int_{|k-k_n(0)|=r_n}(k-k_n(0))\left(\frac{\partial_k(\frac{q_0}{\pi}-q_1e(k))}{e(k)q_0}-\frac{(\frac{q_0}{\pi}-q_1e(k))\partial_k(e(k)q_0)}{(e(k)q_0)^2}\right)dkw\ln(w)$$
$$-\frac{1}{2i\pi}\int_{|k-k_n(0)|=r_n}(k-k_n(0))\left(\frac{\partial_k(C_1q_0-e(k)q_2)}{e(k)q_0}-\frac{(1+C_1q_0-e(k)q_2)\partial_k(e(k)q_0)}{(e(k)q_0)^2}\right)dkw$$
$$+o(w).$$

By Residue Theorem, we find

$$\int_{|k-k_n(0)|=r_n}(k-k_n(0))\frac{\partial_k(e((k)q_0)}{e(k)q_0}dk=0$$
$$\int_{|k-k_n(0)|=r_n}(k-k_n(0))\frac{\partial_k(\frac{q_0}{\pi}-q_1e(k))}{e(k)q_0}dk=0$$
$$\int_{|k-k_n(0)|=r_n}(k-k_n(0))\frac{\partial_k(C_1(k)q_0-e(k)q_2)}{e(k)q_0}dk.$$

Then

$$k_n(w)-k_n(0)=$$
$$\frac{1}{2i\pi}\int_{|k-k_n(0)|=r_n}(k-k_n(0))\frac{(\frac{q_0}{\pi}-q_1e(k))\partial_k(e(k)q_0)}{(e(k)q_0)^2}dkw\ln(w)$$
$$+\frac{1}{2i\pi}\int_{|k-k_n(0)|=r_n}(k-k_n(0))\frac{(1+C_1(k)q_0-e(k)q_2)\partial_k(e(k)q_0)}{(e(k)q_0)^2}dkw+o(w).$$

We have equivalently

$$\int_{|k-k_n(0)|=r_n}(k-k_n(0))\frac{(\frac{q_0}{\pi}-q_1e(k))\partial_k(e(k)q_0)}{(e(k)q_0)^2}dk=2i\pi\frac{\frac{q_0}{\pi}-q_1e(k_n(0))}{\partial_k(e.q_0)(k_n(0))}.$$

$$\int_{|k-k_n(0)|=r_n}(k-k_n(0))\frac{(1+C_1(k)q_0-e(k)q_2)\partial_k(e(k)q_0)}{(e(k)q_0)^2}dk$$
$$=2i\pi\frac{1+C_1(k_n(0))q_0-e(k_n(0))q_2}{\partial_k(e.q_0)(k_n(0))}.$$

Then

$$k_n(w)-k_n(0)=\frac{\frac{q_0}{\pi}-q_1e(k_n(0))}{\partial_k(e.q_0)(k_n(0))}w\ln(w)+\frac{1+C_1(k_n(0))q_0-e(k_n(0))q_2}{\partial_k(e.q_0)(k_n(0))}w+o(w)$$
$$k_n(w)-k_n(0)=\frac{\frac{q_0}{\pi}-q_1e(k_n(0))}{\partial_k(e.q_0)(k_n(0))}w\ln(w)+\frac{1+C_1(k_n(0))q_0-e(k_n(0))q_2}{\partial_k(e.q_0)(k_n(0))}w+$$
$$o(w)$$
$$=\frac{1}{\pi\partial_ke(k_n(0))}w\ln(w)+\frac{1+C_1(k_n(0))q_0(k_n(0))}{q_0(k_n(0))\partial_ke(k_n(0))}w+o(w),$$

which finishes the proof. □

3.5.2 The case $d = mw$

In this part, we consider the asymptotic regime where $d = mw$ where $m > 0$ is a fixed constant. The asymptotic expansion of the Green function G_i is the same as in the previous section.

Asymptotic of G_e

Recall the expression of the Green function

$$G_e(wx_1, 0; wy_1, 0) = \frac{1}{mw} \sum_{l=-\infty}^{+\infty} \frac{1}{\alpha_l} e^{-i\frac{2\pi l}{m}(x_1-y_1)} \tag{3.5.6}$$

$\forall k > 0$, $\exists w_0(k)$, such that $\forall w < w_0(k)$ we have $\mathrm{Re}((\theta + \frac{2\pi l}{mw})^2 - k^2) > 0$. Then $\forall w < w_0(k)$,$\forall l \neq 0$, we have

$$\alpha_l(k, w) = -\sqrt{(\theta + \frac{2\pi l}{mw})^2 - k^2}.$$

Therefore

$$G_e(wx_1, 0; wy_1, 0) = \frac{1}{m\alpha_0 w} + \frac{1}{mw} \sum_{l=1}^{\infty} \frac{1}{\alpha_l} e^{-i\frac{2\pi l}{m}(x_1-y_1)} + \frac{1}{\alpha_{-l}} e^{i\frac{2\pi l}{m}(x_1-y_1)}.$$

To extract the singularity of G_e, we proceed by a expansion of $\alpha_l(k, \theta)$ when l goes to $+\infty$ and w goes to zero.

$$\begin{aligned}
\alpha_l(k, w) &= -\sqrt{(\theta + \frac{2\pi l}{mw})^2 - k^2} \\
&= -\sqrt{\theta^2 - k^2 + \frac{4\theta\pi}{mw} l + \frac{(2\pi)^2}{m^2 w^2} l^2} \\
&= -\frac{2\pi}{m}\frac{l}{w}\sqrt{1 + \frac{\theta m}{\pi}\frac{w}{l} + \frac{(\theta^2 - k^2)m^2}{(2\pi)^2}\frac{w^2}{l^2}}.
\end{aligned}$$

Then

$$\frac{1}{\alpha_l} = -\frac{m}{2\pi}\frac{w}{l}(1 + \frac{\theta m}{\pi}\frac{w}{l} + \frac{(\theta^2 - k^2)m^2}{(2\pi)^2}\frac{w^2}{l^2})^{-\frac{1}{2}},$$

and

$$\frac{1}{\alpha_l} = -\frac{m}{2\pi}\frac{w}{l} + \frac{\theta m^2}{8\pi^2}\frac{w^2}{l^2} - \frac{(2\theta^2 + k^2)m^3}{16\pi^3}\frac{w^3}{l^3} - \frac{(129\theta^3 - 144\theta k^2)m^4}{48(2\pi)^4}\frac{w^4}{l^4} + O(\frac{w^5}{l^5}).$$

We can write the following expansion:

$$\frac{1}{\alpha_l} = -\sum_{n=1}^{+\infty} a_n \frac{w^n}{l^n},$$

and

$$\frac{1}{\alpha_{-l}} = \sum_{n=1}^{+\infty} a_n \frac{w^n}{(-l)^n},$$

with a_i, $i = 1, \cdots, 4$, are known explicitly.

Therefore

$$\begin{aligned}
&G_e(wx_1, 0; wy_1, 0) = \\
&\frac{1}{m\alpha_0 w} + \frac{1}{mw}\sum_{l=1}^{+\infty} \frac{1}{\alpha_l} e^{-i\frac{2\pi l}{m}(x_1-y_1)} \\
&+\frac{1}{mw}\sum_{l=1}^{+\infty} \frac{1}{\alpha_{-l}} e^{i\frac{2\pi l}{m}(x_1-y_1)} \\
&= \frac{1}{m\alpha_0 w} - \frac{1}{mw}\sum_{l=1}^{+\infty}\sum_{n=1}^{+\infty} a_n \frac{w^n}{l^n} e^{-i\frac{2\pi l}{m}(x_1-y_1)} \\
&+\frac{1}{mw}\sum_{l=1}^{+\infty}\sum_{n=1}^{+\infty} a_n \frac{w^n}{(-l)^n} e^{i\frac{2\pi l}{m}(x_1-y_1)} \\
&= \frac{1}{m\alpha_0 w} - \frac{1}{mw}\sum_{n=1}^{4} a_n \sum_{l=1}^{+\infty} \frac{e^{-i\frac{2\pi l}{m}(x_1-y_1)}}{l^n} w^n \\
&-\frac{1}{mw}\sum_{l=1}^{+\infty}(\frac{1}{\alpha_l} - \sum_{n=1}^{4} \frac{a_n w^n}{l^n}) e^{-i\frac{2\pi l}{m}(x_1-y_1)} \\
&+\frac{1}{mw}\sum_{n=1}^{4} a_n \sum_{l=1}^{+\infty} \frac{e^{i\frac{2\pi l}{m}(x_1-y_1)}}{(-l)^n} w^n \\
&+\frac{1}{mw}\sum_{l=1}^{+\infty}(\frac{1}{\alpha_{-l}} - \sum_{n=1}^{4} \frac{a_n w^n}{(-l)^n}) e^{i\frac{2\pi l}{m}(x_1-y_1)}.
\end{aligned}$$

On the other hand

$$(\frac{1}{\alpha_l} - \sum_{n=1}^{4} \frac{a_n w^n}{l^n}) = O(\frac{w^5}{l^5}).$$

Then

$$
\begin{aligned}
G_e(wx_1, 0; wy_1, 0) = \\
\frac{1}{m\alpha_0 w} - \frac{1}{mw}\sum_{n=1}^{4} a_n(\sum_{l=1}^{+\infty}\frac{e^{-i\frac{2\pi l}{m}(x_1-y_1)}}{l^n} \\
-\sum_{l=1}^{+\infty}\frac{e^{i\frac{2\pi l}{m}(x_1-y_1)}}{(-l)^n})w^n + O(w^4) \\
= \frac{1}{m\alpha_0 w} - \frac{1}{m}a_1(\sum_{l=1}^{+\infty}\frac{e^{-i\frac{2\pi l}{m}(x_1-y_1)}}{l} \\
+\sum_{l=1}^{+\infty}\frac{e^{i\frac{2\pi l}{m}(x_1-y_1)}}{l}) - \frac{1}{m}a_2(\sum_{l=1}^{+\infty}\frac{e^{-i\frac{2\pi l}{m}(x_1-y_1)}}{l^2} - \sum_{l=1}^{+\infty}\frac{e^{i\frac{2\pi l}{m}(x_1-y_1)}}{l^2})w \\
-\frac{1}{m}a_3(\sum_{l=1}^{+\infty}\frac{e^{-i\frac{2\pi l}{m}(x_1-y_1)}}{l^3} + \sum_{l=1}^{+\infty}\frac{e^{i\frac{2\pi l}{m}(x_1-y_1)}}{l^3})w^2 + O(w^3)
\end{aligned}
$$

$$
= \frac{1}{m\alpha_0 w} - \frac{1}{m}a_1(\sum_{l=1}^{+\infty}\frac{e^{-i\frac{2\pi l}{m}|x_1-y_1|}}{l} \tag{3.5.7}
$$

$$
+\sum_{l=1}^{+\infty}\frac{e^{i\frac{2\pi l}{m}|x_1-y_1|}}{l}) - \frac{1}{m}a_2\frac{(x_1-y_1)}{|x_1-y_1|}(\sum_{l=1}^{+\infty}\frac{e^{-i\frac{2\pi l}{m}|x_1-y_1|}}{l^2} \tag{3.5.8}
$$

$$
-\sum_{l=1}^{+\infty}\frac{e^{i\frac{2\pi l}{m}|x_1-y_1|}}{l^2})w - \frac{1}{m}a_3(\sum_{l=1}^{+\infty}\frac{e^{-i\frac{2\pi l}{m}|x_1-y_1|}}{l^3} + \sum_{l=1}^{+\infty}\frac{e^{i\frac{2\pi l}{m}|x_1-y_1|}}{l^3})w^2 + O(w^3). \tag{3.5.9}
$$

Using the explicit sums cited in the previous section, we obtain

$$
\begin{aligned}
&G_e(wx_1,0;wy_1,0)=\\
&\frac{1}{m\alpha_0(k)w}+\frac{2}{m}a_1\ln(2\sin\frac{\pi|x_1-y_1|}{m})\\
&-\frac{1}{m}a_2\frac{(x_1-y_1)}{|x_1-y_1|}(\sum_{l=1}^{+\infty}\frac{e^{-i\frac{2\pi l}{m}|x_1-y_1|}}{l^2}\\
&-\sum_{l=1}^{+\infty}\frac{e^{i\frac{2\pi l}{m}|x_1-y_1|}}{l^2})w\\
&-\frac{1}{m}a_3(\sum_{l=1}^{+\infty}\frac{e^{-i\frac{2\pi l}{m}|x_1-y_1|}}{l^3}+\sum_{l=1}^{+\infty}\frac{e^{i\frac{2\pi l}{m}|x_1-y_1|}}{l^3})w^2+O(w^3),
\end{aligned}
$$

and finally

$$
\begin{aligned}
G_e(wx_1,0;wy_1,0)&=\frac{1}{m\alpha_0(k)w}+\frac{1}{\pi}\ln(2\sin\frac{\pi|x_1-y_1|}{m})\\
&+\frac{\theta m}{8\pi^2}\frac{(x_1-y_1)}{|x_1-y_1|}(\sum_{l=1}^{+\infty}\frac{e^{-i\frac{2\pi l}{m}|x_1-y_1|}}{l^2}-\sum_{l=1}^{+\infty}\frac{e^{i\frac{2\pi l}{m}|x_1-y_1|}}{l^2})w\\
&-\frac{(2\theta^2+k^2)m^3}{16\pi^3}(\sum_{l=1}^{+\infty}\frac{e^{-i\frac{2\pi l}{m}|x_1-y_1|}}{l^3}+\sum_{l=1}^{+\infty}\frac{e^{i\frac{2\pi l}{m}|x_1-y_1|}}{l^3})w^2+O(w^3).
\end{aligned}
$$

Asymptotic of S(w,k)

Lemma 3.5.4. *The kernel of $S(w,k)$ has the following asymptotic expansion as w tends to zero*

$$
G_e(wx_1,0;wy_1,0)+G_i(wx_1,0;wy_1,0)=\theta_w+s_1+s_2w+s_3w^2, \quad (3.5.10)
$$

where

$$
\begin{cases}
\theta_w(k) & =\frac{1}{m\alpha_0(k)w}+\frac{e(k)}{w}+\frac{2\ln(2)}{\pi}+\ln(\pi)-\ln(m)\\
s_1(x_1,y_1) & =\frac{1}{\pi}\ln(2|(x_1-y_1)\sin(\frac{\pi}{2}(x_1-y_1))\sin(\frac{\pi}{2}(x_1+y_1+1))|)+ie(k)\theta(x_1-y_1)\\
& +\frac{1}{\pi}\ln(\frac{\sin\frac{\pi|x_1-y_1|}{m}}{\frac{\pi}{m}|x_1-y_1|})\\
s_2(x_1,y_1) & =-\frac{2}{h}\left(\frac{1}{6}+\frac{1}{8}((x_1+y_1+1)^2+(x_1-y_1)^2)-\frac{1}{4}(x_1+y_1+2+|x_1-y_1|)\right)\\
& +i\left(\frac{2\ln(2)}{\pi}+\frac{1}{\pi}\ln(|\sin(\frac{\pi}{2}(x_1-y_1))\sin(\frac{\pi}{2}(x_1+y_1+1))|)\right)\theta(x_1-y_1)\\
& -e(k)\theta^2(x_1-y_1)^2+\frac{\theta m}{8\pi^2}\frac{(x_1-y_1)}{|x_1-y_1|}(\sum_{l=1}^{+\infty}\frac{e^{-i\frac{2\pi l}{m}|x_1-y_1|}}{l^2}-\sum_{l=1}^{+\infty}\frac{e^{i\frac{2\pi l}{m}|x_1-y_1|}}{l^2})\\
s_3(w,x_1,y_1) & =O(1)
\end{cases}
$$

We define the following integral operators from $\widetilde{H}^{-\frac{1}{2}}(-\frac{1}{2},\frac{1}{2})$ to $H^{\frac{1}{2}}(-\frac{1}{2},\frac{1}{2})$:

$$\begin{cases} \Theta(w,k)\phi(x) & := & \theta_w(k) < 1, \phi > \\ S_1\phi(y) & := & \int_{-\frac{1}{2}}^{\frac{1}{2}} s_1(x,y)\phi(x)dx \\ S_2\phi(y) & := & \int_{-\frac{1}{2}}^{\frac{1}{2}} s_2(x,y)\phi(x)dx \\ S_3\phi(y) & := & \int_{-\frac{1}{2}}^{\frac{1}{2}} s_3(x,y)\phi(x)dx \end{cases}$$

Theorem 27. *There exists m_0 large enough such that for $m > m_0$ the linear operator S_1 is invertible if k is in a small neighborhood of the zeros of $e(k) + \dfrac{1}{m\alpha_0(k)w}$.*

Proof. The operator S_1 can be decomposed to two operators:

$$S_1 = S_0 + S_{0,m} + ie(k)\theta\tilde{S_1},$$

where

$$S_0\phi(y) = \int_{-\frac{1}{2}}^{\frac{1}{2}} \frac{1}{\pi} \ln(2|(x_1 - y_1)\sin(\frac{\pi}{2}(x_1 - y_1))\sin(\frac{\pi}{2}(x_1 + y_1 + 1))|)\phi(x)dx,$$

$$S_{0,m}\phi(y) = \int_{-\frac{1}{2}}^{\frac{1}{2}} \frac{1}{\pi} \ln(\frac{\sin\frac{\pi|x_1-y_1|}{m}}{\frac{\pi}{m}|x_1 - y_1|})\phi(x)dx,$$

and

$$\tilde{S_1}\phi(y) = \int_{-\frac{1}{2}}^{\frac{1}{2}} (x - y)\phi(x)dx.$$

In [5], it was proved that S_0 is invertible. We can show that $\exists m_1$, such that $\forall m > m_0$ the norm of ${S_0}^{-1}S_{0,m}$ is less that 1. Consequently, $\forall m > m_0$, $S_0 + S_{0,m}$ is invertible.

Then

$$S_1 = (S_0 + S_{0,m})\left(I + ie(k)\theta(S_0 + S_{0,m})^{-1}\tilde{S_1}\right).$$

On the other hand, there if k is close to a zero of $e(k) + \dfrac{1}{m\alpha_0(k)w}$, there exists m_2 large enough such that the norm of $ie(k)\theta(S_0+S_{0,m})^{-1}\tilde{S_1}$ becomes less than 1 for $m > m_2$.

In conclusion there exists $m_0 = max(m_1, m_2)$ such that $\forall m > m_0$ and inside some neighborhood of the zeros of $e(k) + \dfrac{1}{m\alpha_0(k)w}$, S_1 is invertible.

□

Theorem 28. *The linear operators $S_j, j = 2, 3$ are compact.*

Proof. The proof is provided in [5]. □

Corollary 29. *$S(w, k)$ is bounded and satisfies the following asymptotic expansion:*

$$S(w, k) = \Theta_w + S_1 + wS_2 + w^2 S_3. \tag{3.5.11}$$

We deduce from the previous corollary that $S(w, k)$ is a compact perturbation of the operator S_1 which is invertible. Therefore $S(w, k)$ is a Freedholm operator with index zero. In the next subsection, we derive the asymptotic expansion of its inverse and of its characteristic values.

Theorem 30.

1. *The operator-valued function $S(w, k)$ is finitely meromorphic and of Freedholm type in D.*
2. *The operator-valued function $S(w, k)$ is invertible except some discrete points.*
3. *The operator-valued function $S^{-1}(w, k)$ is finitely meromorphic on $\mathbb{C}\backslash\mathbb{R}_-$ and its poles are exactly the resonances of the scattering domain Ω*

Proof. The proof is similar to the one of Theorem 22.

□

Define

$$L(w, k) = S_1 + wS_2 + w^2 S_3.$$

Since S_1 is invertible and $S_j, j = 2, 3$ are compact, the operator $L(w, k)$ is Fredholm of index zero and it is invertible for w small enough and k near the zeros of $e(k)$. Using the Neumann series, its inverse can be rewritten as

$$L^{-1}(w, k) = S_1^{-1} + \sum_{p=1}^{\infty} (-1)^p \left(wS_1^{-1}S_2 + w^2 S_1^{-1}S_3\right)^p S_1^{-1}.$$

Theorem 31. *Fix $w_0 > 0$ small enough. For $w < w_0$ the following expression holds near the zeros of $e(k)$:*

$$S^{-1}(w, k) = L^{-1}(w, k) - \frac{L^{-1}(w, k)1}{\Theta_w(k)L^{-1}(w, k)1 + 1}\Theta_w(k)L^{-1}(w, k).$$

The resonances frequencies are exactly the zeros of the function

$$f_w(k) := \Theta_w(k)L^{-1}(w, k)1 + 1.$$

Lemma 3.5.5. *The function $f_w(k)$ has the following asymptotic when w goes to zero,*

$$f_w(k) = \frac{1}{w}\left(q_0(k)g_m(k) + (1 + q_0(k)c(m) - q_1(k)g_m(k))w\right)$$

where:

$$\begin{cases} q_0(k) &= \langle 1, S_1^{-1}1\rangle \\ q_1(k) &= \langle 1, S_1^{-1}S_2S_1^{-1}1\rangle \\ g_m(k) &= \frac{1}{m\alpha_0(k)} + e(k) \\ c(m) &= \frac{2\ln(2)}{\pi} + \ln(\pi) - \ln(m) \end{cases}$$

Proof. Recall $f_w(k) = \Theta_w(k)L^{-1}(w,k)1 + 1 = \theta_w(k)\langle 1, L^{-1}(w,k)1\rangle + 1$.

Froward calculation gives

$$L^{-1}(w,k) = S_1^{-1} - S_1^{-1}S_2S_1^{-1}w + o(w).$$

Then

$$\langle 1, L^{-1}(w,k)1\rangle = \langle 1, S_1^{-1}1\rangle - \langle 1, S_1^{-1}S_2S_1^{-1}1\rangle w + o(w).$$

$f_w(k) = \theta_w(k)\langle 1, L^{-1}(w,k)1\rangle + 1 = (\dfrac{1}{m\alpha_0(k)w} + \dfrac{e(k)}{w} + c(m))(q_0 - q_1w + o(w)) + 1.$

Therefore:

$$f_w(k) = \frac{1}{w}\left(q_0(e(k) + \frac{1}{m\alpha_0(k)}) + (1 + q_0c(m) - q_1(\frac{1}{m\alpha_0(k)} + e(k)))w\right).$$

□

Lemma 3.5.6. *The function $q_0(k) = \langle 1, S_1^{-1}1\rangle$ is different from zero.*

Proof. The proof is similar to the one of lemma 3.5.3. □

We note $\{k_j(0), j \in J\}$ the set of all the zeros of $g_m(k)$ in $D_{\frac{\pi}{w_0}}$, that is

$$g_m(k_j(0)) = 0. \tag{3.5.12}$$

A long computation shows that these zeros are all simple and located in the low complex half plan.

Theorem 32. *Let $k_n(0)$ be a fixed zero of the function $g_m(k)$, that verifies $k_n(0) < \frac{\pi}{w_0}$, and r_n be a fixed positive real such that the set $\{k_j(0), j \in J\} \cap D_{r_n}(k_n(0))$ is reduced to $k_n(0)$. Then, for $w < w_1 < w_0$ where w_1 is small enough, there exists a unique resonance $k_n(w)$ in $D_{r_n}(k_n(0))$.*

Proof. We first observe that

$$\frac{\partial_k f_w(k)}{f_w(k)} = \frac{\partial_k(g_m(k))}{g_m(k)} + O(w).$$

Therefore, the function $\frac{\partial_k f_w(k)}{f_w(k)}$ tends to $\frac{\partial_k(g_m(k))}{g_m(k)}$ when w goes to zero, uniformly on every compact far from the isolated zeros and poles of $g_m(k)$.

There exists $r_n > 0$ small enough such that:

$$\frac{1}{2i\pi}\int_{|k-k_n(0)|=r_n} \frac{\partial_k(g_m(k))}{g_m(k)} dk = 1.$$

Moreover, as $\lim_{w\to 0} \frac{\partial_k f_w(k)}{f_w(k)} = \frac{\partial_k(g_m(k))}{g_m(k)}$ uniformly with respect to k on the circle $|k - k_n(0)| = r_n$, we have

$$\lim_{w\to 0} \frac{1}{2i\pi}\int_{|k-k_n(0)|=r_n} \frac{\partial_k f_w(k)}{f_w(k)} dk = 1,$$

It follows from the Rouché Theorem that $\frac{1}{2i\pi}\int_{|k-k_n(0)|=r_n} \frac{\partial_k f_w(k)}{f_w(k)} dk = 1$, for w small enough. Thus, there exists a unique resonance $k_n(w)$ in the complex disc $|k - k_n(0)| < r_n$. □

Theorem 33. *Let $k_n(0)$ be a fixed zero of the function $g_m(k)$, that verifies $k_n(0) < \frac{\pi}{w_0}$. Then, for $w < w_0$, the unique resonance $k_n(w)$ located near $k_n(0)$ has the following expansion:*

$$k_n(w) = k_n(0) - \frac{1}{2i\pi}\left(\frac{1}{\partial_k g_m(k_n(0))q_0(k_n(0))} + \frac{c(m)}{\partial_k g_m(k_n(0))}\right)w + o(w).$$

$$\begin{aligned} Im(k_n(w)) &= Im(k_n(0)) \\ &+ \frac{1}{2i\pi}\frac{Im(\partial_k g_m(k_n(0))q_0(k_n(0)))}{Re^2(\partial_k g_m(k_n(0))q_0(k_n(0))) + Im^2(\partial_k g_m(k_n(0))q_0(k_n(0)))} \\ &+ \frac{1}{2i\pi}\frac{c(m)Im(\partial_k g_m(k_n(0)))}{Re^2(\partial_k g_m(k_n(0))) + Im^2(\partial_k g_m(k_n(0)))}w + o(w). \end{aligned}$$

Proof. Since $k_n(0)$ is a simple pole of the operator-valued function, the generalized Rouché theorem yields

$$k_n(w) - k_n(0) = -\frac{1}{2i\pi} tr\left[\int_{|k-k_n(0)|=r_n} (k - k_n(0))S^{-1}(w,k)\frac{\partial_k S(w,k)}{\partial k} dk\right],$$

which reduces to

$$k_n(w) - k_n(0) = -\frac{1}{2i\pi}\int_{|k-k_n(0)|=r_n}(k-k_n(0))\frac{\partial_k f_w(k)}{f_w(k)}dk.$$

On the other hand

$$\frac{\partial_k f_w(k)}{f_w(k)} =$$
$$\frac{\partial_k(q_0(k)g_m(k))}{q_0(k)g_m(k)} + \frac{c(m)\partial_k g_m(k) - \partial_k q_1(k)g_m(k) - \partial_k g_m(k)q_1(k)}{q_0(k)g_m(k)}w$$
$$-\frac{(1+q_0(k)c(m) - q_1(k)g_m(k))(\partial_k(q_0(k)g_m(k)))}{(q_0(k)g_m(k))^2}w + o(w).$$

Since $k_n(0)$ is a simple zero of the function $g_m(k)$, we deduce from the Residue Theorem that for every holomorphic function ϕ in $\{|k-k_n(0)| \leq r_n\}$ the following equalities hold

$$\int_{|k-k_n(0)|=r_n}(k-k_n(0))\frac{\partial_k g_m(k)}{g_m(k)}\phi(k)dk = 0,$$

$$\int_{|k-k_n(0)|=r_n}(k-k_n(0))\frac{\partial_k g_m(k)}{g_m(k)^2}\phi(k)dk = \frac{\phi(k_n(0))}{\partial_k g_m(k_n(0))}.$$

Then

$$k_n(w) - k_n(0) =$$
$$-\frac{1}{2i\pi}\int_{|k-k_n(0)|=r_n}(k-k_n(0))\frac{(1+q_0(k)c(m))(\partial_k(q_0(k)g_m(k)))}{(q_0(k)g_m(k))^2}dkw + o(w),$$

$$k_n(w) - k_n(0) = -\frac{1}{2i\pi}\frac{(1+q_0(k_n(0))c(m))}{\partial_k(q_0 g_m)(k_n(0))}w + o(w),$$

$$k_n(w) - k_n(0) = -\frac{1}{2i\pi}\frac{(1+q_0(k_n(0))c(m))}{\partial_k g_m(k_n(0))q_0(k_n(0))}w + o(w),$$

which achieve the proof of the theorem. □

Chapter 4

Green's function for a real metallic slab cladded in a dielectric media

Sommaire

4.1 Introduction 111
4.2 Position of the problem 112
4.2.1 Description of the geometry and notations 112
4.2.2 Problem formulation 113
4.2.3 Drude's model for real conductor permittivity . . . 114
4.3 Thin layer limit model 115
4.3.1 Motivation 115
4.3.2 The Green function of the limiting problem 116
4.3.3 Behavior of G_0 as a function of the contrast η . . 126
4.4 Numerical results 132

4.1 Introduction

The first works on plasmonic waveguide date back to the end of the nineties with the discovery of nanowires that have the ability to highly confine plasmon modes [35]. The metal ribbon waveguides then have been widely studied thanks to their particular optical properties and to the fact that they are easily realizable by lithography methods [36, 37]. Their shape is somehow similar to rectangular section guides studied in [38]. However, they are much thinner than the latter: about $50nm$ thick for a width of a few micrometers. Moreover, their localized modes are resulting from the lateral confinement of the surface plasmon polariton, which differs clearly from the modes of the dielectric waveguides interpreted as resulting from the confinement of volume

electromagnetic modes of the dielectric. The plasmonic waveguides can be found in many high-technology products such compact lasers, electro-optic modulators, and biosensors.

In this chapter we focus on a particular structure of plasmonic waveguides which consists in a metal slab cladded in a dielectric media. Our objective consists in studying the quasi-static resonances of the system. We first compute the associated Green function using Fourier analysis. We then investigate the set of frequencies and the spatial region where it blows up. These frequencies correspond to plasmonic surface waves resonances.

The chapter is organized as follows. In the second section, we introduce the physical problem. The second section is dedicated to the reconstruction of the Green function of the quasi-static problem, and its behavior with respect to the contrast and the spatial position. The explicit expression of the Green function is given in theorem 36 while the discussion on its singular behavior is provided in subsection 4.3.3 (Theorems 37, 38, and the discussion at the end of the subsection). In section 4, we present some numerical examples that validate the asymptotic analysis performed in the previous section. This chapter is the subject of a research report [**?**].

4.2 Position of the problem

For simplicity many studies on scattering problems dealing with metallic structures have considered the metal as a perfect conductor. In that case the electromagnetic permittivity ε is a real function, and the electromagnetic waves are totally reflected, and do not penetrate the metal. However, the permittivity of real conductors is a complex function, does depend on the frequency ω of the incident fields, that is $\varepsilon = \varepsilon_m(\omega) \in \mathbb{C}$, and the electromagnetic fields can propagate inside the metal layer. In this context surface plasmon resonances may occur. Resonance phenomena related to the surface waves along the interface may be responsible of the extraordinary transmission of electromagnetic waves through thin metallic layers.

4.2.1 Description of the geometry and notations

We consider an homogeneous infinite conductor layer of thickness $2h$ (Figure 4.1). We denote $M = \{(x, y, z) \in \mathbb{R}^3, -h \leq x \leq h\}$ the region occupied by this layer. We assume that the conductor is real, that is the electric permittivity $\varepsilon_m(\omega)$ is a complex function of the frequency ω of the incident wave. In other words, the incident wave can change the optical properties of the metal layer [39]. The regions $x > h$ and $x < -h$ are denoted D_+ and

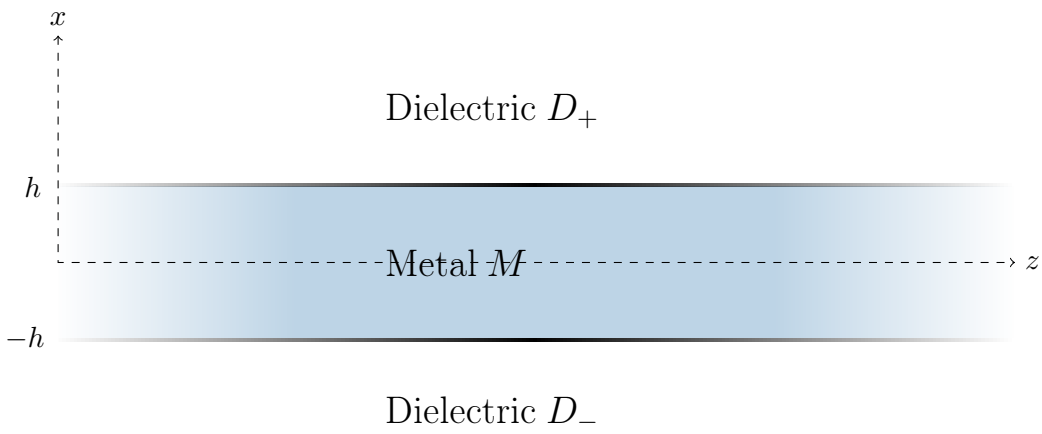

Figure 4.1: Problem geometry

D_- respectively. We assume that $D = D_+ \cup D_-$ is filled with an homogeneous dielectric media with a positive permittivity $\varepsilon_d \in \mathbb{R}^+$. Therefore, the permittivity is given by

$$\varepsilon(x) = \begin{cases} \varepsilon_d & \text{for} \quad |x| \geq h \\ \varepsilon_m(\omega) & \text{for} \quad |x| < h. \end{cases}$$

We also denote by Γ^+ the plane $x = h$ and Γ^- the plane $x = -h$.

4.2.2 Problem formulation

We restrict our work to a non magnetic media with permeability $\mu = 1$ and a magnetization $\mathbf{M} = 0$. Let us consider the Maxwell's equations:

$$\begin{aligned} &\nabla.\mathbf{D} = 0 \\ &\nabla.\mathbf{B} = 0 \\ &\nabla \wedge \mathbf{E} = -i\omega\mathbf{B} \\ &\nabla \wedge \mathbf{B} = \frac{i\omega}{c^2}\varepsilon(\omega)\mathbf{E} \end{aligned}$$

Where D is the displacement field $\mathbf{D} = \varepsilon_0\varepsilon(\omega)\mathbf{E}$, c is the light of speed in the vacuum and ε_0 is the vacuum permittivity.

The metallic layer is illuminated by an harmonic incident plane wave $\mathbf{E^{inc}} = \mathbf{E_0^{inc}}\mathbf{e^{i(\omega t + K.x)}}$. We can suppose without any loss of generality that the incident wave vector $\mathbf{K}$ lies in the zOx plane. The problem geometry and the incident electromagnetic field are invariants by translation in direction y. Consequently, the fields $\mathbf{B}$ and $\mathbf{E}$ do not depend on variable y.

We have chosen the transverse magnetic polarization to excite the SPP as seen in the first chapter. In this case the electric field has the expression $\mathbf{E} = (E_x, 0, E_z)$ and the magnetic field is given by $\mathbf{B} = (0, B_y, 0)$. Then, Maxwell's equations can be reduced to the following equation on $B_y(x, z)$ for $(x, z) \in \mathbb{R}^2$:

$$\operatorname{div}(\frac{1}{\varepsilon}\nabla B_y) + \frac{\omega^2}{c^2} B_y = 0,$$

with the transmission conditions at metal-dielectric interfaces:

$$\begin{aligned} [B_y]_{\Gamma^\pm} &= 0, \\ \left[\frac{1}{\varepsilon}\partial_x B_y\right]_{\Gamma^\pm} &= 0. \end{aligned}$$

The electric field components can be easily found using the relation

$$\nabla \wedge \mathbf{B} = \frac{i\omega}{c^2}\varepsilon \mathbf{E}.$$

Finally, this problem rewrites

$$(P) \begin{cases} \Delta u + \varepsilon_d k^2 u = 0 & \text{in} \quad D_+ \cup D_- \\ \Delta u + \varepsilon_m(\omega) k^2 u = 0 & \text{in} \quad M \\ [u]_{\Gamma^\pm} = 0 \\ \left[\frac{1}{\varepsilon}\partial_x u\right]_{\Gamma^\pm} = 0, \end{cases} \tag{4.2.1}$$

with $k = \frac{\omega}{c}$.

The physical radiation conditions required to close the system and ensure the uniqueness of solution can be found in [40].

4.2.3 Drude's model for real conductor permittivity

According to the first chapter, the permittivity of a real metal can be described by the Drude model

$$\varepsilon_m(\omega) = 1 - \frac{\omega_p^2}{\omega^2 + i\gamma\omega},$$

where $\gamma = 1/\tau$ is the characteristic electrons collision frequency and ω_p the plasma frequency of this metal. The real and imaginary part of $\varepsilon_m(\omega)$ are:

$$\operatorname{Re}[\varepsilon_m(\omega)] = 1 - \frac{\omega_p^2 \tau^2}{1 + \omega^2\tau^2},$$

$$\operatorname{Im}[\varepsilon_m(\omega)] = \frac{\omega_p^2 \tau}{\omega(1 + \omega^2\tau^2)}.$$

For noble metals (e.g Au, Ag, Cu) an extension of this model is needed for $\omega > \omega_p$ due to residual polarization of ions. More precisely we need to introduce a dielectric constant ε_∞ ($1 \leq \varepsilon_\infty \leq 10$) to describe this effect. Then, the permittivity can be written as :

$$\varepsilon_m(\omega) = \varepsilon_\infty - \frac{\omega_p^2}{\omega^2 + i\gamma\omega}.$$

Figure 4.2 illustrates the validity limit of the previous description for silver. We observe that the Drude model does not fit the experimental data anymore

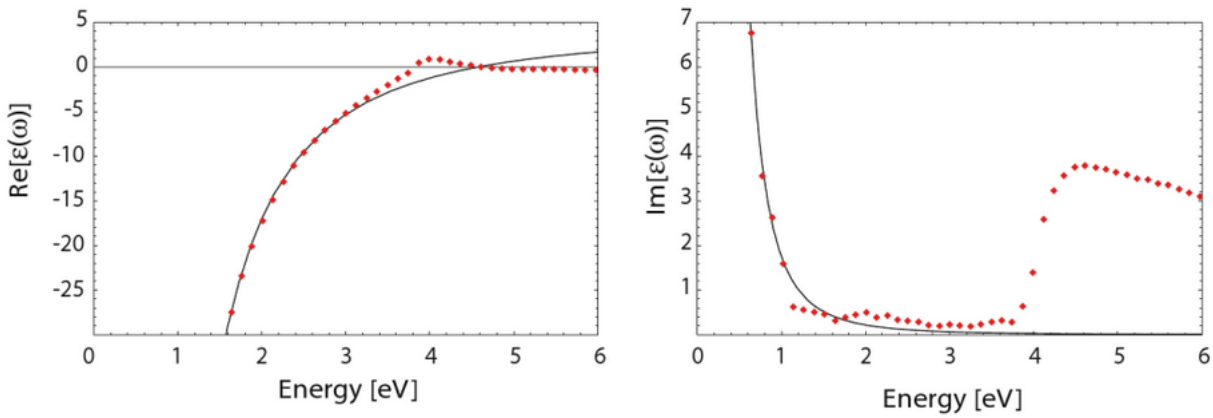

Figure 4.2: The real and imaginary part of $\varepsilon(\omega)$ for silver (dots) determined by Johnson and Christy [41] and Drude model (continuous curve).

for high energy. This is a consequence of inter-band transitions regions, seen in the first chapter, leading to an increase of $\mathrm{Im}[\varepsilon_m(\omega)]$. Then we restrict ourselves to regions where the Drude's model is still valid and we assume for metal permittivity that

$$\begin{cases} \mathrm{Im}[\varepsilon_m(\omega)] > 0 \\ \mathrm{Re}[\varepsilon_m(\omega)] < 0 \end{cases}$$

We recall that the dielectric permittivity ε_d is a positive real number.

4.3 Thin layer limit model

4.3.1 Motivation

Our objective here is to understand the optical response of the considered metallic structure to an electromagnetic excitation in the dielectric layer, when the metal layer thickness h goes to zero. We first formally derive a

limiting model called the quasi-static approximation, and we calculate the its Green function. Based on the explicit expression of this Green function we shall quantify the electromagnetic fields localization and confinement depend in terms of the contrast $\frac{\epsilon_m(\omega)}{\epsilon_d}$, and the frequency ω of the excitation.

Let $u = u(x, y)$ be a solution of the problem (4.2.1). We apply the rescaling $u_h = u(\frac{x}{h}, \frac{y}{h})$ and we get the following equivalent problem (radiation conditions are omitted):

$$(P_h) \begin{cases} \Delta u_h + h^2 \varepsilon_d k^2 u_h = 0 & \text{in} \quad \mathbb{R} \times]-\infty, -1[\cup]1, +\infty[\\ \Delta u_h + h^2 \varepsilon_m(\omega) k^2 u_h = 0 & \text{in} \quad \mathbb{R} \times [-1, 1] \\ [u_h]_{y=\pm 1} = 0 \\ \left[\frac{1}{\varepsilon} \partial_y u_h\right]_{y=\pm 1} = 0 \end{cases}$$

We then write the limit problem when $h \to 0$:

$$(P_0) \begin{cases} \Delta u_0 = 0 & \text{in} \quad \mathbb{R}^2 \\ [u_0]_{y=\pm 1} = 0 \\ \left[\frac{1}{\varepsilon} \partial_y u_0\right]_{y=\pm 1} = 0 \end{cases}$$

Or equivalently

$$(P_0) \qquad \operatorname{div}(\frac{1}{\varepsilon} \nabla u_0)(x, y) = 0, \qquad (x, y) \in \mathbb{R}^2$$

The problem (P_0) is physically meaningful when the coefficient $|h^2 k^2 \varepsilon| = |h^2 \frac{\omega^2}{c^2} \varepsilon|$ is much smaller than 1. This condition is satisfied when $h << L$ where L is the wavelength. So the limit model is acceptable when there is no propagation at the scale of the layer. The problem (P_0) is called the quasi-static limit of the problem (P_h), and u_0 the quasi-static solution [42] [39].

4.3.2 The Green function of the limiting problem

We further study the Green function G_0 of the problem:

$$\operatorname{div}(\frac{1}{\varepsilon} \nabla G_0)(x, y) = \delta_{x_0}(x) \delta_{y_0}(y), \qquad (x, y) \in \mathbb{R}^2$$

The physical radiation conditions satisfied by the Green function will be fixed later in the reconstruction of its spectral expression.

The first step in deriving G_0 is to consider $\hat{G}_0(t, y) = FT_x(G_0(x, y))$, where FT_x is the Fourier transform with respect to the x variable.

Forward calculation shows that $\widehat{G}_0$ solves the following equation:

$$\left[-\frac{t^2}{\varepsilon(y)}\widehat{G}_0 + \partial_y\left(\frac{1}{\varepsilon(y)}\partial_y\widehat{G}_0\right)\right](t,y) = e^{-itx_0}\delta_{y_0}(y), \qquad (t,y)\in\mathbb{R}^2$$

We can rewrite the previous problem as $\widehat{G}_0$ solves the next equation for $(t,y)\in\mathbb{R}\times]-\infty,-h[\cup]-h,h[\cup]h,+\infty[$

$$[-t^2+\partial_{yy}]\widehat{G}_0(t,y) = \varepsilon(y)e^{-itx_0}\delta_{y_0}(y), \tag{4.3.1}$$

with the following jump conditions:

$$[\widehat{G}_0]_{\pm h} = 0 \tag{4.3.2}$$

$$[\frac{1}{\varepsilon}\partial_y\widehat{G}_0]_{\pm h} = 0. \tag{4.3.3}$$

We now construct the Green function using the Wronskian method.

Let $\Phi_+(t,y)$ in the region $y>y_0$, be the homogeneous solution to the previous problem, decaying as $y\to+\infty$:

$$\Phi_+(t,y) = e^{-|t|y}, \qquad y>y_0$$

Let $\Phi_-(t,y)$ in the region $y<y_0$, be the homogeneous solution to the previous problem, decaying as $y\to-\infty$:

$$\Phi_-(t,y) = \begin{cases} e^{|t|y}, & y<-h \\ Ae^{|t|y}+Be^{-|t|y}, & y\in]-h,h[\\ Ce^{|t|y}+De^{-|t|y}, & y\in]h,y_0[, \end{cases}$$

where $A,B,C,D\in\mathbb{C}$ need to be determined using jump conditions at $\pm h$.

Remark 34. *Here we are looking for solutions decaying in the dielectric and propagating along x direction. Indeed we suppose that t is real so we restrict the calculation only to propagating modes along the x direction, and decaying along the y direction. Physicists call this family of waves surface plasmons. The constant t may also be viewed as the x component of the wave-vector of a wave propagating along the x direction. In our case the source point generates a family of plasmons waves and we sum all the contributions (we do the summation over $t\in\mathbb{R}$ so we remove the propagation along y) to obtain the Green function corresponding to our physical radiation conditions.*

Using the continuity condition (4.3.2) at $y=-h$, we get:

$$e^{-|t|h} = Ae^{-|t|h}+Be^{|t|h} \tag{4.3.4}$$

The derivative continuity condition (4.3.3) at $y = -h$ implies:

$$\frac{1}{\varepsilon_d} e^{-|t|h} = \frac{1}{\varepsilon_m}(Ae^{-|t|h} - Be^{|t|h})$$

Then

$$2Ae^{-|t|h} = (1+\kappa)e^{-|t|h}$$
$$2Be^{|t|h} = (1-\kappa)e^{-|t|h},$$

where

$$\kappa = \varepsilon_m/\varepsilon_d, \tag{4.3.5}$$

is the contrast at fixed frequency ω. So, we get

$$A = \frac{1}{2}(1+\kappa)$$
$$B = \frac{1}{2}(1-\kappa)e^{-2|t|h}$$

Continuity (4.3.2) and derivative continuity (4.3.3) conditions at $y = +h$ give

$$Ae^{|t|h} + Be^{-|t|h} = Ce^{|t|h} + De^{-|t|h}$$
$$\frac{1}{\varepsilon_m}(Ae^{|t|h} - Be^{-|t|h}) = \frac{1}{\varepsilon_d}(Ce^{|t|h} - De^{-|t|h})$$

Then

$$2Ce^{|t|h} = A(1+\frac{1}{\kappa})e^{|t|h} + B(1-\frac{1}{\kappa})e^{-|t|h}$$
$$2De^{-|t|h} = A(1-\frac{1}{\kappa})e^{|t|h} + B(1+\frac{1}{\kappa})e^{-|t|h}$$

Hence

$$C = \frac{1}{4}(1+\kappa)(1+\frac{1}{\kappa}) + \frac{1}{4}(1-\kappa)(1-\frac{1}{\kappa})e^{-4|t|h}$$
$$D = \frac{1}{4}(1+\kappa)(1-\frac{1}{\kappa})e^{2|t|h} + \frac{1}{4}(1+\frac{1}{\kappa})(1-\kappa)e^{-2|t|h}$$

We now consider

$$\widehat{G}_0(t,y,x_0,y_0) = \frac{1}{d}\begin{cases}\Phi_+(t,y)\Phi_-(t,y_0), & y > y_0\\ \Phi_-(t,y)\Phi_+(t,y_0), & y < y_0,\end{cases}$$

with d the Wronskian such that

$$\frac{1}{d}(\Phi_-\partial_y\Phi_+ - \Phi_+\partial_y\Phi_-)(t,y_0) = \varepsilon_d e^{-itx_0}, \forall t \in \mathbb{R}$$

The fact that

$$\partial_y \Phi_+(t, y_0) = -|t| e^{-|t| y_0}$$
$$\partial_y \Phi_-(t, y_0) = |t| (C e^{|t| y_0} - D e^{-|t| y_0})$$

implies

$$d = -2C|t| \frac{1}{\varepsilon_d} e^{itx_0}$$

with

$$C = \frac{1}{4} \left(\frac{(1+\kappa)^2}{\kappa} - \frac{(1-\kappa)^2}{\kappa} e^{-4|t|h} \right) = \frac{1}{4} \frac{(1-\kappa)^2}{\kappa} \left(\eta^2 - e^{-4|t|h} \right)$$

and

$$\eta = \frac{1+\kappa}{1-\kappa}, \tag{4.3.6}$$

is the normalized contrast [**?**, 43].

Finally, under the conditions $\kappa \neq 0$ and $\kappa \neq 1$ we have

$$d = -\frac{|t| e^{itx_0}}{2\varepsilon_d} \frac{(1-\kappa)^2}{\kappa} \left(\eta^2 - e^{-4|t|h} \right)$$

Lower dielectric part of $\widehat{G}_0$

Let $y < -h < y_0$, then we can write

$$\begin{aligned} \widehat{G}_0(t, y, x_0, y_0) &= \frac{1}{d} \Phi_-(t, y) \Phi_+(t, y_0) \\ &= \frac{1}{d} e^{|t|(y - y_0)} \end{aligned}$$

Finally for $y < -h < y_0$ and $t \in \mathbb{R}$

$$\widehat{G}_0(t, y, x_0, y_0) = \frac{2\kappa\varepsilon_d}{(1-\kappa)^2} \frac{e^{-itx_0}}{|t|} \frac{e^{|t|(y-y_0)}}{e^{-4|t|h} - \eta^2} \tag{4.3.7}$$

This expression corresponds to the *transmitted part* of the Green function.

Upper dielectric part of $\widehat{G}_0$

For the upper dielectric part we have two case: $y > y_0$ and $y < y_0$.
Let first $y > y_0 > h > 0$, then

$$\begin{aligned}\widehat{G}_0(t, x_0, y, y_0) &= \frac{1}{d}\Phi_-(t, y_0)\Phi_+(t, y) \\ &= \frac{1}{d}\left(Ce^{-|t|(y-y_0)} + De^{-|t|(y+y_0)}\right)\end{aligned}$$

Using

$$D = \frac{(\kappa^2 - 1)}{2\kappa}\sinh(2|t|h)$$

We get

$$\widehat{G}_0(t, x_0, y, y_0) = -\frac{\varepsilon_d e^{-itx_0}}{2|t|}e^{-|t|(y-y_0)} - \eta\frac{\varepsilon_d e^{-itx_0}\sinh(2|t|h)}{|t|(e^{-4|t|h} - \eta^2)}e^{-|t|(y+y_0)} \tag{4.3.8}$$

$$= -\frac{\varepsilon_d e^{-itx_0}}{|t|}\left(\frac{1}{2}e^{-|t|(y-y_0)} + \eta\frac{\sinh(2|t|h)e^{-|t|(y+y_0)}}{e^{-4|t|h} - \eta^2}\right) \tag{4.3.9}$$

This expression corresponds to the *reflected* part of the Green's function. The first term is the wave generated by the source going upward and not interacting with the metal layer. The second term is the reflected wave. It vanishes when $h = 0$ (no perturbation) and when $\eta = 0$.

Let now $h < y < y_0$ then

$$\begin{aligned}\widehat{G}_0(t, x_0, y, y_0) &= \frac{1}{d}\Phi_-(t, y)\Phi_+(t, y_0) \\ &= \frac{1}{d}\left(Ce^{|t|(y-y_0)} + De^{-|t|(y+y_0)}\right)\end{aligned}$$

So we get

$$\widehat{G}_0(t, x_0, y, y_0) = -\frac{\varepsilon_d e^{-itx_0}}{|t|}\left(\frac{1}{2}e^{|t|(y-y_0)} + \eta\frac{\sinh(2|t|h)e^{-|t|(y+y_0)}}{e^{-4|t|h} - \eta^2}\right) \tag{4.3.10}$$

Metal part of $\widehat{G}_0$

Let $h \geq y \geq -h$, then

$$\begin{aligned}\widehat{G}_0(t, x_0, y, y_0) &= \frac{1}{d}\Phi_-(t, y)\Phi_+(t, y_0) \\ &= \frac{1}{d}\left(Ae^{|t|(y-y_0)} + Be^{-|t|(y+y_0)}\right)\end{aligned}$$

We get

$$\widehat{G}_0(t, x_0, y, y_0) = -\frac{\varepsilon_m}{(1-\kappa)}\frac{e^{-itx_0}}{|t|(\eta^2 - e^{-4|t|h})}\left(\eta e^{|t|(y-y_0)} + e^{-|t|(y+y_0+2h)}\right) \tag{4.3.11}$$

Remark 35. *In the case $\eta \neq 0$ the function $\widehat{G}_0$ is always decaying exponentially when $|t| \to +\infty$. However when $\kappa = -1$ we have $\eta = 0$ and then*

$$\widehat{G}_0(t, x_0, y, y_0) = \frac{\varepsilon_m}{2}e^{-itx_0}e^{-|t|(y+y_0-2h)}$$

$\widehat{G}_0$ is decaying exponentially when $|t| \to +\infty$ under the condition $y+y_0-2h > 0$. Because $h > y > -h$ the condition rewrites $y_0 > 3h$. If $y+y_0-2h = 0$ we get a delta Dirac function at $x = 0$ and $y = 2h - y_0$. In the case $y + y_0 - 2h$ is negative then $\widehat{G}_0$ is not integrable with respect to t for all the values of y satisfying the previous condition. In other words if the source is close enough to the metal layer with $\eta = 0$ we expect that the Green function blows up.

We easily verify that $\widehat{G}_0$ as a function of variable t decays exponentially as $t \to \pm\infty$. However it is not integrable at 0 and then does not belong to $L^1(\mathbb{R})$ space for t variable. So the inverse Fourier transform is undefined in the classical sense of integration. For the same reason $\widehat{G}_0$ is not a tempered distribution with respect to t variable. To give a sense to inverse Fourier transform we are going to regularize such an integral using Hadamard finite part method.

$\widehat{G}_0$ can be interpreted as the amplitude of a wave propagating along the x direction with a wavevector t. Moreover zeros of the dispersion relation $\eta^2 - e^{-4|t|h}$ correspond to the poles of the amplitude. In other words if t is such that the relation dispersion is almost zero then the amplitude of the wave propagating along x direction with wavevector t is highly amplified. The value of t in this case is called surface plasmon wavevector by physicists. In Figure 4.3, we plotted the absolute value of G_0 in the lower dielectric part for different values of the parameter η^2. We observe that when $\mathrm{Im}\eta^2 \to 0$ a propagating wave along the x direction appears. That corresponds to the surface plasmon described by physicists. Moreover the frequency of this wave corresponds (visualized using a FFT) to $t_0/2\pi$ where t_0 is a zero of the relation dispersion: $t_0 = -\frac{1}{4h}\ln(\eta^2)$.

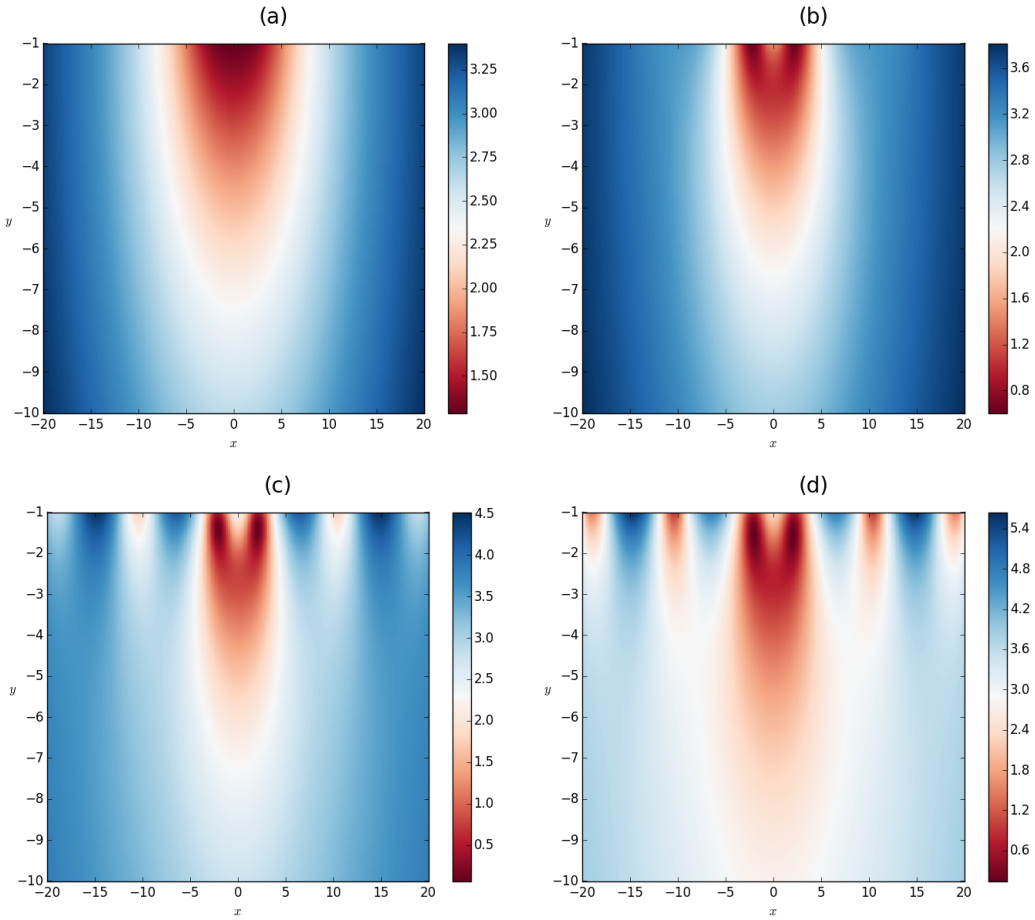

Figure 4.3: Plots of $|G_0|$ in the lower dielectric part ($-10 \leq y \leq -h$, $-20 \leq x \leq 20$ with $h = 1$) for different values of η^2 such that $\mathrm{Im}\eta^2 \to 0$. For figure (a): $\eta^2 = 0.05 + 0.5i$, (b): $\eta^2 = 0.05 + 0.1i$, (c): $\eta^2 = 0.05 + 0.01i$, (d): $\eta^2 = 0.05 + 0.0001i$

Hadamard finite part

Let $f \in C^1_{pw}(\mathbb{R})$ such that $f(t) = o(\frac{1}{t})$ when $t \to \pm\infty$. Here $C^1_{pw}(\mathbb{R})$ is the space of continuous functions with piecewise continuous derivative. We now consider the following undefined integral

$$I = \int_{\mathbb{R}} \frac{f(t)}{|t|} dt$$

To regularize it we denote the truncated integral by

$$I_\rho = \int_{|t|\geq\rho} \frac{f(t)}{|t|} dt = \int_{1\geq|t|\geq\rho} \frac{f(t)}{|t|} dt + \int_{|t|\geq 1} \frac{f(t)}{|t|} dt$$

We first remark the second integral is finite, then we denote the first integral by

$$J_\rho = \int_{1\geq|t|\geq\rho} \frac{f(t)}{|t|}dt$$

Now using $f(t) = f(0) + (f(t) - f(0))$ we write

$$J_\rho = \int_{1\geq|t|\geq\rho} \frac{f(0)}{|t|}dt + \int_{1\geq|t|\geq\rho} \frac{f(t)-f(0)}{|t|}dt$$

Because f derivative is piecewise continuous on $\mathbb{R}$ we can state the second integral is finite when $\rho \to 0$:

$$\lim_{\rho\to 0} \int_{1\geq|t|\geq\rho} \frac{f(t)-f(0)}{|t|}dt < +\infty$$

So we isolated the part of I_ρ which diverges when $\rho \to 0$:

$$\int_{1\geq|t|\geq\rho} \frac{f(0)}{|t|}dt = -2f(0)\ln(\rho)$$

Then by subtracting the divergent part of I_ρ to I_ρ itself we get the finite part of it:

$$\lim_{\rho\to 0}\{I_\rho + 2f(0)\ln(\rho)\} = \lim_{\rho\to 0}\{\int_{|t|\geq 1} \frac{f(t)}{|t|}dt + \int_{1\geq|t|\geq\rho} \frac{f(t)-f(0)}{|t|}dt\} < +\infty$$

The Hadamard finite part of I is

$$\widetilde{I} = \lim_{\rho\to 0}\{I_\rho + 2f(0)\ln(\rho)\} = \lim_{\rho\to 0}\{\int_{|t|\geq\rho} \frac{f(t)}{|t|}dt + 2f(0)\ln(\rho)\}$$

Inverse Fourier transform of $\widehat{G}_0$

Because we denoted by FT_x the Fourier transform with respect to x variable we now denote FT_x^{-1} its inverse formally defined by:

$$FT_x^{-1}(\Phi)(t) = \int_{\mathbb{R}} \Phi(x)e^{ixt}dx$$

Let $\Phi \in \mathcal{S}(\mathbb{R})$ where $\mathcal{S}(\mathbb{R})$ is a Swartz space. In the sense of distributions

$$\begin{aligned} I =< FT_x^{-1}(\widehat{G}_0), \Phi > =< \widehat{G}_0, FT_x^{-1}(\Phi) > \\ = \int_{\mathbb{R}} \frac{2\kappa\varepsilon_d}{(1-\kappa)^2} \frac{e^{-itx_0}}{|t|} \frac{e^{|t|(y-y_0)}}{e^{-4|t|h} - \eta^2} FT_x^{-1}(\Phi)(t)dt \end{aligned}$$

Because the last integral is undefined we will give it a sense using Hadamard finite part introduced in subsection (4.3.2). We now consider the regularization of the previous integral

$$\widetilde{I} = \lim_{\rho \to 0} \{ I_\rho^1 + I_\rho^2 \}$$

Where

$$\begin{aligned}
I_\rho^1 &= \int_{|t| \geq \rho} \frac{h(t)}{|t|} FT_x^{-1}(\Phi) dt \\
I_\rho^2 &= 2h(0) FT_x^{-1}(\Phi)(0) \ln(\rho) \\
h(t) &= \frac{2\kappa\varepsilon_d}{(1-\kappa)^2} \frac{e^{|t|(y-y_0)}}{e^{-4|t|h} - \eta^2} e^{-itx_0}
\end{aligned}$$

We observe that

$$\begin{aligned}
I_\rho^2 &= \frac{2\kappa\varepsilon_d}{(1-\kappa)^2} \frac{2\ln(\rho)}{1-\eta^2} FT_x^{-1}(\Phi)(0) \\
&= \frac{2\kappa\varepsilon_d}{(1-\kappa)^2} \frac{2\ln(\rho)}{1-\eta^2} \int_{\mathbb{R}} \Phi(x) dx \\
&= \frac{2\kappa\varepsilon_d}{(1-\kappa)^2} \frac{2\ln(\rho)}{1-\eta^2} < 1, \Phi > \\
&=< C_\rho, \Phi >
\end{aligned}$$

With $C_\rho = \frac{2\kappa\varepsilon_d}{(1-\kappa)^2} \frac{2\ln(\rho)}{1-\eta^2}$. Moreover

$$\begin{aligned}
I_\rho^1 &= \int_{|t| \geq \rho} \frac{h(t)}{|t|} \int_{\mathbb{R}} \Phi(x) e^{ixt} dx.dt \\
&= \int_{\mathbb{R}} \Phi(x) \left(\int_{|t| \geq \rho} \frac{h(t)}{|t|} e^{ixt} dt \right) dx \\
&=< P_\rho, \Phi >
\end{aligned}$$

With $P_\rho(x) = \int_{|t| \geq \rho} \frac{h(t)}{|t|} e^{ixt} dt$ which is a convergent integral $\forall x \in \mathbb{R}$. So

$$I_\rho^1 + I_\rho^2 =< P_\rho + C_\rho, \Phi >$$

And then

$$\widetilde{I} = \lim_{\rho \to 0} < P_\rho + C_\rho, \Phi >$$

Lemma 4.3.1. *Let* $\Phi \in \mathcal{S}(\mathbb{R})$ *then*

$$\widetilde{I} = \lim_{\rho \to 0} < P_\rho + C_\rho, \Phi >=< \lim_{\rho \to 0} \{ P_\rho + C_\rho \}, \Phi >$$

Proof. The proof relies on convergence dominated theorem. We first know that $\forall x \in \mathbb{R},\ \lim_{\rho\to 0}\{P_\rho + C_\rho\}$ is finite. Moreover we can write

$$I_\rho^1 + I_\rho^2 = \int_{|t|\geq 1} \frac{h(t)e^{ixt}}{|t|}dt + \int_{1\geq|t|\geq\rho} \frac{h(t)e^{ixt} - h(0)}{|t|}dt$$

The first integral is uniformly bounded for $x \in \mathbb{R}$. For the second integral we write

$$\int_{1\geq|t|\geq\rho} \frac{h(t)e^{ixt} - h(0)}{|t|}dt = \int_\rho^1 \frac{h(t)e^{ixt} - h(0)}{t}dt + \int_{-1}^{-\rho} \frac{h(t)e^{ixt} - h(0)}{-t}dt$$

Then, we can use the Taylor formula with integral reminder:

$$\frac{h(t)e^{ixt} - h(0)}{t} = \frac{1}{t}\int_0^t (h'(r)e^{ixr} + ixh(r)e^{ixr})dr$$

So we get

$$\begin{aligned}\left|\int_\rho^1 \frac{h(t)e^{ixt} - h(0)}{t}dt\right| &\leq \int_\rho^1 \frac{1}{t}\int_0^t |h'(r)| + |x||h(r)|dr.dt \\ &\leq \int_\rho^1 \sup_{[0,1]}(h') + |x|\sup_{[0,1]}(h)dt \\ &\leq \sup_{[0,1]}(h') + |x|\sup_{[0,1]}(h)\end{aligned}$$

Similarly we get:

$$\left|\int_{-1}^{-\rho} \frac{h(t)e^{ixt} - h(0)}{-t}dt\right| \leq \sup_{[-1,0]}(h') + |x|\sup_{[-1,0]}(h)$$

Let us remember that $\mathrm{Im}\eta^2 \neq 0$ therefore $e^{-4|t|h} - \eta^2$ is never zero. So it can be said that $h \in C^\infty(\mathbb{R}^+)$ and $h \in C^\infty(\mathbb{R}^-)$. We deduce $\sup_{[0,1]}(h')$, $\sup_{[0,1]}(h)$, $\sup_{[-1,0]}(h')$ and $\sup_{[-1,0]}(h)$ are finites. Consequently $\left|I_\rho^1 + I_\rho^2\right|$ is bounded by $A(|x|)$ where A is affine. As $\Phi \in \mathcal{S}(\mathbb{R})$, $A(|x|)\Phi(x)$ is integrable over $\mathbb{R}$. Finally the lemma is proved using the dominated convergence theorem. □

We proved the regularization of $FT_x^{-1}(\widehat{G}_0)$ with $y < -h < y_0$ is

$$G_0(x, x_0, y, y_0) = \lim_{\rho\to 0}\{\int_{|t|\geq\rho} \frac{2\varepsilon_m}{(1-\kappa)^2}\frac{e^{|t|(y-y_0)}}{|t|(e^{-4|t|h} - \eta^2)}e^{it(x-x_0)}dt + \frac{2\varepsilon_m}{(1-\kappa)^2}\frac{2\ln(\rho)}{1-\eta^2}\}$$

The expression of the Green function

Here we finally provide the expression of the Green function.

Theorem 36. *The explicit expression of the Green function in different regions.*
In the upper dielectric part $y > y_0 > h$:

$$G_0^u(x, x_0, y, y_0) = \lim_{\rho \to 0} \{ \int_{|t| \geq \rho} \frac{\varepsilon_d}{|t|} \left(\frac{1}{2} e^{-|t|(y-y_0)} + \eta \frac{\sinh(2|t|h) e^{-|t|(y+y_0)}}{e^{-4|t|h} - \eta^2} \right) e^{it(x-x_0)} dt + \varepsilon_d \ln(\rho) \}$$

In the upper dielectric part $y_0 > y > h$:

$$G_0^u(x, x_0, y, y_0) = \lim_{\rho \to 0} \{ \int_{|t| \geq \rho} \frac{\varepsilon_d}{|t|} \left(\frac{1}{2} e^{|t|(y-y_0)} + \eta \frac{\sinh(2|t|h) e^{-|t|(y+y_0)}}{e^{-4|t|h} - \eta^2} \right) e^{it(x-x_0)} dt + \varepsilon_d \ln(\rho) \}$$

In the metal part $-h \leq y \leq h$:

$$G_0^m(x, x_0, y, y_0) = \lim_{\rho \to 0} \{ \int_{|t| \geq \rho} \frac{\varepsilon_m}{(1-\kappa)} \frac{e^{it(x-x_0)}}{|t|(\eta^2 - e^{-4|t|h})} \left(\eta e^{|t|(y-y_0)} + e^{-|t|(y+y_0+2h)} \right) dt + \frac{\varepsilon_m}{1-\kappa} \frac{2\ln(\rho)}{1-\eta} \}$$

In the lower dielectric part $y < -h$:

$$G_0^l(x, x_0, y, y_0) = \lim_{\rho \to 0} \{ \int_{|t| \geq \rho} \frac{2\varepsilon_m}{(1-\kappa)^2} \frac{e^{|t|(y-y_0)}}{|t|(e^{-4|t|h} - \eta^2)} e^{it(x-x_0)} dt + \frac{2\varepsilon_m}{(1-\kappa)^2} \frac{2\ln(\rho)}{1-\eta^2} \}$$

4.3.3 Behavior of G_0 as a function of the contrast η

Assuming that the source is located at $(x_0, y_0) \in \{y > h\}$, we are interested in the behavior of the Green function $G_0(x_0, x_0, y, y_0)$ in terms of the contrast parameter η in the lower dielectric region $\{y > h\}$. Recall the expressions (4.3.5) and (4.3.6) of the contrast κ and the normalized contrast η respectively:

$$\kappa = \varepsilon_m / \varepsilon_d, \quad \eta = \tfrac{1+\kappa}{1-\kappa}.$$

The following quantity corresponds to the transmitted part in the lower dielectric region of the waves generated by the point source in the upper dielectric region:

$$I(\eta^2) = \int_{\rho}^{+\infty} \frac{e^{t(y-y_0)}}{t(e^{-4th} - \eta^2)} \cos(t(x - x_0))dt. \tag{4.3.12}$$

Let us now investigate the behavior of $I(\eta^2)$.

Lemma 4.3.2. *Since $Re(\epsilon_m) < 0$ and $Im(\epsilon_m) > 0$, the contrast η lies in the unit disk, that is*

$$|\eta| < 1.$$

Case $\eta^2 \neq 0$

We first investigate the regularity of the function $I(\eta^2)$.

Theorem 37. *$I(\eta^2)$ is piecewise continuous as a function of η^2 for $0 < |\eta^2| \leq 1$.*

The proof will be provided in three following lemmas.

Lemma 4.3.3. *Let C be a compact set included in the unit disk and such that it does not intersect the positive real axis. Then, $I(\eta^2)$ is continuous on C.*

Proof. Since $e^{-4th} \in [0, 1]$, there exist a constant $0 < c < 1$ such that $\forall \eta^2 \in C, \forall t \in [\rho, +\infty[, |e^{-4th} - \eta^2| > c$. Consequently

$$\left| \frac{e^{t(y-y_0)}}{t(e^{-4th} - \eta^2)} \cos(t(x - x_0)) \right| < \frac{1}{c\rho} e^{t(y-y_0)}$$

Since $(y - y_0) < 0$, the lemma is proved using the dominated convergence theorem. □

Lemma 4.3.4. *If η^2 is a positive real number such that $1 > |\eta^2| > 0$, then $I(\eta^2)$ is finite.*

Proof. We denote by $t_0 = -\frac{\ln(\eta^2)}{4h} > 0$ the only root of $e^{-4th} - \eta^2$. We verify that

$$\partial_t(e^{-4th} - \eta^2)(t_0) = \partial_t(e^{-4th} - e^{-4t_0 h})(t_0) \neq 0$$

Then t_0 is a root of order one. So there exists a smooth function R such that close to t_0 it satisfies

$$e^{-4th} - \eta^2 = (t - t_0)R(t_0)$$

where $R(t_0) \neq 0$. Consequently, the integral $I(\eta^2)$ is an improper integral that converges by Cauchy principal value. □

Lemma 4.3.5. *If $Re(\eta^2) \neq 0$, then the function $I(\eta^2)$ has a finite limit when $Im(\eta^2) \to 0^+$ or when $Im(\eta^2) \to 0^-$.*

Proof. We use the Plemelj formula to prove this lemma. □

Considering the previous lemmas we conclude the Green function does not blow up for $\eta^2 \neq 0$ in the closed unit disk. In other words, $\eta^2 = 0$ is the only candidate to be a resonance. In the next part, we study the behavior of $I(\eta^2)$ as η^2 goes to zero.

Case η^2 goes to zero

Let us denote $\alpha = -\frac{(y-y_0)}{4h} - 1$. We distinguish two different cases depending on the sign of α. These kinds of conditions are called *localization conditions*. For example, knowing that $y < -h$ and $y_0 > h$, the condition $\alpha > 0$ is always $(\forall h < -h)$ fulfilled when $y_0 > 3h$. We will see below that this condition corresponds to the case where $I(\eta^2)$ remains bounded when $\eta^2 \to 0$. So if the source if far enough from the metal layer, then I is bounded for all values of $y < -h$.

The case $y < y_0 - 4h$ (or $\alpha > 0$)

Lemma 4.3.6. *If $y < y_0 - 4h$, then $I(\eta^2)$ stays bounded when η^2 goes to zero.*

Proof. We first apply the change of variables $z = e^{-4th}$, and obtain

$$I = \int_0^{e^{-4\rho h}} \frac{z^\alpha}{\ln(z)(z-\eta^2)} \cos\left(-\frac{\ln(z)(x-x_0)}{4h}\right) dz,$$

which implies

$$|I| < \int_0^{e^{-4\rho h}} \frac{\frac{z^\alpha}{|\ln(z)|}}{|z-\eta^2|} dz$$

Let now $\phi(z) = \frac{z^\alpha}{|\ln(z)|}$.
Then

$$\int_0^{e^{-4\rho h}} \frac{\frac{z^\alpha}{|\ln(z)|}}{|z-\eta^2|} dz = \int_0^{e^{-4\rho h}} \frac{\phi(z)-\phi(\eta^2)}{|z-\eta^2|} dz + \phi(\eta^2) \int_0^{e^{-4\rho h}} \frac{1}{|z-\eta^2|} dz,$$

Since ϕ is Hölder continuous there exist constants $C > 0$ and $0 < \theta \leq 1$ such that

$$|\phi(t) - \phi(\eta^2)| < C|t-\eta^2|^\theta$$

So the first integral is finite when $\eta^2 \to 0$. Moreover a primitive of $1/|z-\eta^2|$ is $-\ln(|z-\eta^2| + \mathrm{Re}(\eta^2) - z)$. Then

$$\int_0^{e^{-4\rho h}} \frac{1}{|z-\eta^2|} dz = -\ln(|e^{-4\rho h} - \eta^2| + \mathrm{Re}(\eta^2) - e^{-4\rho h}) + \ln(|\eta^2| + \mathrm{Re}(\eta^2))$$

We easily see that

$$\lim_{\eta^2\to 0}\phi(\eta^2)\left|-\ln(|e^{-4\rho h}-\eta^2|+\mathrm{Re}(\eta^2))+\ln(|\eta^2|+\mathrm{Re}(\eta^2))\right|<+\infty$$

So we deduce $|I|$ is bounded when $\eta^2\to 0$.

□

The case $y > y_0 - 4h$ (or $\alpha < 0$)

Theorem 38. *For $x = x_0$, we have*

$$|I(\eta)|\geq\frac{-C_1|\sin(\gamma)|}{e\epsilon^{1-\tilde{\alpha}}\ln(\epsilon)}\int_0^{\frac{e^{-\beta\rho}}{\epsilon}}\frac{1}{(s-\cos(\gamma))^2+\sin^2(\gamma)}\frac{1}{s^{1-\tilde{\alpha}}s^{\frac{1}{\ln(\epsilon)}}}ds$$

$$|I(\eta)|\leq\frac{-C_2e}{\epsilon^{1-\tilde{\alpha}}\ln(\epsilon)}\int_0^{\frac{e^{-\beta\rho}}{\epsilon}}\frac{1}{|s-e^{i\gamma}|}\frac{s^{\tilde{\alpha}-1}s^{\frac{1}{\ln(\epsilon)}}}{(1-e^{-1}s^{-\frac{1}{\ln(\epsilon)}})}ds,$$

where $\eta^2=\epsilon e^{i\gamma}$ and $\tilde{\alpha}=-\frac{y-y_0}{4h}>0$.

We will begin by proving a useful result for our coming analysis.

Lemma 4.3.7. *There exist two positive constants C_1 and C_2 such that, $\forall t\in]0,1[$, $\forall\theta>0$,*

$$\frac{C_2t^\theta(1-t^\theta)}{\theta}<|\ln(t)|<\frac{C_1}{\theta t^\theta}$$

Proof. On the one hand, we have that $\exists C_1>0$, $\forall t\in]0,1[$, $|t\ln(t)|<C_1$. In particular, $\forall\theta>0$, $|t^\theta\ln(t^\theta)|<C_1$.

$$\forall t\in]0,1[,\forall\theta>0,|\ln(t)|<\frac{C_1}{\theta t^\theta}$$

On the other hand, $\exists\tilde{C}_2>0$, $\forall t\in]0,1[$, $|\frac{t(1-t)}{\ln(t)}|<\tilde{C}_2$. In particular, $\forall\theta>0$, $|\frac{t^\theta(1-t^\theta)}{\theta\ln(t)}|<\tilde{C}_2$.

$$\forall t\in]0,1[,\forall\theta>0,\frac{t^\theta(1-t^\theta)}{\theta\tilde{C}_2}<|\ln(t)|$$

□

Back to the Green function and the quantity

$$I(\eta)=\int_\rho^{+\infty}\frac{e^{t(y-y_0)}}{t(e^{-4th}-\eta^2)}cos(t(x-x_0))dt$$

$$I(\eta)=\frac{1}{2}\int_\rho^{+\infty}\frac{e^{t(y-y_0+i(x-x_0))}}{t(e^{-4th}-\eta^2)}dt+\frac{1}{2}\int_\rho^{+\infty}\frac{e^{t(y-y_0-i(x-x_0))}}{t(e^{-4th}-\eta^2)}dt$$

We apply the change of variables $z = e^{-4th}$. We note $\alpha = y - y_0$ and $\beta = 4h$. Then

$$I(\eta) = -\frac{1}{2}\int_0^{e^{-\beta h}} \frac{z^{-\frac{\alpha+i(x-x_0)}{\beta}-1}}{\ln(z)(z-\eta^2)}dz - \frac{1}{2}\int_0^{e^{-\beta h}} \frac{z^{-\frac{\alpha-i(x-x_0)}{\beta}-1}}{\ln(z)(z-\eta^2)}dz$$

Let $\eta^2 = \epsilon e^{i\gamma}$.

$$I(\eta) = -\frac{1}{2}\int_0^{e^{-\beta \rho}} \frac{z^{-\frac{\alpha+i(x-x_0)}{\beta}-1}}{\ln(z)(z-\epsilon e^{i\gamma})}dz - \frac{1}{2}\int_0^{e^{-\beta \rho}} \frac{z^{-\frac{\alpha-i(x-x_0)}{\beta}-1}}{\ln(z)(z-\epsilon e^{i\gamma})}dz$$

By a change of variables $z = \epsilon s$, we find

$$I(\eta) = -\frac{1}{2}\int_0^{\frac{e^{-\beta\rho}}{\epsilon}} \frac{(\epsilon s)^{-\frac{i(x-x_0)}{\beta}}}{(\epsilon s)^{\frac{\alpha}{\beta}+1}\ln(\epsilon s)(s-e^{i\gamma})}ds - \frac{1}{2}\int_0^{\frac{e^{-\beta\rho}}{\epsilon}} \frac{(\epsilon s)^{\frac{i(x-x_0)}{\beta}}}{(\epsilon s)^{\frac{\alpha}{\beta}+1}\ln(\epsilon s)(s-e^{i\gamma})}ds$$

We note $\tilde{\alpha} = -\frac{\alpha}{\beta} = -\frac{y-y_0}{4h} > 0$.

$$I(\eta) = -\frac{1}{2}\int_0^{\frac{e^{-\beta\rho}}{\epsilon}} \frac{(\epsilon s)^{-\frac{i(x-x_0)}{\beta}}}{(\epsilon s)^{1-\tilde{\alpha}}\ln(\epsilon s)(s-e^{i\gamma})}ds - \frac{1}{2}\int_0^{\frac{e^{-\beta\rho}}{\epsilon}} \frac{(\epsilon s)^{\frac{i(x-x_0)}{\beta}}}{(\epsilon s)^{1-\tilde{\alpha}}\ln(\epsilon s)(s-e^{i\gamma})}ds$$

On the other hand

$$|-\frac{1}{2}\int_0^{\frac{e^{-\beta\rho}}{\epsilon}} \frac{(\epsilon s)^{\pm\frac{i(x-x_0)}{\beta}}}{(\epsilon s)^{1-\tilde{\alpha}}\ln(\epsilon s)(s-e^{i\gamma})}ds| \leq -\frac{1}{2}\int_0^{\frac{e^{-\beta\rho}}{\epsilon}} \frac{1}{(\epsilon s)^{1-\tilde{\alpha}}\ln(\epsilon s)|s-e^{i\gamma}|}ds$$

Therefore

$$|I(\eta)| \leq -\int_0^{\frac{e^{-\beta\rho}}{\epsilon}} \frac{1}{(\epsilon s)^{1-\tilde{\alpha}}\ln(\epsilon s)|s-e^{i\gamma}|}ds$$

Lemma 4.3.8. *There exist two positive constants C_1 and C_2 such that $\forall s \in]0, \frac{e^{-\beta\rho}}{\epsilon}[$,*

$$\frac{-C_1}{e\epsilon^{1-\tilde{\alpha}}\ln(\epsilon)s^{1-\tilde{\alpha}}s^{\frac{1}{\ln(\epsilon)}}} < \frac{-1}{\ln(\epsilon s)(\epsilon s)^{1-\tilde{\alpha}}} < \frac{-C_2 e}{\epsilon^{1-\tilde{\alpha}}\ln(\epsilon)s^{1-\tilde{\alpha}}s^{-\frac{1}{\ln(\epsilon)}}(1-e^{-1}s^{-\frac{1}{\ln(\epsilon)}})}$$

Proof. It suffices to apply lemma 4.3.7 with $\theta = -\frac{1}{\ln(\epsilon)}$. □

Proof of the theorem.

Proof. By applying lemma 3.3.2, we find:

$$|I(\eta)| \leq \frac{-C_2 e}{\epsilon^{1-\tilde{\alpha}}|\ln(\epsilon)|}\int_0^{\frac{e^{-\beta\rho}}{\epsilon}} \frac{1}{|s-e^{i\gamma}|}\frac{s^{\tilde{\alpha}-1}s^{\frac{1}{\ln(\epsilon)}}}{(1-e^{-1}s^{-\frac{1}{\ln(\epsilon)}})}ds. \tag{4.3.13}$$

We are in the case where $\tilde{\alpha}-1<0$. So, the integral

$$\int_0^{\frac{e^{-\beta\rho}}{\epsilon}} \frac{1}{|s-e^{i\gamma}|}\frac{s^{\tilde{\alpha}-1}s^{\frac{1}{\ln(\epsilon)}}}{(1-e^{-1}s^{-\frac{1}{\ln(\epsilon)}})}ds$$

is convergent. Moreover, $|I(\eta)| \geq |\mathrm{Im}(I(\eta))|$.

$$I(\eta) = -\int_0^{\frac{e^{-\beta\rho}}{\epsilon}} \frac{\cos(\frac{(x-x_0)}{\beta}\ln(\epsilon s))}{(\epsilon s)^{1-\tilde{\alpha}}\ln(\epsilon s)(s-e^{i\gamma})}ds$$

$$\mathrm{Im}(I(\eta)) = -\int_0^{\frac{e^{-\beta\rho}}{\epsilon}} \frac{\sin(\gamma)}{(s-\cos(\gamma))^2+\sin^2(\gamma)}\frac{\cos(\frac{(x-x_0)}{\beta}\ln(\epsilon s))}{(\epsilon s)^{1-\tilde{\alpha}}\ln(\epsilon s)}ds$$

If we take $x = x_0$.

$$|\mathrm{Im}(I(\eta))| = |\sin(\gamma)|\int_0^{\frac{e^{-\beta\rho}}{\epsilon}} \frac{1}{(s-\cos(\gamma))^2+\sin^2(\gamma)}\frac{-1}{(\epsilon s)^{1-\tilde{\alpha}}\ln(\epsilon s)}ds$$

By lemma 3.3.2, we find that:

$$|I(\eta)| \geq |\mathrm{Im}(I(\eta))| \geq \frac{C_1|\sin(\gamma)|}{e\epsilon^{1-\tilde{\alpha}}|\ln(\epsilon)|}\int_0^{\frac{e^{-\beta\rho}}{\epsilon}} \frac{1}{(s-\cos(\gamma))^2+\sin^2(\gamma)}\frac{1}{s^{1-\tilde{\alpha}}s^{\frac{1}{\ln(\epsilon)}}}ds, \tag{4.3.14}$$

which finishes the proof of the theorem.

□

Discussion

Theorems 37 and 38 show that the Green function remains bounded if the contrast η is not degenerated ($\kappa = -1$). When η tends to zero (or κ goes to -1), the Green function $G(x_0, x_0, y, y_0)$ blows up like $\frac{1}{|\eta|^{\frac{y_0-y}{4h}}\ln(|\eta|)}$ in the region close to the metallic layer, that is $\frac{y_0-y}{4h} > 0$ and $y < -h < h < y_0$. Then, the only plasmonic resonances ω_j of the metallic slab are the solutions to the following dispersion relation:

$$\varepsilon_m(\omega) \quad = \quad -\varepsilon_d. \tag{4.3.15}$$

Simple calculation leads to

$$\omega_j \quad = \quad -i\frac{\gamma}{2} + (-1)^j \left(\frac{\omega_p^2}{1+\varepsilon_d} - \frac{\gamma^2}{4} \right)^{\frac{1}{2}}, \quad j = 1, 2.$$

These resonances correspond exactly to the plasmonic resonances of a plasmonic spherical small nanoparticle (see for instance Lemma 2.1 in [39]). We observe that when the attenuation γ tends to zero, these resonances converge to the real axis, that is $\mathrm{Im}(\omega_j) \to 0$. Moreover, when γ becomes large, which means that the metal becomes a perfect conductor, these resonances move away from the real axis and will have no influence on the confinement and localization of the electromagnetic fields.

4.4 Numerical results

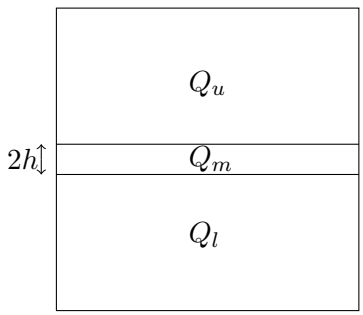

Figure 4.4: Simulation domain Q

We propose to calculate a numerical solution to the scattering problem (4.2.1) defined on an unbounded domain. To do this we need to restrict ourselves to a square bounded domain Q. We denote by Q_m, Q_u, Q_l the metal part, the upper dielectric part and the lower dielectric part of Q respectively (see Figure 4.4). We solve the following problem on Q:

$$\begin{cases} \Delta u + \varepsilon_d k_0^2 u_h = f & \text{in} \quad Q_u \cup Q_l \\ \Delta u + \varepsilon_m(\omega) k_0^2 u = 0 & \text{in} \quad Q_m \\ [u_h]_{y=\pm h} = 0 \\ \left[\frac{1}{\varepsilon}\partial_y u_h\right]_{y=\pm h} = 0 \end{cases}$$

Additionally, we set appropriates absorbing boundary conditions on ∂Q to avoid reflection on the boundaries. The source term f is a compactly supported function whose support is included in the upper dielectric region Q_l. Because we study a limit model when the layer thickness h is small compared to the wavelength we suppose that $k_0 << 1$. For the numerical simulation

we chose $k_0 = 10^{-4}$ and $\varepsilon_d = 1$. Firstly we simulated the previous problem with $\varepsilon_m = -1$ ($\eta^2 = 0$). We showed earlier that $\eta^2 = 0$ is a critical value. Indeed we proved the Green's function is always well-defined for $\eta^2 \neq 0$. However in the case $\eta^2 = 0$ it may not be well-defined when the source comes close to the metal layer. We now explore the numerical behaviour of the solution when $\eta^2 = 0$ and when the source comes close to the metal layer.

The results of the simulation are given in Figure 4.5. The constant d_{src} controls the source position y_0 such that $y_0 = h + d_{src} * h$. So here we moved the source from $y_0 = 2h$ to $y_0 = h$. Then, we measured the L^2 norm of the solution denoted E_{conf} (confined energy) in different regions (see figure 4.5 for the corresponding region to each curve) and we plotted the proportion of the total energy (E_{tot}) confined in this region E_{conf}/E_{tot}. We observe that when the source becomes very close to the metal layer, the energy confined in the region $-3h < y < 3h$ growths to reach 90% of the total energy (black curve). We also plotted the repartition of the confined energy, inside and around the metal layer (red, green, blue curves). We observe the same growth in the tree regions when d_{src} goes to 0. The difference between the region $-3h < y < -h$ and the region $h < y < 3h$ can be explained by the presence of the source in the second region increasing the measured energy. So we showed that moving the source very close to the metal layer increases the proportion of the energy confined around the layer. However some could

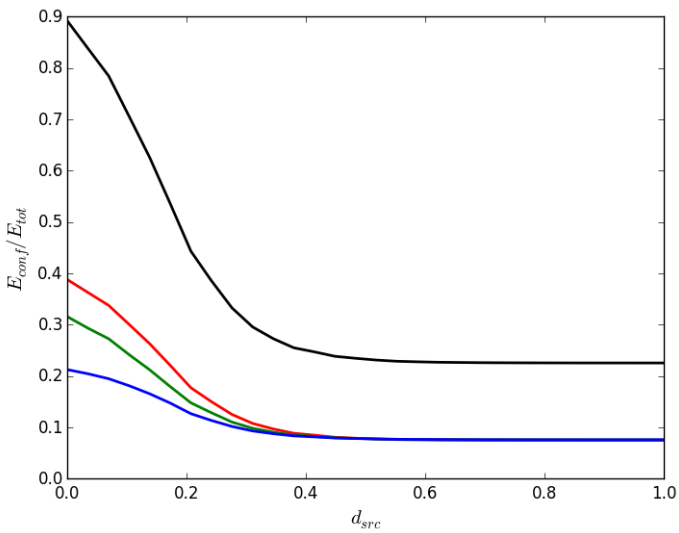

Figure 4.5: Black curve: Proportion of total energy confined in the region $-3h < y < 3h$. Green curve: Proportion of total energy confined in the region $h < y < 3h$ (reflective part). Red curve: Proportion of total energy confined in the region $-h < y < h$ (metal layer part). Blue curve: Proportion of total energy confined in the region $-3h < y < -h$ (transmission part).

argue the previously observed behaviour is just the consequence of moving the source very close to the layer, such that the growth of the confinement is only explained by the proximity between the source and the metal layer. But that is not the case. We plotted the energy ratio confined in the region $-3h < y < 3h$ when the source come close to the metal layer for different values of ε_m close to -1 (see Figure 4.6). That we observe is when the source comes close to the metal, the confined energy growth rate highly depends on ε_m. When ε_m is far from -1 ($\mathrm{Im}(\varepsilon_m) > 0.001$), the growth rate is almost constant (green curve). But when we come close to -1 the growth rate increases.

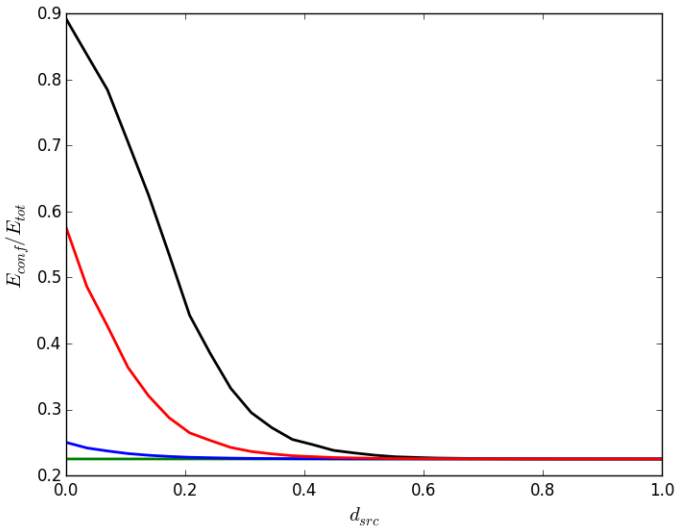

Figure 4.6: We observe the proportion of total energy confined in region $-3h < y < 3h$ for different values of ε_m. The black curve corresponds to the case $\varepsilon_m = -1$. The red curve corresponds to the case $\varepsilon_m = -1 + 0.00001i$. The blue curve to $\varepsilon_m = -1 + 0.0001i$. The green curves corresponds to the cases $\varepsilon_m = -1.1$, $\varepsilon_m = -1 + 0.001i$, $\varepsilon_m = -1 + 0.01i$, $\varepsilon_m = -1 + 0.1i$ which gives identical results at the figure scale.

Conclusion

We derived the asymptotic behavior of the plasmonic resonances of rough metallic surfaces containing subwavelength apertures and thin metallic plane layers. We showed that the these resonances converge to the zeros of some dispersion equations when the ratio between the roughness parameter and the wavelength tends to zero. The obtained dispersion equations (2.4.17), (3.5.12), (3.5.5), and (4.3.15) are independent of the roughness parameter, provide a precise localization of the resonances in the complex plane, and are suited for numerical approximation, shape and material optimization. We are confident that the derived results will help physicists and engineers in understanding the amplification and confinement of electromagnetic fields in sub-wavelength metallic structures. We plan in future works, to derive the asymptotic expansion of the electromagnetic fields and to validate numerically the obtained results.

Bibliography

[1] P. Quémerais, A. Barbara, J. Le Perchec, and T. López-Ríos. Efficient excitation of cavity resonances of subwavelength metallic gratings. *Journal of Applied Physics*, 97(5):053507, 2005.

[2] J. Le Perchec, P. Quémerais, A. Barbara, and T. López-Ríos. Controlling strong electromagnetic fields at subwavelength scales. *Phys. Rev. Lett.*, 97:036405, Jul 2006.

[3] A. Barbara, P. Quémerais, E. Bustarret, T. López-Rios, and T. Fournier. Electromagnetic resonances of sub-wavelength rectangular metallic gratings. *The European Physical Journal D - Atomic, Molecular, Optical and Plasma Physics*, 23(1):143–154, 2003.

[4] Faouzi Triki and Habib Ammari. Resonances for microstrip transmission lines. *SIAM Journal on Applied Mathematics*, 64(2):601–636, 2004.

[5] E. Bonnetier and F. Triki. Asymptotic of the green function for the diffraction by a perfectly conducting plane perturbed by a subwavelength rectangular cavity. *Mathematical Methods in the Applied Sciences*, 33(6):772–798, 2010.

[6] Jean-François Babadjian, Eric Bonnetier, and Faouzi Triki. Enhancement of electromagnetic fields caused by interacting subwavelength cavities. *Multiscale Modeling & Simulation*, 8(4):1383–1418, 2010.

[7] P. Drude. Zur Elektronentheorie der Metalle. *Ann. Phys.*, 306(3):566–613, January 1900.

[8] P. Drude. Zur elektronentheorie der metalle; ii. teil. galvanomagnetische und thermomagnetische effecte. *Annalen der Physik*, 308(11):369–402, 1900.

[9] A. Sommerfeld. *Zur Elektronentheorie der Metalle auf Grund der Fermischen Statistik*. Z. Phys. A-Hadron. Nucl, 1928.

[10] P. B. Johnson and R. W. Christy. Optical constants of the noble metals. *Phys. Rev. B*, 6:4370–4379, Dec 1972.

[11] Kittel. *Introduction to solid state physics.* Wiley India Pvt, 2007.

[12] Stefan Alexander Maier. *Plasmonics: Fundamentals and Applications.* Springer, 2007.

[13] H. Ehrenreich and H. R. Philipp. Optical properties of ag and cu. *Phys. Rev.*, 128:1622–1629, Nov 1962.

[14] Lewi Tonks and Irving Langmuir. Note on "oscillations in ionized gases". *Phys. Rev.*, 33:990–990, Jun 1929.

[15] R. H. Ritchie. Plasma losses by fast electrons in thin films. *Phys. Rev.*, 106:874–881, Jun 1957.

[16] Stefan Alexander Maier. *Oxford Dictionaries.* Oxford University Press, 2016.

[17] Shuwen Zeng, Dominique Baillargeat, Ho-Pui Ho, and Ken-Tye Yong. Nanomaterials enhanced surface plasmon resonance for biological and chemical sensing applications. *Chem. Soc. Rev.*, 43:3426–3452, 2014.

[18] A. Otto. Excitation of nonradiative surface plasma waves in silver by the method of frustrated total reflection. *Zeitschrift fur Physik*, 216:398–410, August 1968.

[19] E. Kretschmann and H. Raether. Radiative decay of nonradiative surface plasmons excited by light. *Z. Naturforsch. A*, 23:2135, 1968.

[20] Lukas Novotny and Bert Hecht. *Principles of nano-optics.* Cambridge University Press, 2006.

[21] A. Hessel and A. A. Oliner. A new theory of wood's anomalies on optical gratings. *Appl. Opt.*, 4(10):1275–1297, Oct 1965.

[22] A. Wirgin and T. Lopez-Rios. Can surface-enhanced Raman scattering be caused by waveguide resonances? *Optics Communications*, 48:416–420, January 1984.

[23] Joel Gersten and Abraham Nitzan. Electromagnetic theory of enhanced raman scattering by molecules adsorbed on rough surfaces. *The Journal of Chemical Physics*, 73(7):3023–3037, 1980.

[24] T. López-Rios, D. Mendoza, F. J. García-Vidal, J. Sánchez-Dehesa, and B. Pannetier. Surface shape resonances in lamellar metallic gratings. *Phys. Rev. Lett.*, 81:665–668, Jul 1998.

[25] J Homola. *Surface Plasmon Resonance Based Sensors.* Springer, 2006.

[26] H Ammari, H.Kang and H Lee. *Layer potential techniques in spectral analysis.* American Mathematical Society, 2009.

[27] Mario Durán, Ignacio Muga, and Jean-Claude Nédélec. The helmholtz equation in a locally perturbed half-space with non-absorbing boundary. *Archive for Rational Mechanics and Analysis*, 191(1):143–172, 2009.

[28] NATACHA VIALLE BEREUX. *Etude des resonances pour les equations de maxwell dans quelques structures.* PhD thesis, 1998. Thèse de doctorat dirigée par H. Ammari Physique EP 1998.

[29] J.C Nedelec and F Starling. Integral equation methods in a quasi-periodic diffraction problem for the time-harmonic maxwell's equations. *SIAM Journal on Mathematical Analysis*, 22(6):1679–1701, 1991.

[30] H. D. Alber. A quasi-periodic boundary value problem for the laplacian and the continuation of its resolvent. *Proceedings of the Royal Society of Edinburgh: Section A Mathematics*, 82(3-4):251–272, 1979.

[31] C. H. Wilcox. Scattering theory for diffraction gratings. *Mathematical Methods in the Applied Sciences*, 6(1):158–158, 1984.

[32] T Kato. *Perturbation Theory for Linear operators.* Springer, 1976.

[33] Anne-Sophie Bonnet-Ben Dhia and Felipe Starling. Guided Waves by Electromagnetic Gratings and Non-Uniqueness Examples for the Diffraction Problem. *Mathematical Methods in the Applied Sciences*, 17(5):305–338, April 1994.

[34] Robert E Collin. *Field theory of guided waves.* Wiley-IEEE Press, 1991.

[35] Junichi Takahara, Suguru Yamagishi, Hiroaki Taki, Akihiro Morimoto, and Tetsuro Kobayashi. Guiding of a one-dimensional optical beam with nanometer diameter. *Opt. Lett.*, 22(7):475–477, Apr 1997.

[36] Jean-Claude Weeber, Yvon Lacroute, and Alain Dereux. Optical near-field distributions of surface plasmon waveguide modes. *Phys. Rev. B*, 68:115401, Sep 2003.

[37] M. U. González, J.-C. Weeber, A.-L. Baudrion, A. Dereux, A. L. Stepanov, J. R. Krenn, E. Devaux, and T. W. Ebbesen. Design, near-field characterization, and modeling of 45 surface-plasmon bragg mirrors. *Phys. Rev. B*, 73:155416, Apr 2006.

[38] Rashid Zia, Anu Chandran, and Mark L. Brongersma. Dielectric waveguide model for guided surface polaritons. *Opt. Lett.*, 30(12):1473–1475, Jun 2005.

[39] M Vauthrin F Triki. Mathematical modelization of the photoacoustic effect generated by the heating of metallic nanoparticles. *arXiv preprint arXiv*, 2017.

[40] Giulio Ciraolo and Rolando Magnanini. A radiation condition for uniqueness in a wave propagation problem for 2-d open waveguides. *Mathematical Methods in the Applied Sciences*, 32(10):1183–1206, 2009.

[41] P. B. Johnson and R. W. Christy. Optical constants of the noble metals. *Phys. Rev. B*, 6:4370–4379, Dec 1972.

[42] I. D. Mayergoyz and Zhenyu Zhang. Numerical analysis of plasmon resonances in nanoparticles. *IEEE Transactions on Magnetics*, 42(4):759–762, April 2006.

[43] H. Ammari and H. Kang. *Reconstruction of Small Inhomogeneities from Boundary Measurements*. Springer Science & Business Media, 2004.